APPLICATION OF REMOTE SENSING, GIS, AND GPS IN PRECISION FORESTRY PRACTICES

by

ZENNURE UCAR

BS, Karadeniz Technical University, TURKEY, 2007

MS, Texas A&M University, 2012

A Dissertation Submitted to the Graduate Faculty of The University of Georgia in Partial Fulfillment of the Requirements for the Degree

DOCTOR OF PHILOSOPHY

ATHENS, GEORGIA

2017

APPLICATION OF REMOTE SENSING, GIS, AND GPS IN PRECISION FORESTRY PRACTICES

by

ZENNURE UCAR

(Under the Direction of PETE BETTINGER)

ABSTRACT

This dissertation is composed of three studies that evaluated the use of precision technologies; remote sensing, geographic information systems (GIS), and global positioning systems (GPS) for the capture and development of forestry and natural resources information. We explored the use of new protocols and procedures to collect data with GPS, estimated urban canopy cover with different remotely sensed sources, and assessed the accuracy of the processes.

In the first study, a statistical design was developed to collect data using a type of recreation-grade GPS receiver in the forest, during two different seasons. The dynamically-collected data were used in conjunction with GIS to assess error and accuracy. The results indicated the samples collected in winter showed less variation than the samples collected in summer when compared to the true land area. However, statistical test results suggested the season was not a significant factor. In the second study, two different sampling approaches, random point-sampling and plot/grid were employed for estimating urban tree canopy cover within two U.S. cities, using aerial photography and Google Earth imagery. The results indicated the two different sampling approaches could produce similar estimates of urban canopy cover, although one (point-based) was more time-efficient. Mixed results were observed when

considering the imagery sources. In the third study, the urban canopy cover was again assessed within same two U.S. cities yet this was a remote sensing study that incorporated LiDAR data with high resolution remotely sensed imagery, and urban canopy cover was estimated using the pixel-based supervised maximum likelihood classification method. The results suggested using LiDAR data along with high resolution remotely sensed imagery or using LiDAR data by itself can improve the process of identifying vegetated areas. These tactics increase accuracy of the vegetation class, and produce more accurate estimates of land areas when compared to using high resolution remotely sensed imagery alone.

These studies demonstrate the importance in forestry and natural resources fields of continuous evaluation of advanced technologies with a variety of experimental designs. The results might assist the endeavors of resource managers, the environmental community, manufacturers, and policy makers, and contribute to further advance in the field of precision forestry.

INDEX WORDS: Global positioning systems, geographic information systems, remote sensing, forestry, urban forests, urban vegetation, accuracy assessment, sampling, supervised classification

© 2017

Zennure Ucar

All Rights Reserved

APPLICATION OF REMOTE SENSING, GIS, AND GPS IN PRECISION FORESTRY PRACTICES

by

ZENNURE UCAR

Major Professor: Pete Bettinger
Committee: Jacek Siry
Chris Cieszewski
Marguerite Madden

Electronic Version Approved:

Suzanne Barbour
Dean of the Graduate School
The University of Georgia
August 2017

DEDICATION

To the loving memory of my father Osman Ucar,

a smart, honest and caring man

whom I still miss every day.

ACKNOWLEDGEMENTS

First and foremost, praises and thanks to God for everything that I have today.

I would like to express my deep and sincere gratitude to my advisor Dr. Pete Bettinger, for giving me the opportunity to pursue my PhD degree and providing me invaluable guidance in my dissertation and professional development. I am inspired by his dynamism, vision, sincerity and motivation. His performance, original thoughts and encouragements have pushed me to learn and grow more and more. Without his guidance and persistent help, this dissertation would not have been possible. It was a great privilege and honor to work under his guidance and I am extremely grateful for all his efforts.

I would like to thank my committee members, Dr. Jacek Siry, Dr. Chris Cieszewski, and Dr. Marguerite Madden, for their comments, support and patience on this dissertation, but also for their advices which extend and inform my future research perspective. I also express my appreciation to Krista Merry, for her constant help in developing the methodology for my research, and presenting the research work as clearly as possible. This dissertation would not have been possible without her support and assistance. I would also like to thank our research team members, Steven Weaver, Ramazan Akbulut, and Shingo Obata for helping me in conducting field work and writing-up the research. Their comments and suggestions were useful and definitely improve the quality of work.

I express my gratitude to all members of Warnell School of Forestry and Natural Resources, the University of Georgia (UGA). I had exceptional learning experience during my PhD studies, and without your assistance, invaluable resource and friendship, I would not have

been able to develop as scholar. Special thanks to Dr. Jeff Hepinstall-Cymerman, for giving me opportunity to teach FANR 3800 and FANR 4420/6420; Mr. Eric Schmeckpeper, for giving me opportunity to work as a GIS Intern at the U.S. Forest Service Region 8. I feel very grateful for their support during my studies.

I would like to say thanks to all my friends who offer their help, encouragement, understanding, and love during this process. To Aysegul and Aynur, thanks for being always supportive and believing in me more than I do. To Tugba and Mutlu, thanks for listening and supporting me when I needed to talk to somebody even if I had craziest ideas or irrational concerns about my research or daily life, and being always there to make my grad-life endurable. I am so grateful to have two of you in my life. Although I cannot mention all their names in this limited space, I also had many loving friends; Gulcimen, Gulcin, Merve, Esma, Serap, Bahadir, Gulden, Hakan, Ayca, Suravi, Ike, Kubra, whose friendships directly or indirectly improve my vision.

From the depth of my hearth, I would like to thank my big family, who believed in me, taught me to be honest, and always to strive for the best. Special thanks to my oldest brother Fahri Ucar, his wife Gulenay Ucar, and my younger sister Kezban Ucar Cifci, for encouraging me to begin this long journey. Even though my family is back in Turkey, I always feel their love and endless support in my heart. They will never let me alone.

TABLE OF CONTENTS

Page

ACKNOWLEDGEMENTS v

LIST OF TABLES ix

LIST OF FIGURES x

CHAPTER

1 INTRODUCTION AND LITERATURE REVIEW 1

Introduction 1

GPS Receiver Literature Review 3

Urban Canopy Cover Estimation Literature Review 4

Dissertation Format 6

References 9

2 DYNAMIC ACCURACY OF RECREATION-GRADE GPS RECEIVERS IN OAK-HICKORY FORESTS 15

Abstract 16

Introduction 17

Methods 21

Results 28

Discussion 34

Conclusion 35

References 37

3 A COMPARISON OF TWO SAMPLING APPROACHES FOR ASSESSING THE URBAN FOREST CANOPY COVER FROM AERIAL PHOTOGRAPHY 41

Abstract 42

Introduction 43

Methods 49

Results 58

Discussion 63

Conclusion 71

References 72

4 ESTIMATION OF URBAN VEGETATION COVER USING MULTISPECTRAL DATA AND LiDAR 77

Abstract 78

Introduction 79

Methods 83

Results 95

Discussion 106

Conclusion 110

References 113

5 CONCLUSION 120

REFERENCES 126

LIST OF TABLES

Page

Table 2.1: Results from dynamic study of Garmin Oregon® 450t GPS receiver 29

Table 2.2: Ranking of each Garmin Oregon® 450t GPS receiver after averaging the areas determined during each season 30

Table 2.3: Results of the Mann-Whitney statistical test for significant difference amongst seasons (*n* = 40 each season).....32

Table 3.1: Summary statistics for the point-based sampling approach (1,000 randomly-located sample points) and the plot/grid sampling approach (1,000 randomly-located sample plots) using imagery available through Google Earth and NAIP imagery viewed within ArcGIS 61

Table 4.1: Classification schemes for major classes and subclasses in the two study areas 92

Table 4.2: Classification matrices for four scenarios and six major land classes, Tallahassee 97

Table 4.3: Difference in land cover between LiDAR-related scenarios (1-3) and using NAIP imagery only (Scenario 4), Tallahassee 99

Table 4.4: Classification matrices for two major land classes, Tallahassee 100

Table 4.5: Classification matrices for four scenarios and six major land classes, Tacoma 102

Table 4.6: Area difference of land cover between using LiDAR integrated data (Scenario 1, 2, and 3) and using NAIP imagery only (Scenario 4) into the classification, Tacoma.....104

Table 4.7: The summarized accuracy of two classes among five scenarios with Kappa statistic, Tacoma, WA 105

LIST OF FIGURES

Page

Figure 2.1: A map of the study of the area and the Whitehall Forest GPS Test Site points used in this study 22

Figure 2.2: An example of vertices within 1 m buffers around true area with 40 samples in winter..... 25

Figure 2.3: An example of overlay of one sample area on top of the true area 26

Figure 2.4: The percentage difference between the true area and simulated areas.....33

Figure 3.1: The Tallahassee city boundary (upper left), an example of the random point-based sampling approach (upper right), 0.4 ha plots (lower left), and the 1.83 m grid embedded within the 0.4 ha plots (lower right).....51

Figure 4.1: Administrative boundaries of (*left*) Tallahassee, and (*right*) Tacoma.....84

Figure 4.2: Flowchart describing workflow adapted in the study 87

Figure 4.3: Conceptual model of the stacked images 91

Figure 4.4: Percent area of the major land classes, Tallahassee 98

Figure 4.5: Comparison of land area estimated using the classification scenarios, Tallahassee .100

Figure 4.6: Percent area of the major land classes, Tacoma 103

Figure 4.7: Comparison of land area estimated using the classification scenarios, Tacoma.....105

Figure 4.8: An example of classification results for six major classes (*left*) Tallahassee, and (*right*) Tacoma 108

Figure 4.9: An example of classification results for two major classes (*left*) Tallahassee, and (*right*) Tacoma 111

CHAPTER 1

INTRODUCTION AND LITERATURE REVIEW

Introduction

Precision forestry arose based on principles similar to those used precision agriculture, where advanced technology and sophisticated analytical tools are used to acquire high spatial and spectral resolution information that could be used to assist in the decision making process. (Kovácsová and Antalová, 2010; Olivera and Visser, 2014). In 2001, precision forestry was defined a process that facilitates site specific decision-making issues that require repeatable measurements, activities and procedures to grow and harvest trees, and manage forest in conjunction with desire to protect wildlife habitat, water quality, aesthetics, and other environmental resources (Bare 2001). The practice of precision forestry therefore offers an opportunity to use information of value to research, the environmental community, manufacturers and public policy makers.

Taylor et al. (2006) expanded on the definition of precision forestry in Southeast U.S. as a way to plan and conduct "site-specific forest management activities and operations to improve wood product quality and utilization, reduce waste, and increase profits, and maintain the quality of environment." According Taylor et al. (2006), precision forestry also consisted of three main categories: (1) the use of geospatial information to help forest management and planning, (2) the use of information to assist with site specific silvicultural operations, and (3) the use of the information and advanced technology to address market demands for higher valued products. In

order to actuate these activities, precision forestry uses a variety of new and advanced technologies, which include surveying technologies (e.g., Global Positioning Systems (GPS), terrestrial scanners), remote sensing technologies (airborne and satellite laser scanners), real-time process control scanners (e.g., radio frequency identification, ultrasound decay detectors), geographic information systems (GIS), and decision support systems (DSS) (Kovácsová and Antalová, 2010). For this study, we will consider the definition of precision forestry by Taylor et al. (2006), and employ navigation GPS, remote sensing technologies and GIS.

A variety of research has been conducted under the guise of precision forestry in order to evaluate the use of modern tools and technologies, and their accuracy in forestry because the profitability of forestry, and conservation of natural resources depend upon the accurate resource information (Holopainen et al., 2014). For example, GPS technologies have been studied in many different fields for a variety of purposes, including delineating land ownership and management unit boundaries, locating and mapping vegetation samples, mapping roads and trails, and measuring other natural resources (Deckert and Bolstad, 1996; Veal et al. 2001; Zenner et al., 2007). GPS technologies are also frequently used to monitor the locations of wildlife (e.g., Dussault et al., 2001; Gervasi et al., 2006). Laser devices have also been studied for their benefit to forest inventory purposes (Weaver et al., 2015).

GIS and remote sensing have been widely applied in forestry and natural resource management for monitoring, mapping, and management of the resources at multi-temporal, multi-spectral, and multi-spatial resolution since the 1980s (Ehlers et al., 1989; Loveland and Johnson, 1983; Lyon, 1983; Welch et al., 1988; Wulder et al., 2005). GIS and remote sensing have been used for detailed analysis of forest inventory (e.g., within- stand attributes), land cover characteristics, change detection, monitoring of forest health and natural disturbances (e.g.,

insect disturbance, fire, and invasive species, and information update (Franklin, 2001; Holopainen et al., 2014; Lachowski, 1996; Wulder et al., 2005). Although the use of advanced technology in forestry and natural resources is gradually increasing, it requires continuous evaluation in order to determine the social and scientific issues of forestry (Weaver, 2015). The social issue includes an assessment to sustainable management, goods, and ecological values; the scientific issue involves testing new technologies with application to a variety of experimental designs (Farnum, 2001). We take into account these issues while evaluating new technologies with different experimental designs in these studies.

GPS Receiver Literature Review

For forestry and natural resource management purposes, Global Navigation Satellite Systems (GNSS) help address a number of navigational, positioning, and mapping needs of managers and scientist. In many areas of the world, these systems are simply referred to as GPS, although GPS is shorten version of the United States system, NAVSTAR Global Positioning System. Satellite navigation and positioning systems use signals (electromagnetic energy) emitted by satellites, received by devices often located inside an automobile or airplane, attached to an animal, or held within a person's hand, and decoded to determine a position on the surface of the Earth (Bettinger and Merry, 2011). Satellite positioning systems can often provide highly accurate locational information when compared to accuracies that might be obtained from traditional navigation and mapping techniques (Bettinger and Fei, 2010; Naesset and Jonmeister, 2002). However, accuracy and precision of position determined by GPS under a forest canopy are often relatively low when compared with similar measures captured in open areas (Rodriquez-Perez et al., 2006; Rodriquez-Perez et al., 2007). This is important because resource managers frequently use information collected with GPS technology to delineate land

boundaries, record inventory plots, define roads, and map other features of interest. The spatial accuracy of the devices used (receivers) should be of high interest to both forest managers and scientists, as the application of GPS technology within a forested environment is perhaps one of the most demanding uses due to multipath, masking, and blocking effects caused by leaves, limbs, and boles of trees (Pirti, 2005). Therefore, advances in GPS technology require continual research and review to constantly express and information application of the technology when used under tree canopies. Since 2000, research in this area has evolved from purely observational studies to a blend of observational and hypothesis-driven studies today, as is presented in this dissertation.

Urban Canopy Cover Estimation Literature Review

An urban forest can be described as the woody vegetation within a city that includes street-lined trees located on both public and private lands, trees located in urban parks, and trees located on residential properties, commercial land, and other lands (Berland, 2012; Nowak et al., 2010; Ward and Johnson, 2007). This vegetation resource provides a number of essential benefits to human beings, a few of which include enhancing aesthetic values, reducing energy use, facilitating cooling effects, improving water and air quality, providing diverse wildlife habitat, and increasing human health and well-being (Jensen et al., 2004; Leuzinger et al., 2010; McPherson et al., 2011; Myeong et al., 2006; Nowak, 1993; Nowak et al., 2010; Richardson and Moskal, 2014). The amount of tree canopy cover, often estimated as the percentage of an area covered by the canopies of trees (Richardson and Moskal, 2014), can be used to inform management decision and policy makers. The ecosystem services derived from an urban forest are often directly related to amount of (percent of land) covered by a tree canopy, ideally composed of healthy and well-functioning vegetation (Nowak and Greenfield, 2012).

Urban population growth has an important influence on land cover change processes around the world (Berland, 2012). Since 1950, the world's urban human population has grown rapidly from 746 million to 3.9 billion people (54% of the total world population), partly due to increases in human population and partly due to administrative expansion of urban land designations. While urbanization of land can facilitate employment opportunities, it also increases the need for infrastructure, such as roads, educational facilities, and cultural amenities (Berland, 2012; United Nations, 2015), all of which then exert pressure upon the urban canopy cover (McPherson et al., 2011; Nowak, 1993). Hence, accurately quantifying urban vegetation cover is crucial for proper management of vegetated areas within a city, and through this we may be able to better sustain or improve ecosystem services and our quality of life (Nowak et al., 2008; Richardson and Moskal, 2014; Walton et al., 2008).

Two main approaches have been used to estimate the extent of urban forest: those using sampling methods and those using remote sensing technology. Both approaches have their own advantages and disadvantages in effort to estimate urban tree canopy cover. For example, point-based sampling approaches are relatively easy to implement, and if conducted well, can provide a reasonable estimate of urban forest cover along with a level of confidence. Other sampling efforts are not easy to implement (see Merry et al., 2014), yet more effectively capture the variability in urban tree cover, therefore need to be investigated. Various remote sensing approaches (such as using aerial photography, satellite imagery, or LiDAR (Light Detection and Ranging)) have proved useful for estimating tree canopy cover in urban environment. Remotely-sensed sources of information can be cost-effective when compared to field sampling, and can facilitate comparable analyses among different cities (McPherson et al., 2011). However, they generally require more effort than sampling approaches. As examples, Nowak and Crane (2002)

used advanced very high resolution radiometer (AVHRR) data to estimated carbon storage and sequestration by urban tree at different scales (state, regional, and national level), and Myeong et al. (2006) also developed a method using Landsat images from three different dates in order to quantify aboveground carbon storage of urban trees in Syracuse. However, using these low and mid resolution remote sensing images to assess urban canopy cover might not be adequate when applied to small scale heterogeneous urban environment. Therefore, with advanced technology, high resolution imagery and LiDAR have been begun to use increasingly to determine amount of the area covered by trees in urban environment. Irani and Galvin (2003) used 4 m resolution remotely sensed imagery to assess tree canopy cover in Baltimore, Nowak and Greenfield (2012) conducted a study using paired aerial photographs to determine tree canopy cover changes in 20 cities in the United States, and Parlin and Mead (2009) used 0.6 m resolution remotely sensed imagery to estimate tree cover change in Seattle. In addition, some studies integrated two or more remotely sensed data in order to estimate canopy cover in urban areas. Hartfield et al. (2011), Singh et al. (2012), and Jia (2015) all conducted studies which used LiDAR to estimate tree canopy cover. While efforts have been exerted to understand the value of sampling and remote sensing approaches in estimating urban tree canopy cover, more research is necessary to fully understand the possibilities of interest for urban land managers to estimate tree canopy cover levels.

Dissertation Format

This dissertation is written in the manuscript format, and it represents the results of three studies. Chapter 1 (this chapter) presents an introduction to the dissertation and a brief summary of previous research on GPS receivers and urban canopy cover estimation using sampling and remote sensing. In Chapter 2, “Dynamic accuracy of recreation-grade GPS receivers in oak-

hickory forests," we designed a study to assess the dynamic (kinematic) accuracy of a single model of recreation-grade receiver, within forested conditions, across two seasons of the year (winter and summer). The objectives of the study were to assess the area of agreement with a relatively small but well-defined closed area, to determine the variation of waypoints recorded around true boundaries of the area, and to determine whether significant differences in area determination were evident among the two seasons of the year. The following hypotheses were tested to evaluate the accuracy of this model of recreational-grade GPS receiver:

1. Difference in areas estimated by recreational grade GPS units from the true area is the same whether the GPS data are collected in winter or in summer.
2. Differences in the percentage of vertices within 1 m bands (1 m, 2 m, 3 m, etc.) of the true area boundary are not different during the two seasons.
3. The area of agreement between the true sample area and the areas estimated using the GPS receiver (using an intersect process in a geographic information systems) is the same in winter as in summer.

In addition to these hypotheses, we simulated larger areas of different sizes (1 to 49 ha) using the variation observed around the true boundaries of the sampled. This exercise helped us to understand how the effects of the observed error from our small study area might extend and affect area measurements when applied to larger land areas.

In Chapter 3, "A comparison of two sampling approaches for assessing the urban forest canopy cover from aerial photography," two different sampling approaches for estimating urban tree canopy cover were tested in conjunction with two freely available remotely sensed imagery products. The two sampling approaches were (a) the random point-based and (b) the plot/grid

approach. The two different remote sensing imagery sources used in this study included (a) U.S. Department of Agriculture National Agriculture Imagery Program (NAIP) imagery viewed within ArcGIS (ESRI, 2013) and (b) Google Earth imagery (Google, Inc., 2014). The objectives of the study were to determine the percentage of tree canopy cover in two United States cities using NAIP imagery within ArcGIS and using Google Earth imagery. The goal was to understand whether estimated tree canopy cover levels would be comparable when using either imagery source, and when using either sampling approach. The following hypotheses were developed:

1. When employing the random point-based sampling approach, there is no significant difference in the estimated tree canopy cover derived from using the NAIP imagery in ArcGIS and the estimated tree canopy cover derived from using the Google Earth imagery.
2. When employing the plot/grid sampling approach, there is no significant difference in the estimated tree canopy cover derived from using the NAIP imagery in ArcGIS and the estimated tree canopy cover derived from using the Google Earth imagery.

In Chapter 4, “Estimation of urban vegetation cover using multispectral imagery and LiDAR,” we classified urban vegetation cover using a supervised maximum likelihood classification method. The data included multispectral aerial imagery with 1 m spatial resolution collected in with 4 spectral bands (red, green, blue, and near infrared) and LiDAR data. The objective was to assess whether the addition of the LiDAR data increased the accuracy of urban vegetation cover estimations when using a pixel-based supervised maximum likelihood classification method. The following general hypotheses were developed:

1. When employing LiDAR in a supervised classification of urban vegetation, the overall accuracy of the resulting vegetation level improves when used in conjunction with high spatial resolution remotely sensed imagery.
2. When employing LiDAR data by itself to identify urban vegetation, the overall accuracy of the resulting vegetation level is no different than if it is used in conjunction with high spatial resolution remotely sensed imagery.

Finally, Chapter 5 is a conclusion chapter and presents review of each study's conclusions, their contribution to science, and future endeavors associated with each.

References

Bare, B.B. (2001). Opening remarks and welcome to the First International Precision Forestry Symposium. *In* Proceedings of the First International Precision Forestry Cooperative Symposium. University of Washington, College of Forest Resources, Seattle, WA. pp. 1.

Berland, A.M. (2012). Twin Cities urbanization and implications for urban forest ecosystem services. PhD dissertation. University of Minnesota, Minneapolis, MN. 142 p.

Bettinger, P., and Fei, S. (2010). One year's experience with a recreation-grade GPS receiver. Math. Comp. For. Nat. Res. Sci. 2, 153–160.

Bettinger, P., and Merry, K.L. (2011). Global navigation satellite system research in forest management. LAP Lambert Academic Publishing, Saarbrücken, Germany. 64 p.

Deckert, C. and Bolstad, P.V. (1996). Forest canopy, terrain, and distance effects on global positioning system point accuracy. Photogramm. Eng. Rem. Sens. 62, 317–321.

Dussault, C., Courtios, R., Ouellet, J., and Huot, J. (2001). Influence of satellite geometry and differential correction on GPS location accuracy. Wildl. Soc. Bull. 29, 171–179.

Ehlers, M., Edwards, G., and Bedard, Y. (1989). Integration of remote sensing and GIS: data and data access. Photogramm. Eng. Rem. Sens. 55, 1619–1627.

ESRI. (2013). ArcGIS. http://www.esri.com/software/arcgis (accessed 05/26/2013).

Franklin, S.E. (2001). Remote sensing for sustainable forest management. CRC Press, Boca Raton, FL.

Gervasi, V., Brunberg, S., and Swenson, J.E. (2006). An individual-based method to measure animal activity levels: A test on brown bears. Wildl. Soc. Bull. 34, 1314–1319.

Google, Inc. (2014). Google Earth (Version 7.1.2.2041). https://www.google.com/earth/ (accessed 12/27/2014)

Hartfield, K.A., Landau, K.I., and van Leeuwen, W.J.D. (2011). Fusion of high resolution aerial multispectral and LiDAR data: land cover in the context of urban mosquito habitat. Remote Sens. 3, 2364–2383.

Holopainen, M., Vastaranta, M., and Hyypä, J. (2014). Outlook for the next generation's precision forestry in Finland. Forests. 5, 1682–1694.

Irani, F.M., and Galvin, M.F. (2003). Strategic urban forests assessment: Baltimore, Maryland. Maryland Department of Natural Resources, Annapolis, MD.

Jensen, R., Gatrell, J., Boulton, J., and Harper, B. (2004). Using remote sensing and geographic information systems to study urban quality of life and urban forest amenities. Ecol. Soc. 9(5), 5–15.

Jia, Y. (2015). Object-based land cover classification with orthophoto and Lidar data. Masters Thesis. Royal Institute of Technology, Stockholm, Sweden.

Kovácsová, P., and Antalová, M. (2010). Precision forestry–definition and technologies. Šumarski List. 134(11-12), 603–610.

Leuzinger, S., Vogt, R., and Körner, C. (2010). Tree surface temperature in an urban environment. Ag. For. Meteorol. 150, 56–62.

Loveland, T.R., and Johnson, G.E. (1983). The role of remotely sensed and other spatial data for predictive modelling: The Umatilla, Oregon example. Photogramm. Eng. Rem. Sens. 49, 1183–1192.

Lyon, J.G. (1983). Landsat derived landcover classifications for locating potential Kestrel nesting habitat. Photogramm. Eng. Rem. Sens. 49, 245–250.

McPherson, E.G., Simpson, J.R., Xiao, Q., and Wu, C. (2011). Million trees Los Angeles canopy cover and benefit assessment. Landscape Urban Plan. 99, 40–50.

Merry, K., J. Siry, P. Bettinger, and J.M. Bowker. (2014). Urban tree cover change in Detroit and Atlanta, USA, 1951-2010. Cities. 41, 123–131.

Myeong, S., Nowak, D.J., and Duggin, M.J. (2006). A temporal analysis of urban forest carbon storage using remote sensing. Remote Sens. Environ. 101, 277–282.

Nowak, D.J. (1993). Historical vegetation change in Oakland and its implications for urban forest management. J. Arboric. 19, 313–319.

Nowak, D.J., and Crane, D.E. Carbon storage and sequestration by urban trees in the USA. Environ. Pollution. 116, 381–389.

Nowak, D.J., Crane, D.E., Stevens, J.C., Hoehn, R.E., Walton, J.T., and Bond, J. (2008). A ground-based method of assessing urban forest structure and ecosystem services. Arboric. Urban For. 34, 347–358.

Nowak, D.J., and Greenfield, E.J. (2012). Tree and impervious cover change in U.S. cities.

Urban For. Urban Greening. 11, 21–30.

Nowak, D.J., Stein, S.M., Randler, P.B., Greenfield, E.J., Comas, S.J., Carr, M.A., and Alig, R.J., (2010). Sustaining America's urban trees and forests. General Technical Report NRS-62. U.S. Department of Agriculture, Forest Service, Northern Research Station, State and Private Forestry, Newtown Square, PA.

Olivera, A., and Visser, R. (2014). Integration of GNSS in harvesters as a tool for site-specific management in plantation forests; a literature review. Future Forest Research Ltd. Rotorua, New Zealand.

Parlin, M., and Mead, M. (2009). Seattle, Washington urban tree canopy analysis: Project report: Looking back and moving forward. NCDC Imaging & Mapping, Colorado Springs, CO.

Pirti, A. (2005). Using GPS near the forest and quality control. Surv. Rev. 38, 286–299.

Richardson, J.J., and Moskal, L.M. (2014). Uncertainty in urban forest canopy assessment: Lessons from Seattle, WA, USA. Urban For. Urban Greening 13, 152–157.

Rodriguez-Perez, J.R., Alvarez, M.F., Sanz, E., and Gavela, A. (2006). Comparision of GPS receiver accuracy and precision in forest environments. Practical recommendations regarding methods and reciever selection. Shaping the Change XXIII FIG Congress. Munich, Germany.

Rodriguez-Perez, J.R., Alvarez, M.F., and Sanz-Ablanedo, E. (2007). Assessment of low-cost GPS receiver accuracy and precision in forest enviroments. J. Surv. Eng. 133, 159–167.

Singh, K.K., Vogler, J.B., Shoemaker, D.A., and Meentemeyer, R.K. (2012). LiDAR-Landsat data fusion for large-area assessment of urban land cover: Balancing spatial resolution, data volume and mapping accuracy. ISPRS J. Photogramm. Remote Sens. 74, 110–121.

Taylor, S.E., McDonald, T.P., Fulton, J.P., Shaw, J.N., Corley, F.W., and Brodbeck, C.J. (2006). Precision forestry in the Southeast US. *In* Proceedings of the Precision Forestry in Plantations, Semi-Natural and Natural Forests, Ackerman, P.A., Längin, D.W., and Antonides, M.C. (eds.). pp. 397–414.

United Nations. (2015). World urbanization prospects. United Nations Department of Economic and Social Affairs, Population Division, New York. ST/ESA/SER.A/366. 493 p.

Veal, M.W., Taylor, S.E., McDonald, T.P., McLemore, D.K., and Dunn, M.R. (2001). Accuracy of tracking forest machines with GPS. Trans. ASAE. 44, 1903–1911.

Walton, J.T., Nowak, D.J., and Greenfield, E.J. (2008). Assessing urban forest canopy cover using airborne or satellite imagery. Arboric. Urban For. 34, 334–340.

Ward, K. T., and Johnson, G.R. (2007). Geospatial methods provide timely and comprehensive urban forest information. Urban For. Urban Greening. 6, 15–22.

Weaver, S.A. (2015). Precision forestry studies: Laser calipers and GPS receivers. Master of Science thesis. University of Georgia, Athens, GA. 71 p.

Weaver, S.A., Z. Ucar, P. Bettinger, K. Merry, K. Faw, and C.J. Cieszewski. (2015). Assessing the accuracy of tree diameter measurements collected at a distance. Croatian J. For. Engineering. 36(1), 73–83.

Welch, R., Remillard, M., and Slack, R. (1988). Remote Sensing and geographic information techniques for aquatic resource evaluation. Photogramm. Eng. Rem. Sens. 54, 177–185.

Wulder, M.A., Hall, R.J., and Franklin, S.E. (2005) Remote sensing and GIS in forestry. *In* Remote sensing for GIS managers, Aronoff, S. (ed.). ESRI Press, Redlands, CA. pp. 351–362.

Zenner, E.K., Fauskee, J.T., Berger, A.L., and Puettmann, K.J. (2007). Impacts of skidding

traffic intensity on soil disturbance, soil recovery, and aspen regeneration in north central Minnesota. North. J. Appl. For. 24, 177–183.

CHAPTER 2

DYNAMIC ACCURACY OF RECREATION-GRADE GPS RECEIVERS IN OAK-HICKORY FORESTS[1]

[1] Ucar, Z., Bettinger, P., Weaver, S., Merry, K.L., and Faw, K.

Accepted by *Forestry*, 2014. Reprinted here with permission of publisher

(https://doi.org/10.1093/forestry/cpu019).

Abstract

The study, using 20 individual instruments of one model of recreational-grade GPS receiver, was conducted in a mature predominantly deciduous forest in the southern United States. The true area was delineated from the eight test points which were very accurately located from monuments using survey grade instrument and protocols, within the Whitehall Forest GPS Test Site in northeast Georgia. These same eight test points were used as controls during the dynamic horizontal accuracy assessments of GPS technology conducted within the forest. The test points are very precise compared to recent published literature. Our hypotheses were that the areas determined with the 20 receivers were not significantly different from the true areas, and the percentage of the area of agreement and the variation of the vertices around the true boundary were not different in winter and summer seasons. Also, based on the distribution of the vertices around the true boundary, we conducted simulations for larger areas. The average area of agreement was approximately 93% during the winter season, and approximately 84% during the summer season. The variation in sample areas was also greater for data collected during the summer, and data from the winter had higher association as measured by area of agreement with the true study area than data from the summer. A ranking of receivers by average area during each season did not reveal significant problems within the set of receivers tested. In conclusion, data collected during each season were not significantly different. Given the distribution of vertices around the true boundary of the study area, simulations of larger land areas revealed that there would be a 2% or less error for mature, deciduous forest greater than approximately 25 ha in size in both winter and summer seasons.

Keywords: Global Navigation Satellite Systems, accuracy assessment, dynamic accuracy, geographic information systems.

Introduction

For forestry and natural resource management purposes, Global Navigation Satellite Systems (GNSS) help address a number of navigational, positioning, and mapping needs. In many areas of the world, these systems are referred to as Global Positioning Systems (GPS). Satellite navigation and positioning systems are based on electromagnetic energy emitted by satellites, and received by devices often located inside an automobile or airplane, attached to an animal, or held within a person's hand (Bettinger and Merry, 2011). Satellite positioning systems can often provide highly accurate locational information when compared to traditional navigation and mapping techniques (Naesset and Jonmeister, 2002; Bettinger and Fei, 2010). However, accuracy and precision under a forest canopy are often very low when compared with similar measures in open areas (Rodriquez-Perez et al., 2006; Rodriquez-Perez et al., 2007). This is important because resource managers frequently use the information obtained to delineate land boundaries, and inventory plots, roads, and other features of interest. The spatial accuracy of the devices (receivers) should be of high interest, as the application of GPS technology within a forested environment is perhaps one of the most demanding uses due to masking and blocking effects caused by trees (Pirti, 2005). Therefore, advances in GPS technology require continual research and review for their application under tree canopies. Research in this area has thus evolved from purely observational studies conducted a decade ago to a blend of observational and hypothesis-driven studies today.

GPS receivers can be divided into three general classes: survey-grade, mapping-grade, and consumer-grade (or recreational-grade). Survey-grade GPS receivers are generally able to determine locations within 1 cm horizontal position accuracy in open areas and within 1 m accuracy in forested landscapes (Wing, 2008). The time required to use them, the cost (roughly 10,000 to 25,000 U.S. dollars (USD)), and the size of these units make them inappropriate for field work in a forested landscape (Bettinger and Fei, 2010). Mapping-grade GPS receivers are generally capable of providing accuracy within 1 m in open areas, and 2-5 m accuracy under forest canopies (Ransom et al., 2010). These receivers are frequently used in forest management, and have a price range of 1,000 to 5,000 USD. Recreation-grade receivers provide the least accurate positional information, generally between 5-10 m depending on environmental conditions (Wing, 2011). The cost range of recreational-grade GPS receivers is around 100 to 600 USD. The cost of data collection and the desired accuracy levels of referenced positions should be taken into account when choosing a GPS receiver (Bettinger and Fei, 2010; Wing et al., 2005).

It has been shown that precision and accuracy of data collected with GPS receivers decrease when used in forested landscapes (Danskin et al., 2009; Deckert and Bolstad, 1996; Naesset and Jonmeister, 2002; Rodriquez-Perez et al. 2006; Rodriquez-Perez et al., 2007) because GPS uses microwave signals, and forest vegetation and topography might interfere with the satellite signals (Veal et al., 2001). The highest accuracy in these types of environments requires using expensive and sophisticated equipment. However, some users hesitate to employ the highest accuracy equipment in forested areas because they fear they might damage equipment that is expensive to replace (Wing, 2011). Recreational-grade receivers have thus become popular for a variety of natural resource applications in forested environments because

of their affordable prices and their ease of use. While often a concern, measurement accuracy of these receivers might be adequate depending upon the goals and applications of a project (Wing, 2011).

The techniques employed for the assessment of GPS technology are well-established in the forestry field (Bettinger and Merry, 2011). GPS accuracy (often used interchangeably with *error*) is highly important for mapping, record-keeping, and research purposes, and many (e.g., McRoberts, 2010) have cautioned users on the potential pitfalls of using the information. The two main areas of concern for natural resource management professionals include static horizontal position accuracy (for points) and dynamic (kinematic) accuracy (for areas). A number of studies have recently illustrated the static horizontal accuracy of recreation-based receivers (e.g., Anderson et al., 2009; Bettinger and Fei, 2010; Bettinger and Merry, 2012b; Wing et al., 2005; Wing, 2008; Wing, 2009), yet assessments on the dynamic accuracy of recreation-grade receivers has been lacking. Most studies concerning GPS accuracy involve assessments of commercially-available equipment applied to forest conditions in manners typical of common field data collection processes. For dynamic accuracy studies, GPS accuracy and precision would ideally be compared against an independent control (Tachiki et al., 2005). However, at times the comparison has been reported only against the mean position determined from the epochs (waypoints, position fixes) recorded by other GPS receivers positioned at the same place (Taylor et al., 2004), against other benchmarks (Holden et al., 2001; Veal et al., 2001; Buerkert and Schlecht, 2009), or no control was necessary for the purposes of the associated studies (Zenner et al., 2007).

In a dynamic or kinematic mode, GPS has been used to track the movement of forest machines (Veal et al., 2001; Zenner et al., 2007). Liu and Brantigan (1995) evaluated whether

GPS technology was able to achieve more accurate dynamically-collected data than traditional methods (compass and chain) in closed forest stands. A number of advanced methods have also been tested in order to seek improvements to GPS accuracy levels, such as the correction of satellite orbit and clock errors, the post-processing of data using filters and modeling, and the mitigation of other external effects (Beran et al., 2007). Unfortunately, these latter areas of concern are rarely addressed by natural resource management professionals due to the added time and cost of application. GPS technology is also often used to monitor the locations of wildlife of concern (e.g., Dussault et al., 2001; Gervasi et al., 2006). Therefore the value in understanding the dynamic accuracy of GPS receivers lies in end uses of the information. For example, Kiser et al. (2005) once suggested that GPS could be of value in the design of timber sale areas, replacing other field methods that are based on magnetic fields or control points. In many cases in the management of forests, the edges (boundary) of an area described by GPS-collected data, and the subsequent area that is determined, may be used directly in contracts and research assessments.

As a result of these concerns, increased attention to the dynamic accuracy of new technology is essential. We therefore designed a study to assess the dynamic accuracy of a single model of recreation-grade receiver, the Garmin 450t (Garmin International Inc. 2013), within a forested condition, across two seasons of the year (winter and summer). Receivers were supplied by the University of Georgia's Department of Forestry and Natural Resources. The receivers were purchased not because of their cost (400 USD each) or their size, but because of their user-friendliness with respect to classes taught at the university.

Our objectives were to assess the area of agreement with a relatively small well-defined closed area, to determine the variation of waypoints around true boundaries, and to determine

whether significant differences were evident among the two seasons of the year. The following hypotheses were tested to evaluate the accuracy of this model of recreational-grade GPS receivers:

1. Difference in areas estimated by recreational grade GPS units from the true area is the same whether the GPS data are collected in winter or in summer.
2. The seasons do not cause differences in the percentage of vertices within 1 m bands (1 m, 2 m, 3 m, etc.) of the true area boundary regardless of the season.
3. The area of agreement between the true area and the sample areas (after an intersect process) is the same in winter as in summer.

In addition to these hypotheses, we simulated larger areas of different sizes (1 to 49 ha). It helped us to understand how the effects of the observed error from our small study area might impact area measurements when applied to larger land areas.

Methods

We developed a 0.90 ha (2.22 ac) test area in a mature deciduous (oak-hickory) forest that was 60 -70 years old, with 26.2 m^2 ha^{-1} basal area and 421.7 stems ha^{-1}. Ideally, for a dynamic accuracy study, independent control would arise from a formal survey of a closed area (Bettinger and Merry, 2011).

The true size of the study area was determined using a closed area that was defined by the coordinates of 8 GPS test points located on the Whitehall Forest GPS Test Site near Athens, Georgia (USA) (Figure 2.1). In developing the Whitehall Forest GPS Test Site in 2004, positions of a set of nearby established survey monuments were determined using a survey-grade GPS receiver (Ashtech Locus GPS) according to protocols (static data, 4 hours of data collection, etc.) that would allow the determined positions to be considered and accepted as National Spatial

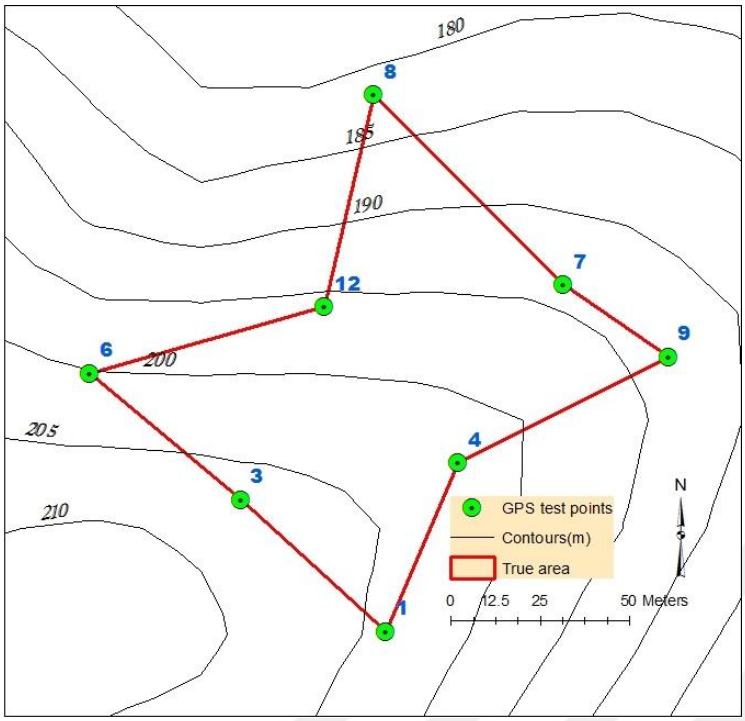

Figure 2.1. A map of the study of the area and the Whitehall Forest GPS Test Site points used in this study.

Reference System (NSRS) positions. The positions of the monuments were processed using the U.S. Department of Commerce, National Oceanic and Atmospheric Administration's Online Positioning User Service (OPUS) (www.ngs.noaa.gov/OPUS). The positional precision of these monuments was less than 2 cm. The closed traverse network that represents the Whitehall Forest GPS Test Site corners was then established by registered surveyors using a Topcon GTS-211D instrument and the NSRS monuments as a base. The closure of the points within the Test Site (as represented by a closed traverse connecting the points) was estimated to be 1/92,137. Given this resource, and for this particular study, we then very carefully delineated a straight line (using string) between the Test Site corners in order to provide the best indication of the position of the perimeter (boundary) of the area as one might expect in field conditions. We therefore consider

the closed area as a highly accurate model around which the recreation-grade GPS equipment could be tested.

In a dynamic horizontal position analysis, data are collected as a field-based receiver travels around a fixed course (an area) or along a fixed line. It is therefore important to maintain the receiver's antenna as close to the boundary of the area when waypoints or vertices are being collected because even tree position can affect positional accuracy (Bettinger and Merry, 2012b). If this is not the case, an unknown amount of error (deviations from the boundary or the line) may be inherent in the sample simply due to a loss of control. Our effort for controlling and understanding the true boundary of the study area is new and unique to the literature published thus far regarding the accuracy of dynamically-collected GPS data in a forested environment.

The data were collected both in winter (leaf-off) and in summer (leaf-on) with 20 different Garmin Oregon® 450t recreational-grade GPS receivers that only utilized satellites from the United States Navigation Satellite Timing and Ranging System (NAVSTAR) GPS program. These GPS receivers were considered state-of-the-art for recreation-grade equipment at the time of the study. Each receiver was used to determine the test area boundary, once per day. The availability of the researchers and the likelihood of non-rainy days were taken into account to determine the time for leaf-off (January 12-13, 2013) and leaf-on (June 5-6, 2013) data collection efforts. Each receiver was randomly chosen and used twice during each season, thus 40 samples of the test area were collected during each season. Before starting to collect data, a warm-up period (3 – 5 min) was required to ensure that each receiver was tracking a sufficient number of satellites. In collecting positional information regarding the boundary of the study area, the researchers collected waypoints (vertices of the boundary) at about 10 m intervals, holding the GPS receiver directly over the string during data collection process.

The dynamically-collected GPS data were downloaded to a personal computer using Minnesota DNRGPS software (Minnesota Department of Natural Resources, 2012). The data were saved in shapefile format to be used in conjunction with a Geographic Information System (ArcGIS 10.0, ESRI 2013). The average number of the vertices for the closed area was 50.78 in winter and 52.78 in summer. In only one case was a waypoint (boundary vertex) manipulated. In this case, the very first vertex of one sample area was obviously well away (50+ m) from the actual starting position, while the other vertices were adequately positioned. We can think of no reason for this anomaly, thus this vertex was removed from the sample. Using the data collected, three measures were reported: difference in areas estimated by the recreational grade GPS units from the true area, percent of vertices within *x* meters of the true boundary (proximity analysis), and area of agreement (after intersecting or overlapping sample areas with the true area). To calculate the difference in area, the closed area determined with each visit during the two different seasons these were compared to true area.

$$\text{Difference in area} = \text{True area} - \text{Sample area} \tag{1}$$

Through a proximity analysis conducted in GIS, buffers were created using the "generate near table," function, which is a tool in ArcGIS, was used to calculate the nearest distance of every point to the study area boundary line. This processes helped us understand the percentage of vertices from each sample area that were within 1 m intervals around the true boundary, up to 4 m (Figure 2.2). The final class included the percentage of vertices 4+ m from the true boundary line.

Percentage of the vertices = (Number of the vertices within certain distance / Total points)*100 (2)

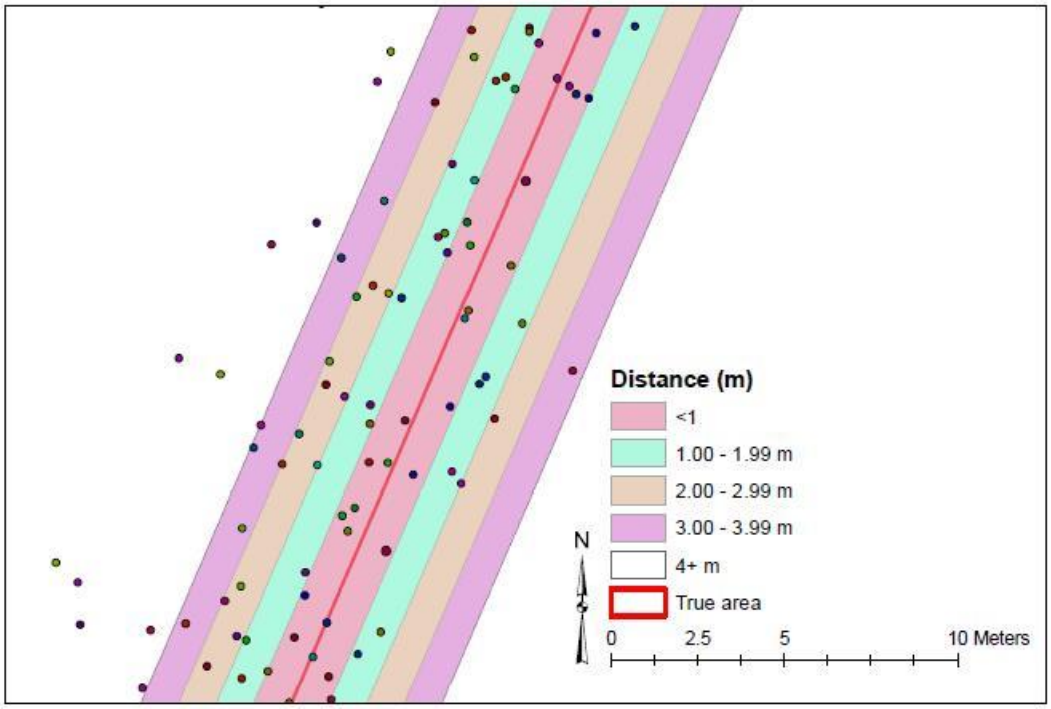

Figure 2.2. An example of vertices within 1 m buffers around true area with 40 samples in winter.

To evaluate the area of agreement, sample areas and the true area were overlaid (intersected) in ArcGIS to determine the area of agreement between the true area and the sample areas. Firstly, data were imported into ArcGIS 10.0 and converted to an area by connecting the waypoints. Then the true area was intersected (an overlay process) with each of the samples collected during the different seasons (Figure 2.3) to determine the area of agreement. The formula below was then used to determine area of agreement.

Area of agreement (%) = (Overlapping area / True area)*100 (3)

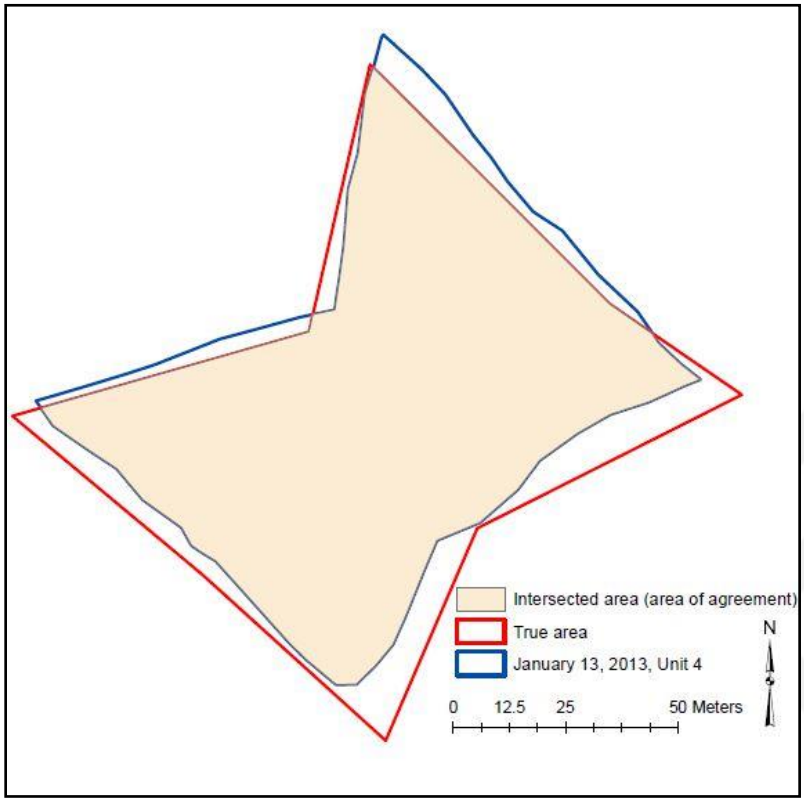

Figure 2.3. An example of overlay of one sample area on top of the true area.

To examine the accuracy of the GPS receiver, the normality of the data were assessed to decide which statistical tests need to be used (parametric or non-parametric). Based on the results of this assessment, we determined that the data in general were not normally distributed, which is very common among GPS studies. Thus, the Mann-Whitney non-parametric test within Minitab 16 software (Minitab Inc., 2013) for independent samples collected in winter and summer was used to test the differences between 40 samples collected in each season. As noted earlier, the hypotheses were (1) that the difference in areas was not significantly different between seasons, (2) that the area of agreement between the sample areas and the true area was not significantly

different between seasons, and (3) that the dispersion of the vertices around the true boundary was not significantly different between seasons.

Recreational grade receivers are frequently used for natural resource applications. In this study, we were able to evaluate only one recreational grade receiver within the small test area due to the effort required. However, most of users in the natural resources field are interested in how error in using the technology relates to larger-sized areas. Hence, after developing information regarding the distribution of observed, field-collected vertices around the true boundary of the study area, simulations of larger areas were conducted. The proximity analysis results of the summer season (representing a worse case than the winter season because leaves affect signals) were used in the development of simulated square areas that were 1, 2, 4, 9, 16, 25, 36, and 49 ha in size. For every 10 m of boundary distance, a random number was drawn and compared to the probability of a vertex falling with the 1-m bands around the true line (up to 5 m). A second random number was then drawn to estimate where the simulated vertex would lie within the 1-m band assuming a normal distribution of distances within each band. Five simulations were developed for each of the square areas in order to represent errors outside of true boundary line, and five simulations were generated for each of the square areas in order to represent errors inside of the true boundary line. These were considered worst-case scenarios, suggesting that the incorrect vertices were always either inside or outside of the true boundary, when in fact they may oscillate back and forth over the true line. In any event, these simulations were meant to help us understand the effects of the observed error (from the small study area) when applied to larger land areas.

Results

As we suspected, the sample (n = 40) average of closed areas collected using the recreation-grade GPS receiver was closer to the true area during the winter season, when the trees in the study area were devoid of leaves (Table 1). Interestingly, the sample average in both winter and summer was lower than the true area. The summer average area was only about 91% of the true area, while the winter average area was about 97%. The standard deviation of sample areas indicates that there was more variation in the summer as well, even though the coefficient of variation of areas during this season was only about 6.1%, which was about twice the coefficient of variation observed in the winter season. The range of the sample areas during the leaf-off season was 0.82 ha to 0.93 ha, while it was 0.67 ha to 0.98 ha during the leaf-on season. When the samples areas were intersected with the true area, the average area of agreement was 92.6% in the winter season, and 84.2% in the summer season. Positional issues related to the vertices that represent the boundary were much more evident in the summer season. When the percentage of vertices within 1 m bands around the true boundary line was assessed, there seemed to be only minor differences among the seasons. However, only the average percentage of vertices within 1.00 to 1.99 m and 3.00 to 3.99 m seemed to show large differences among the seasons (Table 2.1). This analysis did not take into account the direction of error (inside or outside of the true area).

With multiple receivers, we were able to rank the average performance of each when used in winter and spring. The results from ranking of each Garmin Oregon® 450t GPS receiver after averaging show that with the exception of one, in general receivers did not share the same ranking. Receiver number 11 was ranked as 12th (smallest to largest average areas) in both the leaf-off and leaf-on seasons (Table 2.2). However, one receiver (no. 16) was in the top five of

both season's rankings, representing the smaller average areas estimated during the data collection effort. And, two receivers (nos. 15 and 19) were in the bottom five of both season's rankings, representing the larger average areas estimated. The differences in rank were very small (0.1 to 0.2 ha difference between five or more in the list), and one should bear in mind that these seasonal averages arise from a sample size of two per season for each receiver. Therefore, we were not overly concerned that differences in areas estimated by receivers were due to the receivers themselves.

Table 2.1. Results from dynamic study of Garmin Oregon® 450t GPS receiver.

	Winter	**Summer**
True area (ha)	0.90	0.90
Sample average area (ha)	0.88	0.82
Standard deviation of the sample areas	0.03	0.05
Range of the sample areas		
• Smallest area (ha)	0.82	0.67
• Largest area (ha)	0.93	0.98
Average area of agreement (%)	92.6	84.2
Average number of the vertices within < 1. 00 m of the true line (%)	27.4	27.5
Average number of the vertices within 1.00 - 1.99 m of the true line (%)	25.3	19.6
Average number of the vertices within 2.00 - 2.99 m of the true line (%)	17.1	17.7
Average number of the vertices within 3.00 - 3.99 m of the true line (%)	12.1	15.7
Average number of the vertices within 4.01 + m of the true line (%)	18.1	19.6

Table 2.2. Ranking of each Garmin Oregon® 450t GPS receiver after averaging the areas determined during each season.

Receiver number	**Leaf-on season avg. area (ha)**	**Ranking**	**Leaf-off season avg. area (ha)**	**Receiver number**
10	0.77	1	0.85	20
16	0.83	2	0.85	4
14	0.83	3	0.85	13
1	0.84	4	0.86	17
6	0.84	5	0.86	16
8	0.85	6	0.86	7
4	0.86	7	0.87	14
12	0.86	8	0.87	9
2	0.87	9	0.87	10
18	0.87	10	0.87	6
17	0.89	11	0.87	12
11	0.89	12	0.88	11
20	0.90	13	0.88	3
7	0.90	14	0.88	5
3	0.90	15	0.89	1
15	0.91	16	0.89	18
5	0.91	17	0.89	15
13	0.91	18	0.90	19
9	0.93	19	0.90	2
19	0.94	20	0.91	8

Three hypotheses were proposed for this research. The results of the Mann-Whitney non-parametric tests (Table 2.3) indicate that the difference between areas estimated by the recreation-grade GPS receivers and the true area was not significantly different when seasons were compared ($p = 0.77$). Likewise, the percentage of the area of agreement was not significantly different between the seasons ($p = 0.62$). Further, the different seasons did not seem to result in significantly different percentages of vertices within the 1 m bands around the true boundary line. Hence, while the general results (Table 1) hint that there may be differences

among the seasons, based on the non-parametric test results (Table 2.3) no significant differences were observed, and all three hypotheses could not be rejected.

The positional data associated with this study illustrate an interesting situation that has heretofore not been described in the literature. It seems as if the recreation-grade receiver may perform better during dynamic tests of horizontal accuracy than during static tests of horizontal accuracy. The average error of the vertices describing the study area, with respect to the true boundary of the test area, and after accounting for vertices that are both inside the area and outside the area, was approximately 2.2 m in the winter and 2.3 m in the summer. This of course reflects the perpendicular distance between each vertex and the nearest boundary line, and does not take into account larger directional error that may have occurred along (parallel to) the boundary (rather than perpendicular to the boundary). Regardless, recent studies of similar technology (Bettinger and Fei, 2010; Bettinger and Merry, 2012a; Bettinger and Merry, 2012b) suggest that static horizontal positional accuracy should be 4-8 m on average, and recent unpublished static tests of the same technology used in this research suggest that the static error can be perhaps as much as 7-9 m on average.

Table 2.3. Results of the Mann-Whitney statistical test for significant difference amongst seasons (*n* = 40 each season).

Hypotheses	**Results**	**P-value**
Ho: Areas not significantly different	Not significantly different	0.77
Ho: Percentage areas of agreement are not significantly different	Not significantly different	0.62
Ho: Percentage of vertices within < 1 m are not significantly different	Not significantly different	0.49
Ho: Percentage of vertices within 1.00 - 1.99 m are not significantly different	Not significantly different	0.42
Ho: Percentage of vertices within 2.00 - 2.99 m are not significantly different	Not significantly different	0.96
Ho: Percentage of vertices within 3.00 - 3.99 m are not significantly different	Not significantly different	0.37
Ho: Percentage of vertices beyond 4.00 +m are not significantly different	Not significantly different	0.78

After simulating larger areas using the distribution of vertices within 1 m bands observed during the summer season, which assumes that the positional error around a true boundary will be similar regardless of the size of the area, our results suggest that the difference in area (compared to the true area) can be as high as 10 percent for 1 ha forested areas, and as small as about 1.3% for 49 ha areas (Figure 4). At around 9 ha, the simulated error was around 3%, and at around 25 ha the simulated error in estimated land area was below 2%. The results of these simulations were not unexpected. We had assumed that the magnitude of the error in land area estimation would dissipate somewhat as the size of the land area increased; this assumes again that the distribution of error around true boundary lines would not change when land area sizes changed.

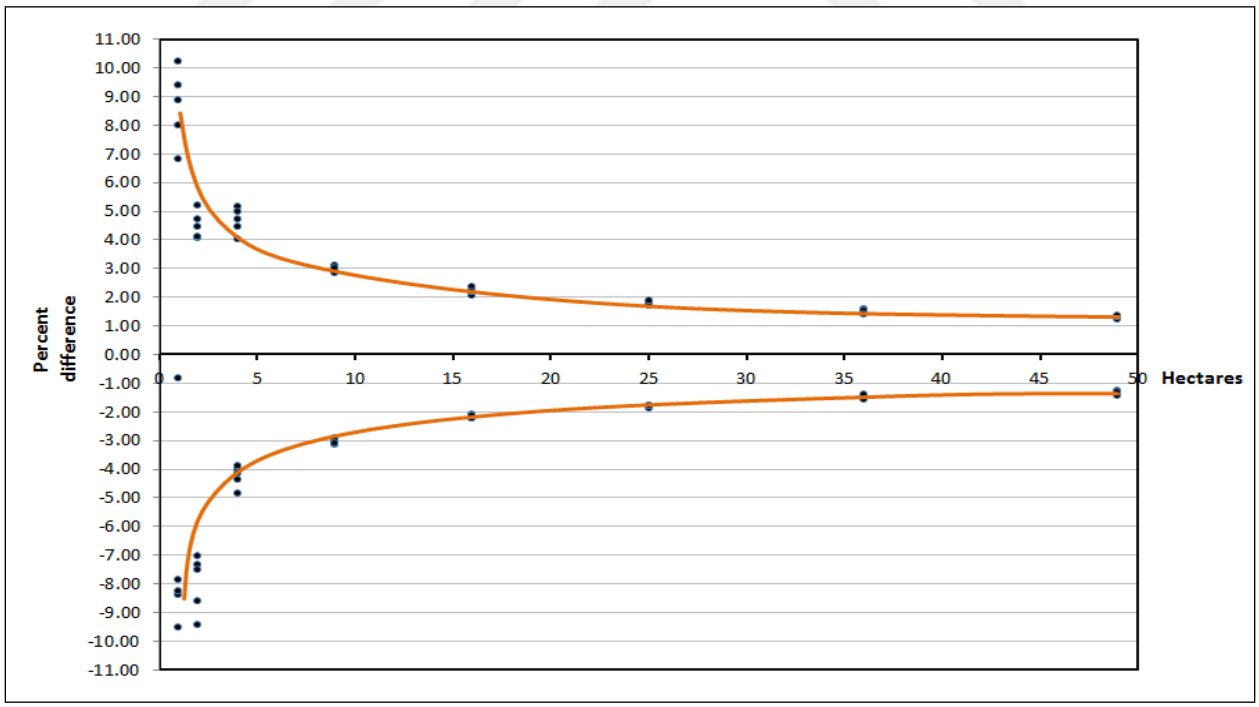

Figure 2.4. The percentage difference between the true area and simulated areas.

Discussion

The accuracy of GPS-collected data when describing land areas and when collected as a person, animal, or vehicle moves is of high importance for some fields of natural resource management. In forestry, practitioners want to use new technologies to quickly and effectively determine land areas associated with potential timber sales, natural or man-made impacts (fires, etc.), and critical habitat. Many people look to GPS as a source of this information. Others (e.g., Bettinger and Merry, 2011) have described the differences in GPS technology. In this study we solely examined recreation-grade GPS receivers, which are typically the least expensive of the vast array of commercially-available devices. While the study was limited to one brand and one type of receiver, 20 different receivers were used to assess the quality of data that could be developed. As this is one of the first reported dynamic accuracy tests, and given the tight control we placed on the boundary of the closed area, we feel that the observational results and the tested hypotheses represent a significant contribution to the literature.

Given the physical effort involved in this research, we considered two options: use one receiver multiple times to generate sample areas, or use multiple receivers a few times. With one receiver, we run the risk of that one being "different" from the norm. With multiple receivers, we were able to observe the average performance of each receiver under forest conditions. Thus, we used 20 GPS receivers (all Garmin 450t, and all purchased at the same time) rather than use one GPS receiver to collect measurements for all 80 sample areas (40 collected during each season). We collected information with each of the 20 receivers only four times, and therefore it was difficult to determine whether any one (or more) of the 20 receivers included measurement error that was statistically and significantly in contrast with the others. However, we evaluated average performance of the each receiver by ranking for both leaf-off and leaf-on season. In general, and

given the small sample size, there seemed to be no reason for concern. However, this issue can be important, as in one study of recreation-grade GPS technology, Wing (2009) showed that one may observe differences in the data obtained from receivers of the same vintage and technology.

We surmise that results will vary when other technologies are applied to the same forest types with similar tests. Obviously, it would be difficult to conduct and report upon every significant variation in technology, and therefore we leave open several questions for others to pursue. There have been very few examples of dynamic accuracy assessments of GPS technology employed in forests and reported in the literature, perhaps due to the difficulties in maintaining control of the boundary being mapped. In general, where it is clear and evident in the methodology of other studies, the control was established using mean positions determined from waypoints recorded by other GPS receivers or through means other than an independently established survey. In fact, none of the previous dynamic accuracy studies within forests reported contain the level of control we imposed on the collection of data along a true boundary line, perhaps with the exception of Tachiki et al. (2005), though the boundary line control in their case was unclear. Therefore, our study design seems to advance the science in this manner.

One could expand on this research by then applying similar study protocol to the assessment of current mapping-grade GPS technology. Others could also explore the impact of variations in receiver settings on the results obtained. For example, we limited our study to the use of the NAVSTAR GPS constellation of satellites because a typical recreation-grade receiver used in the United States can only access signals from this system. However, a number of mapping-grade and survey-grade GPS receivers are now available to capitalize on the signals provided by Russia's GLONASS system, the European Union's GALILEO system, and China's COMPASS system. The increase in accuracy and precision that could be achieved using

mapping-grade and survey-grade GPS receivers is due to the advanced antenna technology and algorithms employed not only to filter out degraded GPS signals (multipathed or otherwise), but also to optimize the use of satellites from other systems. These advancements in technology typically increase the cost of the equipment, perhaps significantly. A choke-ring antenna, for example, which is designed to mitigate the impact of multipathed signals on determined positions, can cost over 1,000 USD, twice the cost of a typical recreation-grade GPS receiver. In areas where Differential Global Positioning Systems (DGPS) capability is available, one could assess whether the near-real time augmentation that these provide will affect the quality of data collected while moving through a forested environment. In cases where GPS-related research conducted in forested environments is limited due to a lack of funding, well-designed studies such as this provide reliable periodic benchmarks for others to compare against.

Conclusion

We developed a highly-controlled dynamic accuracy test of recreation-grade GPS equipment in a deciduous forest located in an oak-hickory forest of the Southeastern United States. The boundary of the test area, which was delineated from accurately located eight points by using survey grade instrument and protocols, was clear and precise when data were collected, as the line was represented by string extending straight from one corner of our study area to the next. When a waypoint (vertex) was collected, the person collecting the data briefly stopped walking, held the receiver over the string, and saved the position. The data were analyzed within GIS to determine the size of the sample areas, the area of agreement with the true area, and the percentage of vertices that were within 1 m bands around the true boundary. While it seemed that there were general differences between the samples collected in the summer and the samples that were collected in the winter, statistical tests did not reject the three main hypotheses of the study.

Therefore, we cannot state with certainty that vegetative conditions associated with a deciduous forest in winter and in summer had any effect on the area determined, the area of agreement (with the true area), or the distribution of vertices around the true area boundary.

Funding

This work was supported by the Warnell School of Forestry and Natural Resources at the University of Georgia and The Republic of Turkey, Ministry of National Education.

References

Anderson, H.E., Clarkin, T., Winterberger, K., and Strunk, J. (2009). An accuracy assessment of positions obtained using survey- and recreational-grade global positioning system receivers across a range of forest conditions within the Tanana Valley of Interior Alaska. West. J. Appl. For. 24, 128–136.

Beran, T., Langley, R.B., Bisnath, S.B., and Serrano, L. (2007). High-accuracy point positioning with low-cost GPS receivers. Navig. 54, 53–63.

Bettinger, P., and Fei, S. (2010). One year's experience with a recreation-grade GPS receiver. Math. Comp. For. Nat. Res. Sci. 2, 153–160.

Bettinger, P., and Merry, K.L. (2011). Global navigation satellite system research in forest management. LAP Lambert Academic Publishing, Saarbrücken, Germany. 64 p.

Bettinger, P., and Merry, K. (2012a). Static horizontal positions determined with a consumer-grade GNSS receiver: One assessment of the number of fixes necessary. Croat. J. For. Eng. 33, 149–157.

Bettinger, P., and Merry, K.L. (2012b). Influence of the juxtaposition of trees on consumer-grade

GPS position quality. Math. Comp. For. Nat. Res. Sci. 4, 81–91.

Buerkert, A., and Schlecht, E. (2009). Performance of three GPS collars to monitor goats' grazing itineraries on mountain pastures. Comput. Electron. Agr. 65, 85–92.

Danskin, S.D., Bettinger, P., Jordan, T.R., and Cieszewski, C. (2009). A comparison of GPS performance in a southern hardwood forest: Exploring low-cost solutions for forestry applications. South. J. Appl. For. 33, 9–16.

Deckert, C. and Bolstad, P.V. (1996). Forest canopy, terrain, and distance effects on global positioning system point accuracy. Photogramm. Eng. Rem. Sens. 62, 317–321.

Dussault, C., Courtios, R., Ouellet, J., and Huot, J. (2001). Influence of satellite geometry and differential correction on GPS location accuracy. Wildl. Soc. Bull. 29, 171–179.

ESRI. (2013). ArcGIS. http://www.esri.com/software/arcgis (accessed 09/21/2013).

Garmin International Inc. (2013). Oregon® 450t. Garmin International Inc., Olathe, KS. https://buy.garmin.com/en-US/US/on-the-trail/handhelds/oregon-450t/prod63350.html (accessed 09/21/2013).

Gervasi, V., Brunberg, S., and Swenson, J.E. (2006). An individual-based method to measure animal activity levels: A test on brown bears. Wildl. Soc. Bull. 34, 1314–1319.

Holden, N.M., Martin, A.A., Owende, P.M.O., and Ward, S.M. (2001). A method for relating GPS performance to forest canopy. Int. J. For. Eng. 12, 51–56.

Kiser, J., Solmie, D., Kellogg, L., and Wing, M.G. (2005). Efficiencies of traditional and digital technologies for forest operations. West. J. Appl. For. 20, 138–143.

Liu, C.J., and Brantigan, R. (1995). Using Differential GPS for forest traverse surveys. Can. J. For. Res. 25, 1795–1805.

McRoberts, R.E. (2010). The effects of rectification and Global Positioning system errors on

satellite image-based estimates of forest area. Remote Sens. Environ. 114, 1710–1717.

Minitab Inc. (2013). Minitab 16. Minitab Inc., State College, PA. www.minitab.com (accessed 09/21/2013).

Minnesota Department of Natural Resources. (2012). DNRGPS application, 6.0.0.15. St. Paul, MN. http://www.dnr.state.mn.us/mis/gis/DNRGPS/DNRGPS.html (accessed 09/21/2013).

Naesset, E., and Jonmeister, T. (2002). Assessing point accuracy of DGPS under forest canopy before data acquisition, in the field and after postprocessing. Scand. J. For. Res. 17, 351–358.

Pirti, A. (2005). Using GPS near the forest and quality control. Surv. Rev. 38, 286–299.

Ransom, M.D., Rhynold, J., and Bettinger, P. (2010). Performance of mapping-grade GPS receivers in southeastern forest conditions. RURALS: Rev. Undergrad. Res. Agric. Life Sci. 5(1), Article 2.

Rodriguez-Perez, J.R., Alvarez, M.F., Sanz, E., and Gavela, A. (2006). Comparision of GPS receiver accuracy and precision in forest environments. Practical recommendations regarding methods and reciever selection. Shaping the Change XXIII FIG Congress. Munich, Germany.

Rodriguez-Perez, J.R., Alvarez, M.F., and Sanz-Ablanedo, E. (2007). Assessment of low-cost GPS receiver accuracy and precision in forest enviroments. J. Surv. Eng. 133, 159–167.

Tachiki, Y., Yoshimura, T., Hasegawa, H., Mita, T., Sakai, T., and Nakamura, F. (2005). Effects of polyline simplification of dynamic GPS data under forest canopy on area and perimeter estimations. J. For. Res. 10, 419–427.

Taylor, R.K., Schrock, M.D., Bora, G., Bloomfield, J., Brockmeier, G., Burton, W., Carlson, B., Gattis, J., Groening, R., Kopriva, J., Oleen, N., Ney, J., Simmelink, C., and Vondracek. J. (2004). Dynamic testing of GPS receivers. Trans. ASAE. 47, 1017–1025.

Veal, M.W., Taylor, S.E., McDonald, T.P., McLemore, D.K., and Dunn, M.R. (2001). Accuracy of tracking forest machines with GPS. Trans. ASAE. 44, 1903–1911.

Wing, M.G. (2008). Consumer-grade Global Positioning Systems (GPS) receiver performance. J. For. 106, 185–190.

Wing, M.G. (2009). Consumer-grade Global Positioning Systems performance in an urban forest setting. J. For. 107, 307–312.

Wing, M.G. (2011). Consumer-grade GPS receiver measurement accuracy in varying forest conditions. Res. J. For. 5, 78–88.

Wing, M.G., Eklund, A., and Kellogg, L.D. (2005). Consumer-grade Global Positioning System (GPS) accuracy and reliability. J. For. 103, 169–173.

Zenner, E.K., Fauskee, J.T., Berger, A.L., and Puettmann, K.J. (2007). Impacts of skidding traffic intensity on soil disturbance, soil recovery, and aspen regeneration in north central Minnesota. North. J. Appl. For. 24, 177–183.

CHAPTER 3

A COMPARISON OF TWO SAMPLING APPROACHES FOR ASSESSING THE URBAN FOREST CANOPY COVER FROM AERIAL PHOTOGRAPHY[2]

[2] Ucar, Z., Bettinger, P., Merry, K., Siry, J., Bowker, J.M., and Akbulut, R. Accepted by *Urban Forestry & Urban Greening*, 2016. Reprinted here with permission of publisher.

Abstract

Two different sampling approaches for estimating urban tree canopy cover were applied to two medium-sized cities in the United States, in conjunction with two freely available remotely sensed imagery products. A random point-based sampling approach, which involved 1,000 sample points, was compared against a plot/grid sampling (cluster sampling) approach that involved a 1.83 m square grid of points embedded within 0.04 ha circular plots. The imagery products included aerial photography from the U.S. Department of Agriculture National Agricultural Imagery Program (viewed within ArcGIS), and Google Earth imagery. For Tallahassee, Florida, the estimate of tree canopy cover was 48.6 to 49.1% using Google Earth imagery and 44.5 to 45.1% using NAIP imagery within ArcGIS. Statistical tests suggested that the two sampling approaches produced significantly different estimates using the two different imagery sources. For Tacoma, Washington, the estimated tree canopy cover was about 19.2 to 20.0% using Google Earth imagery and 17.3 to 18.1% when using NAIP imagery in ArcGIS. Here, there seemed to be no significant difference between the random point-based sampling efforts when used with the two different image sources, while the opposite was true when using the plot/grid sampling approach. However, our findings showed some similarities between the two sampling approaches; hence, the random point-based sampling approach might be preferred due to the time and effort required, and because fewer opportunities for classification problems might arise. Continuous review of urban canopy cover estimation procedures suggested by organizations such as the Climate Action Reserve and others can provide society with information on the accuracy and effectiveness resource assessment methods employed for

making wise decisions about climate change and carbon management.

Keywords: Aerial photography, tree canopy cover, urban forestry, sampling, Google Earth

Introduction

An urban forest can be described as the woody vegetation within a city that includes street trees located on both public and private lands, urban parks, and other trees located on residential properties, commercial land, and other lands. This resource provides a number of essential benefits to human beings, a few of which include providing aesthetic value, reducing energy use, facilitating cooling effects, improving water and air quality, providing diverse wildlife habitat, and increasing human health and well-being (Jensen et al., 2004; Leuzinger et al., 2010; Nowak, 1993; Nowak et al., 2010; McPherson et al., 2011; Richardson and Moskal, 2014). The ecosystem services derived from an urban forest are often directly related to the amount of tree canopy cover, which is ideally composed of healthy and functioning vegetation (Nowak and Greenfield, 2012). Tree canopy cover, generally estimated as the percentage of a site covered by tree canopies, is the simplest and most often used metric to quantify urban forest extent (Richardson and Moskal, 2014) and can be used to inform management decisions and policy analyses. For instance, a tree canopy assessment was conducted for Los Angeles to determine the capacity of the city to plant an additional one million trees (McPherson et al., 2011).

The human population of the United States increased from 281.4 million to 308.7 million between 2000 and 2010, and over 83.7% of the population now lives in metropolitan areas (large cities), where the population grew almost twice as fast as micropolitan areas (small cities with

10,000 to 50,000 people) (Mackun et al., 2011). Unless the administrative boundaries of cities expand, growth in the human population applies certain types of pressure upon the urban forests found there (Nowak, 1993; McPherson et al., 2011). For many United States cities, developed areas were created from areas once previously forested. In the 1990s, approximately 0.4 million hectares (ha) of forested land was converted each year to developed or other uses. Even if tree canopy cover increases in association with urban expansion of Great Plains and desert states, it is estimated that by 2050, an additional 9.3 million ha of forested area will become some other land use in the United States due to urbanization (Alig et al., 2003), thus population growth may result in direct or indirect negative impact on the structure, pattern and function of urban ecosystems in and around urban areas (Nowak, 1993).

In recent years, various approaches such as aerial photography interpretation, satellite-based image analysis, and aerial LiDAR (Light Detection and Ranging) analysis have proved useful for estimating tree canopy cover. These remotely-sensed sources of information can be both cost-effective when compared to field sampling, and can facilitate comparable analyses among different cities (McPherson et al., 2011). As examples, Irani and Galvin (2003) used 4 m resolution remotely sensed imagery to assess tree canopy cover in Baltimore. Nowak and Greenfield (2012) conducted a study using paired aerial photographs to determine tree canopy cover changes in 20 cities in the United States. And Parlin and Mead (2009) used digital land cover maps developed from 0.6 m resolution remotely sensed imagery to estimate tree cover change in Seattle. Remotely sensed imagery thus provides an opportunity to efficiently and effectively measure canopy cover across both space and time.

Specific tree canopy cover estimates can be developed using several different sampling approaches. The most common sampling approach involves random point-based sampling,

where random points are located within the boundary of a city, and then are classified through aerial photo interpretation as either falling on a tree crown or not falling on a tree crown. The observation value from this sampling approach is binary (yes/no or 1/0), indicating presence or absence of tree canopy at the sample point, as interpreted from the imagery. As suggested above, for 20 cities in the United States, Nowak and Greenfield (2012) used random point sampling to assess tree cover change over a five year period. They found that there was a decreasing trend in tree cover, about 0.27% per year on average, in these cities. Walton et al. (2008) also used a random point sampling approach and compared their results to classified satellite images.

A second sampling approach for estimating tree canopy cover might be to create random polygons and delineate tree crowns within these polygons. Nowak et al. (1996) were perhaps the first to use a fixed polygon approach like this for estimating tree cover. Nowak et al. (2008) studied the impact of polygon size on urban forest estimates, and noted that an increase in polygon size meant (logically) an increase in time required to perform the assessment. For Detroit and Atlanta, Merry et al. (2014) used a polygon approach to estimate tree canopy cover from aerial photography, and noted that the estimate of tree canopy cover using a polygon sampling approach could be slightly different than the estimate derived from using a point-based approach. The combined effects of mis-registration, feature displacement, and shadows could have imposed minor challenges to either method.

A third sampling approach may be to create a random polygon and then create a grid of points within the polygon in order to estimate canopy cover. Therefore, rather than draw the outline of tree canopies within the polygon and compute the proportion of tree canopy cover using the tree canopy and non-tree canopy areas (as in Merry et al., 2014), the proportion of grid points that fall on tree canopies within the polygon is used as the estimate of canopy cover for

the polygon. From this juncture forward we will refer to this cluster sampling process as the *plot/grid sampling approach*. This approach was proposed by the Climate Action Reserve (Nickerson, 2014a), in their draft Urban Forest Project Protocol. The Climate Action Reserve is a private nonprofit environmental organization and leading entity in the measurement of forest resources for carbon policy implementation. Their aim is to provide support to activities that decrease greenhouse gas emissions (GHG) by assuring the environmental entirety and economic benefits of emissions reduction projects. Along these lines, the Climate Action Reserve has a goal of establishing high quality standards for carbon offset projects and supporting activities that reduce air pollution, enhance growth in new green technologies, and facilitate the attainment of emission reduction goals. Since the cluster sampling approach for estimating canopy cover (when proposed) was different than other approaches described in the literature, we embarked on a study of its effectiveness for this purpose.

Interestingly, the cluster sampling process described in the draft Climate Action Reserve protocol (Nickerson, 2014a) was absent from the final protocol to allow people involved in these assessments the flexibility to respond to improvements in methodological and technological tools. However, they refer to desired sampling error in the *Quantification Guidance* (Climate Action Reserve, 2014a) and to verification of tree canopy cover estimates through a point-based sampling approach in the final protocol. Comments received with respect to the draft Urban Forest Project protocol (Climate Action Reserve, 2014b) suggested that the plot/grid sampling approach may have been reasonable for large, contiguous forest areas, but may have been unsuitable for urban areas that include a scattered arrangement of trees (street trees and others). However, this limitation would also seem to affect a point-based sampling approach. Further, it was suggested through feedback on the draft protocol that the processes used for estimating

urban canopy cover needed to be less detailed and structured, and needed to allow for the use of other equally valid tree canopy cover sampling protocols. While not included in the final protocols for urban forest projects by the Climate Action Reserve, the plot/grid sampling approach has not heretofore been assessed; therefore, it is the focus of this study.

Our goal was to compare two sampling approaches for estimating urban tree canopy cover in two United States cities (Tacoma, Washington and Tallahassee, Florida), using remotely sensed imagery from two different sources. We wanted to determine the feasibility of each sampling approach and to compare the results of canopy cover estimates using the two different remotely sensed imagery sources. The two sampling approaches are (a) the random point-based and (b) the plot/grid approach. The two remote sensing imagery sources used in this study included (a) U.S. Department of Agriculture National Agriculture Imagery Program (NAIP) imagery viewed within ArcGIS (ESRI, 2013) and (b) Google Earth imagery (Google, Inc., 2014). The NAIP imagery presents features in natural color (0.4-0.7 μm wavelengths of energy), is contained in compressed county mosaic form, and has a 1 m spatial resolution. The imagery is provided by the U.S. Department of Agriculture's Farm Service Agency (U.S. Department of Agriculture, 2013), and was captured between September 16th, 2013 and October 28th, 2013. Google Earth imagery arises from a variety of sources such as the U.S. Department of Agriculture, DigitalGlobe, GeoEye-1, Ikonos, MODIS Terra, city or state governments, and commercial aerial photographers (Taylor, 2014). Thus due to the use of third-party sources of imagery contained in Google Earth, and because the imagery is aggregated, the spatial resolution varies. The Google Earth imagery was dated as May 5th, 2013 and April 1st 2013 for Tacoma and Tallahassee, respectively. The most recent imagery available through Google Earth also presents features in natural color; the historical imagery available through Google Earth may be

panchromatic. These two imagery sources (NAIP and Google Earth) were selected because they are freely available and temporally current. The Google Earth imagery is also temporally consistent with the NAIP imagery within the two cities studied. NAIP imagery has been used in other recently published assessments of urban tree canopy cover (e.g., McGee et al., 2012; Merry et al., 2014), while Google Earth imagery has not.

In summary, we conducted a study to determine the percentage of tree canopy cover using NAIP imagery within ArcGIS and using Google Earth imagery in order to compare whether estimated tree canopy cover levels would be comparable when using either imagery source. We also conducted the study in a manner that would allow us to compare the two sampling approaches. Statistical tests were employed to determine whether significant differences existed. The following hypotheses were developed:

1. When employing the random point-based sampling approach across Tallahassee, there is no significant difference in the estimated tree canopy cover derived from using the NAIP imagery in ArcGIS and the estimated tree canopy cover derived from using the Google Earth imagery.
2. When employing the random point-based sampling approach across Tacoma, there is no significant difference in the estimated tree canopy cover derived from using the NAIP imagery in ArcGIS and the estimated tree canopy cover derived from using the Google Earth imagery.
3. When employing the plot/grid sampling approach across Tallahassee, there is no significant difference in the estimated tree canopy cover derived from using the NAIP imagery in ArcGIS and the estimated tree canopy cover derived from using the Google Earth imagery.

4. When employing the plot/grid sampling approach across Tacoma, there is no significant difference in the estimated tree canopy cover derived from using the NAIP imagery in ArcGIS and the estimated tree canopy cover derived from using the Google Earth imagery.

Methods

In the sections below, the study areas (cities) and the remotely sensed data around which the study was conducted are described, along with the sampling approaches employed and the statistical tests used to address the hypotheses.

Study Areas

As we suggested earlier, we selected two United States cities (Tallahassee, Florida and Tacoma, Washington) as case studies within which to estimate tree canopy cover using two sampling approaches and two imagery sources. We wanted to select two medium-sized cities that were located in two different regions of the United States, which contained in theory different forms of vegetative cover. These two cities were further selected based on the availability of both NAIP imagery and Google Earth imagery for the year 2013, and because Tallahassee and Tacoma have similar human population sizes. According to the U.S. Census Bureau (2014), Tallahassee was the seventh largest city in Florida with an estimated total population of about 186,000 people in 2013 and a population density of about 700 people per square kilometer (km^2). Comparably, Tacoma was the third largest city in Washington with an estimated total population of about 203,000 people in 2013 and a population density of about 1,541 people per km^2. The percent change in population from April 1, 2010 to July 1, 2013 was 2.5% for Tacoma and 2.8% for Tallahassee.

For both cities, we used NAIP imagery viewed within ArcGIS and Google Earth

imagery, both captured in 2013. Google Earth compiles imagery from multiple imagery sources including USDA NAIP imagery. However, through visual analysis we confirmed that the imagery used when analyzing sampling methods in Google Earth was not NAIP imagery.

Sampling Approaches for Tree Canopy Cover Estimates

Two different approaches were employed: a random point-based approach and a plot/grid approach. We randomly located 1,000 points each within the boundaries of each city (Figure 3.1). Suggested minimum samples were 100 per class for a large area by Congalton and Green (2009). Our sample size, 1,000 points, goes beyond the minimum requirements presented by Congalton and Green (2009) and is comparable to recent studies by Nowak and Greenfield (2012) and Richardson and Moskal (2014). These random points were created using the random point generator in ArcGIS. They were converted to a .KMZ format for use in Google Earth. For the plot/grid approach, the plots were centered on the points of the point-based approach.

The point-based approach uses binary data that are typically expressed as a proportion or percent when reported for an entire population (or sample area). The samples involve a determination from a random or systematic dot grid whether tree canopy is present or absent. This metric is often reported as the percent canopy cover for the sample area. In this study, through aerial photo interpretation we determined whether the location of every single point fell onto a tree crown (1), or did not fell onto a tree crown (0) representing a presence / absence type of analysis. We used the same 1,000 sample points to assess canopy cover with the NAIP imagery in ArcGIS and with the Google Earth imagery. Points were analyzed simultaneously in the two imagery sources in order to make sure they fell on the same location and to limit mis-classification, but the order of the sample was randomly assigned for each data set, so as to not introduce bias into the presence / absence decision. Also, in estimating canopy cover a fixed

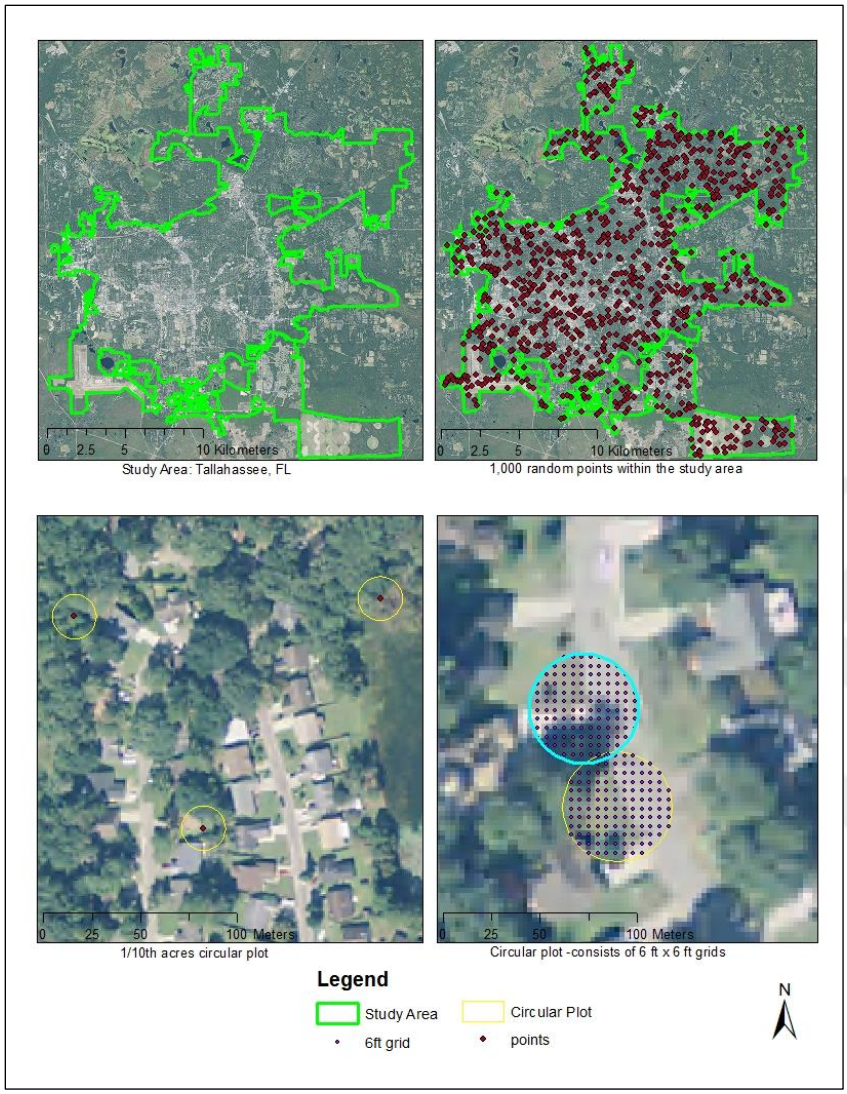

Figure 3.1. The Tallahassee city boundary (upper left), an example of the random point-based sampling approach (upper right), 0.4 ha plots (lower left), and the 1.83 m grid embedded within the 0.4 ha plots (lower right).

scale was utilized (1:600 to 1:800) when interpreting NAIP imagery within ArcGIS, and a fixed eye altitude was utilized (200 to 300 meters (m)) when interpreting Google Earth imagery. The percentage of tree canopy cover (p) was calculated by dividing the number of samples (x) indicating tree canopy cover by the total number of sample points (n) within each city ($p = x/n$).

The standard error (SE) for the tree canopy cover of an individual sample was defined using following equation:

$$SE = (p\ (1 - p) / n)^{0.5} \quad (1)$$

We also derived the pooled sample proportion

$$p^* = ((p_1\ (1 - p_1) / n_1) + (p_2\ (1 - p_2) / n_2))^{0.5} \quad (2)$$

for the estimates of tree canopy cover between NAIP imagery (p_1) and Google Earth imagery (p_2), and the SE of the difference between two samples:

$$SE^* = (p^*\ (1 - p^*))((1 / n_1) + (1 / n_2)))^{0.5} \quad (3)$$

where p^* is the pooled sample proportion, n_1 is the size of sample 1, and n_2 is the size of sample 2.

For the plot/grid (cluster sampling) approach, the original 1,000 randomly sampled points were buffered in ArcGIS to create circular polygons of a size (0.04 ha) that was suggested by Nickerson (2014a) as appropriate for this type of analysis. A grid of points was then placed inside each plot in order to estimate canopy cover. The spacing between the points within the circular plots was 1.83 m, and a large number of points (121) were created for each circular plot (Figure 1). Thus, 121,000 points were interpreted (1,000 plots *x* 121 points per plot) for each imagery product. Some plots were very quickly interpreted, if all or most points fell inside or

outside of tree canopies, thus the average rate of interpretation per point in this method is much faster than the per-point rate for the point-based approach. A Visual Basic program was used to create the grid of points based on the center location of the plot. A shapefile of these grids was created for use in ArcGIS, and a .KMZ file was created for use in Google Earth. The number of the points within the circular points that fell on a tree canopy was counted and the percentage canopy cover was estimated for each plot by dividing through by the total number of points in the grid. While the order of plot assessment was randomized, for consistency, we followed the same order for assessing the grid of points within each plot (north to south and laterally west to east). Also, some of the circular plots overlapped, overlapping points were not discarded but treated as a separate plot/grid sample. After interpretation of the grid within each plot, each plot became associated with an observation of the percentage canopy cover that ranged between 0-100 percent.

For the plot/grid approach, the mean and standard error for the entire sample within each city were calculated, along with 95% confidence intervals for tree canopy cover. We also calculated SE for each plot to compare with standard error of the entire sample. Similar to the point-based sampling approach, we reordered the sample randomly for each imagery source (NAIP and Google Earth) to avoid introducing sampling bias in the tree canopy cover estimation. We also used the same fixed viewing scale for the random point-based sampling approach (1:600 to 1:800 for NAIP imagery within ArcGIS and 200 to 300 m eye altitude for Google Earth imagery, respectively). Although Nickerson (2014a) suggests progressive sampling of plots until "a confidence estimate for average canopy cover for each urban forest class is achieved at ±10% at the 90% confidence interval", we initially used the same number of samples (1,000) as we used in the point-based sampling approach. However, we re-analyzed the data collected to

determine how many samples would have been required had the stopping point been determined where the ±10% range in average canopy cover equaled the 90% confidence interval for canopy cover.

The plot/grid (cluster sampling) approach that we employ is a form of simple random one-stage cluster sampling process that involves a geographic sampling frame or cluster (a city) in which there are listing units (the 0.10 acre plots) and elementary units (the collection of points within the plots) from which we estimate the proportion of tree cover. The clusters (cities) however are not selected randomly from the entire population (sampling frame) of cities within the United States. The listing units were randomly dispersed (or selected) within each city. Given that the plots could differ in tree canopy characteristics by simply shifting them a meter or so in any direction, the sampling frame for the plots might be considered infinite or very large. The feasibility and economics of cluster sampling have been noted as reasons for using this type of sampling process. In our case these reasons may not be viewed as advantages for our sampling effort, since the listing units are positioned in the same locations as the random sample points, and since more time is required to assess the elementary units (points) within the plots. High standard errors within samples have also been suggested as a disadvantage of cluster sampling approaches (Levy and Lemeshow 1991). However, an estimate of the percent canopy cover for each of the listing units (plots) is obtained from the binary data associated with each elementary unit (the points within the plots). This continuous value (range 0-100 percent) is then used to determine canopy closure within each city rather than the binary value associated with the point-based sampling approach noted previously.

Statistical Tests Related to Tree Canopy Cover Estimates

For hypotheses H_1 and H_2 (referencing the random point-based approach) we tested the difference between proportions (H_0: $p_1 = p_2$, H_a: $p_1 \neq p_2$). We developed the pooled sample proportion and the standard error of the sampling distribution difference between two proportions. A *Z*-score was determined using the following equation;

$$Z = (p_1 - p_2) / SE^* \quad (4)$$

We then assessed the probability (*P*-value) associated with the *Z*-score to determine whether significant differences existed, and to determine whether to accept or reject the hypotheses. Because the data collected from the plot/grid sampling approach resulted in a continuous value estimate (from 0 to 100%) of tree canopy cover (as opposed to the presence / absence response from the random point-based sampling approach), to test H_3 and H_4 we first examined the normality of the data by employing the Shapiro-Wilk test, since our data set were smaller than 2,000 elements. The results indicated that the tree canopy estimates from the plot/grid sampling approach, using both the NAIP imagery viewed within ArcGIS and the Google Earth imagery, were not normally distributed. Hence, the non-parametric Wilcoxon Signed Rank Test was used to test hypotheses H_3 and H_4.

Assessment of Classification Error, Mis-Registration and Feature Displacement

Inevitably when conducting analysis with two remotely sensed imagery sources, issues such as image mis-registration and the resulting mis-classification of a point between imagery sources will need to be addressed. As suggested by Nowak and Greenfield (2012) these components of image analysis may lead to incorrect estimations of land cover, for example a

point may be reported as falling on tree canopy in one imagery source and not falling on a tree in a different imagery source. Using a second interpreter can help mitigate this mis-classification; therefore, we randomly selected 10% of the points from the 1,000 sampling points in each city and with a second interpreter analyzed the presence / absence of trees using the NAIP and Google Earth imagery in the two cities. There was a 95 to 98% agreement between the analyses of the two interpreters across the two imagery sources and two cities, which is similar to that found in Nowak and Greenfield (2012). Differences were due to the subjective nature of the classification near the edges of tree crowns.

For further clarity on the potential for mis-classification of a point due to its proximity to a tree canopy edge and potential mis-registration between the two imagery sources on the point classification, four independent sets of randomly selected points were generated from the original 1,000 point-based sample. For both the NAIP and Google Earth imagery, 100 of the points classified as having fallen on a tree were selected. These were not paired points but 100 unique points for each imagery source. Additionally, 100 points that were classified as having not fallen on a tree were selected. For each point, a measurement was made to estimate the proximity of the point to the nearest tree canopy edge (those points not classified as having fallen on a tree) as well as the proximity of points classified as having fallen on a tree to nearest edge of the tree canopy. These measurements were of interest in assessing whether potential mis-classification by the interpreter may have contributed to the cause of some error.

For large areas, mis-registration of images may not be very important in estimating tree cover for a single point in time. Yet when comparing points between images taken at different points in time (e.g., to perform a landscape change analysis), the mis-registration of images may lead to false differences. When assessing two temporally different images, ideally an image

interpreter may be able to account for mis-registration by locating on the second image the original position of each point from the first image. However, this is difficult in circumstances where points fall on tree crowns or within groups of trees. Therefore in order to further understand mis-registration (or registration inconsistencies) between the imagery sources, another 100 independent points of the original 1,000 point sample were randomly selected for analysis in both cities. From these points, a linear distance measurement was made to a place on a clearly visible, permanent feature using both the NAIP imagery and the Google Earth imagery. Since it is impossible to know which of the two imagery sources is correct, the absolute difference in the distances between these measurements was used to understand the average mis-registration distance among the two imagery sources. These estimates of mis-registration distances are compared to the distances of points to the nearest canopy edge, using the sub-sets of sample points noted in the previous paragraph.

Finally, feature displacement can be a significant issue along the edges of individual aerial images, depending on a number of factors (flying height of the aircraft, focal length of the camera or sensor, etc.). With composited images, one would hope that feature displacement would be minimized, but through casual observation, the effects can occasionally be seen. Unfortunately, feature displacement depends also on the height of the features and the distance of the features from the nadir of each individual aerial image, two measurements that are elusive for a study such as ours; the image nadir is especially difficult to determine within composite images. To determine the nadir, one would need to locate the places in the composite images where feature displacement is negligible, which is difficult if these areas include a high density of trees, or if tree crowns are rounded (i.e., deciduous trees). For these reasons, we failed to provide a process for estimating feature displacement in the study areas.

Results

In evaluating the tree canopy cover of Tallahassee through the use of the point-based sampling approach, we estimated that 49.1% of the land within the boundary of the city was covered with trees in 2013 when viewed with Google Earth imagery, while 44.5% was covered with trees when viewed with NAIP imagery in ArcGIS (Table 1). Therefore, the difference between two imagery sources seemed to be about 4.6% in tree canopy cover estimates (standard error of the difference = 2.23%). The standard errors employed for the confidence intervals were 1.50% for the Google Earth and 1.40% for NAIP analyses and the resulting 95% confidence intervals were [46.2 to 52.0%] and [41.7 to 47.3%] for Google Earth and NAIP analyses, respectively. For Tacoma, through the use of the point-based sampling approach our estimate of tree cover in 2013 using the Google Earth imagery was 19.2%. The estimate of tree canopy cover was 18.1% when using NAIP imagery within ArcGIS. The estimated tree cover difference between Google Earth imagery and NAIP imagery within ArcGIS was thus 1.1% (standard error of the difference = 1.74%). The standard errors employed for developing confidence intervals were the same (1.20%) for both Google Earth imagery and NAIP imagery within ArcGIS, and hence the 95% confidence intervals were [16.8 to 21.6%] and [15.7 to 20.5%] for Google Earth imagery and NAIP imagery within ArcGIS, respectively.

With respect to the point-based sampling approach results, after performing the statistical tests associated with the hypotheses, we encountered some interesting findings. For Tallahassee, the results suggested that we cannot accept the H_1 null hypothesis ($p < 0.05$). There seemed to be a significant difference between the estimated percentage tree canopy cover using the random point-based approach with NAIP imagery within ArcGIS and the estimated percentage tree canopy cover using the random point-based approach with Google Earth imagery. On the other

hand, the results for Tacoma suggested that we can accept the H_2 null hypothesis ($p > 0.05$). There seemed to be no significant difference between the estimated percentage tree canopy cover with the random point-based approach when using either NAIP imagery within ArcGIS or Google Earth imagery.

In assessing tree cover using the plot/grid sampling approach, we estimated that 48.6% of the land within the city boundary of Tallahassee was covered with tree canopy in 2013 when viewed with imagery contained within Google Earth, and 45.1% was covered with tree canopy when viewed with NAIP imagery within ArcGIS (Table 1). Thus, the difference between the estimates of tree canopy cover was 3.5%. The estimate using Google Earth imagery was slightly lower than what we found using the point-based approach with Google Earth imagery, and the estimate from using NAIP imagery within ArcGIS was slightly higher than the result we found from the point-based approach. The standard errors were 1.29% and 1.30% for Google Earth imagery and NAIP imagery within ArcGIS, respectively, hence the 95% confidence intervals were [46.1% - 51.1%] and [42.7% - 47.7%] for Google Earth imagery and NAIP imagery within ArcGIS, respectively. For Tacoma, tree canopy cover was estimated to be about 20.0% in 2013 when viewed with Google Earth imagery, and 17.3% when viewed with NAIP imagery in ArcGIS, a difference in estimated tree canopy cover of 2.7%. Contrary to the Tallahassee results, the estimate from using NAIP imagery within ArcGIS was slightly lower than what we found using the point-based approach; however, the estimated tree canopy cover from using Google Earth imagery was slightly higher than the results we found from the point-based approach. The standard errors were 0.92% and 0.93% for the Google Earth imagery and using NAIP imagery within ArcGIS, respectively, hence the 95% confidence intervals were [18.2 to 21.8%] and [15.4 to 19.1%] for Google Earth imagery and NAIP imagery within ArcGIS, respectively.

With respect to the plot/grid sampling approach results, after performing the statistical tests associated with the hypotheses, we encountered some unexpected findings. The results suggested rejecting the H_3 and H_4 hypotheses ($p < 0.05$), since for both cities there seemed to be significant differences between the use of Google Earth imagery and NAIP imagery within ArcGIS for estimating tree canopy cover.

In re-analyzing the set of 1,000 samples from the plot/grid approach, we found that the point at which the ±10% range in average canopy cover equaled the 90% confidence interval for canopy cover was greater when using the NAIP imagery than when using Google earth imagery for both cities. Further, the number of plot/grid samples that would have been required in Tacoma was greater than the number of plot/grid samples that would have been required in Tallahassee using this rule. For Tacoma, the number of plot/grid samples required would have been 796 using the NAIP imagery in ArcGIS, and 504 using Google Earth imagery. For Tallahassee, the number of plot/grid samples required would have been 200 using the NAIP imagery in ArcGIS, and 140 using Google Earth imagery. However, estimates of canopy cover using these sample sizes were greater (2-8%) than the estimates of canopy cover using 1,000 samples.

From measurements made to a sub-set of sample points, on average for the two cities, those points that fell on a tree were within approximately 25 m (Tacoma) to 35 m (Tallahassee) of the edge of the canopy when using the NAIP imagery and approximately 15 m (Tacoma) to 24 m (Tallahassee) when using Google Earth imagery. Those points that were classified as not falling on a tree were, on average, approximately 37 m (Tallahassee) to 46 m (Tacoma) from a canopy edge when using the NAIP imagery and approximately 24 (Tallahassee) to 69 m (Tacoma) from a tree canopy edge when using Google Earth imagery.

Table 3.1. Summary statistics for the point-based sampling approach (1,000 randomly-located sample points) and the plot/grid sampling approach (1,000 randomly-located sample plots) using imagery available through Google Earth and NAIP imagery viewed within ArcGIS.

S.E. =Standard Error

	City											
	Tallahassee						Tacoma					
	Point-based Sampling Approach			Plot/grid Sampling Approach			Point-based Sampling Approach			Plot/grid Sampling Approach		
Imagery source	Estimated Canopy Cover (%)	S.E. (%)	95% Confidence Interval (%)	Estimated canopy cover (%)	S.E. (%)	95% Confidence Interval (%)	Estimated Canopy Cover (%)	S.E. (%)	95% Confidence Interval (%)	Estimated Canopy Cover (%)	S.E. (%)	95% Confidence Interval (%)
NAIP	44.5	1.50	41.7-47.3	45.1	1.30	42.7-47.7	18.1	1.20	15.7-20.55	17.3	0.93	15.4-19.1
Google Earth	49.1	1.40	46.2-52.0	48.6	1.29	46.1-51.1	19.2	1.20	16.8-21.6	20.0	0.92	18.2-21.8

Therefore, the likelihood of a mis-classification due to a point falling on the edge of a tree canopy in one image and not in the other was deemed minimal for the point-based sampling approach. The variation in these distances to canopy edges was high, however. In Tacoma, when points within tree canopies were considered, 12% were within 1 m from the edge of the canopy. When points not falling on tree canopies were considered, 1.5% were within 1 m from the canopy edge. In Tallahassee, when the sub-sample of points within tree canopies were considered, 2.5% were within 1 m from the edge of the canopy. When points not falling on tree canopies were considered, 5.5% were within 1 m from the canopy edge. As a result, photo interpretation error due to close, subjective classifications along the edges of tree crowns seems minimal, but likely contributes to some of the differences observed between sampling systems and imagery products. This is particularly of concern with the plot/grid approach where many points within a grid imposed within a plot may be close to the edge of a tree canopy.

The average absolute difference between specific points located on both the NAIP and Google Earth imagery, using locations of a sub-sample of paired points, was 1.19 m in Tacoma and 1.70 m in Tallahassee. These can be viewed as estimates of image registration differences. For Tacoma, using the NAIP imagery, 10% of the previous sub-sampled points classified as having fallen on a tree canopy were closer to the edge of the canopy than the corresponding image registration difference. Comparatively, none of the previous sub-sampled points classified as not being on a tree canopy were closer to the edge of the canopy than the corresponding image registration difference. When using Google Earth imagery, these were 20% and 4% of the previous sub-sampled points, respectively. For Tallahassee, using the NAIP imagery, less than 1% of the previous sub-sampled points that fell on a tree canopy were closer to the edge of the canopy than the corresponding image registration difference, while 3% of the points classified as

not having fallen on tree canopy were closer to the edge of the canopy than the corresponding image registration difference. When using Google Earth imagery, these were 12% and 15% of the previous sub-sampled points, respectively. As a result of this analysis, it becomes obvious that some of the differences in tree canopy classification estimates may be associated with registration differences among the two imagery products. Again, this is particularly of concern with the plot/grid approach where many points within a grid imposed within a plot may be close to the edge of a tree canopy.

Discussion

In this study, our findings show similarities to other recent findings (e.g., Merry et al., 2014) that indicate tree canopy cover estimates can be statistically significantly different when different sampling approaches or imagery sources are employed, even when the sample units are basically positioned in the same location within the study areas. However, the sampling process itself should not be the cause of these differences; as we noted earlier the combined effects of mis-registration, feature displacement, and mis-classification could have imposed minor challenges to either method.

Given the large number of sample observations collected (1,000 sample points, which exceeded the minimum requirement represented by Congalton and Green (2009)), it should be of no surprise that the standard errors are relatively small, and therefore slight differences in sample means might be considered statistically significant. For example, when employing point-based sampling, the differences in canopy cover between using NAIP imagery and Google Earth imagery were 4.6% and 1.1% for Tallahassee and Tacoma, respectively. Statistical test results showed that these were significantly different than the estimated tree canopy cover for Tallahassee but not Tacoma. However, when the plot/grid sampling approach was employed the

differences in canopy cover between using NAIP imagery and Google Earth imagery are 3.5% and 2.7% for Tallahassee and Tacoma, respectively, and these were not significantly different. This might be a result of the plot/grid sampling approach minimizing the impact of image mis-registration and feature displacement. The SEs for the plot/grid sampling approach are slightly smaller than the SEs for the point-based approach. However, the average SE of each plot within the plot/grid sampling approach was 1.80% when using the NAIP imagery and 1.88% when using the Google Earth imagery for Tallahassee. For Tacoma, the average SE for the individual plots was 1.48% and 1.80% with the NAIP imagery and Google Earth imagery, respectively. These are slightly larger than the SEs for the point-based sampling approach. Even though many more points were employed in the plot/grid sampling approach, the SE of this approach should be similar to the SE of the point-based approach given that the plot is the sample unit, not the grid of 121 points used within each plot. Had a smaller number of sample observations been utilized, and larger standard errors observed, statistical tests may have suggested that there were no significant difference in the mean values of the Tallahassee results when using the point-based sampling approach. As it stands, the significant differences in results are more likely associated with some combination of mis-classification, mis-registration, and feature displacement issues of the sampling protocol.

A number of factors could have introduced bias or error into our findings. These include problems inherent in the imagery, such as topographic displacement, spatial resolution, minor georeferencing problems, mis-registration, parallax, shadows, image tone and texture issues along edges of individual image frames, and other image processing issues for which users are unaware. During the image interpretation process, the majority of the differences were attributed to points falling on the edge of tree canopies within shadows of one imagery source and not

within a shadow on the other imagery source. This was due to differences in the timing of the capture of the imagery (time of day, time of year). This was also particularly evident within the NAIP imagery. Further, due to the spatial resolution of the NAIP imagery, pixilation at a larger scale resulted in some challenges related to the classification of points. Google Earth imagery was advantageous in that regard because it has a finer spatial resolution at larger scales. Allowing the interpreter to vary the scale may also be beneficial to image interpretation efforts and canopy cover assessments using Google Earth imagery, but may have less benefits to similar efforts employing NAIP imagery. Finally, while the imagery used for analysis were captured within months of each other, the variation in season between the two imagery sources may have attributed to the differences in canopy estimates specifically when a point fell on a deciduous tree species.

Without sub-meter accurate horizontal positions to compare against, it is difficult to tell which of the two imagery sources had more mis-registration problems. Orthophotos like those offered by the USDA, by nature, have been processed and corrected to limit these sorts of issues (Lillesand et al., 2004) while the same corrections may not have been applied to the composite imagery offered from Google Earth. Overall, a small level of inconsistent registration was evident across both imagery sources and cities, and therefore likely had some impact on the point classification process. Given that both are composite images, the registration differences are not consistent across the landscape, and a correction process employed for an analysis such as this (estimating tree canopy cover in urban areas) would be time-intensive.

Shadows may result in urban trees not being easily distinguishable from other nearby features. Shadows can also result in mis-classification of the vegetation because of dense appearance of tree canopies (Merry et al., 2014). In addition, we assumed a fixed viewing scale

for interpretation purposes, and this may compound the effect of the shadows; hence it may be better to change scales in order to more clearly interpret the image. Also, the finer spatial resolution of the Google Earth imagery may have played a role in the generally higher canopy cover estimates when compared to using the NAIP imagery. Other factors that could have played a role in the results we obtained included photo interpretation error caused by fatigue or distraction (blunders, random error), and photo interpretation error in the assessment of vegetation (e.g., trees vs. bushes). However, it is comforting to know that our estimated tree canopy cover for Tacoma was similar to other recent estimates (Nowak and Greenfield, 2012) and the results of our mis-registration and mis-classification tests showed that these issues were minimal in influencing our analysis.

Estimation of tree canopy cover using different sampling approaches and different imagery sources provides us with an understanding of the time, effort, and complexity of the processes. The time required to implement each process associated with this study was important, as the use of different sampling approaches and imagery sources required a significantly different amount of time for interpretation and determination of tree cover. The plot/grid sampling approach may seem to represent a more precise way to estimate tree canopy cover, but it also required more time and attention to detail than when simply interpreting individual random points - when using the same number of sample. For instance, for the photo interpreter associated with this project, the plot/grid approach required approximately one hour to assess 100 plot/grid sample locations (1/10 of the sample size), but for the point sampling approach about 200 to 250 points were interpreted within same period of time (1/4 of the sample size). It may seem that the plot/grid sampling approach would be more time consuming than reported but the interpreter did not always have to count each point within each grid. There were

many instances when the plot/grid fell completely onto a forested area or the area of canopy cover fell within one continuous section of the grid requiring only a portion of the points to be interpreted. Conversely, there were instances when the plot/grid fell completely onto a developed area or water, so only a minimal number of points within the grid (or no points at all) had to be analyzed, allowing the interpreter to move on to the next plot quickly. Had we ceased to sample using the plot/grid approach when the point at which the ±10% range in average canopy cover equaled the 90% confidence interval for canopy, the time required for sampling (as compared to the point-based approach) would have actually been less for Tallahassee, but not for Tacoma. This may be related to the lower level of canopy cover in Tacoma and the larger standard error as a proportion of the mean canopy cover. In addition, the higher spatial resolution of Google Earth imagery may reduce the number of samples required under this rule.

With regard to viewing scale, the NAIP imagery analysis within ArcGIS provided a fixed scale option which made it easier to provide and apply a consistent process for canopy cover estimation. However, the Google Earth imagery analysis required more attention on the photo interpreter's behalf to the fixed eye altitude in order to maintain a consistent scale while interpreting canopy cover for the sample points. Hence, more time was required for tree canopy cover analysis with the Google Earth imagery than when using the NAIP imagery within ArcGIS.

Several sampling approaches have been tested recently for their usefulness in assessing urban canopy cover in addition to the cluster sampling approach evaluated here. These include sampling processes that use satellite or aerial imagery (such as the random point and cluster sampling approaches) and integrated tools for field-based assessments of canopy cover. For example, the iTree application tool, developed by the U.S. Forest Service and their cooperators,

was designed to help users assess and manage the character of urban forests (King and Locke 2013, Nowak at al. 2008). The iTree application tool allows one to collect field based measurements of urban tree canopy cover at sample points and to collect estimates of other forest information (tree size, species, etc.) needed for management purposes. In comparing different approaches using the iTree application tool, high-resolution land cover data (GIS), and skyward-oriented hemispherical photographs, King and Locke (2013) found that estimates of canopy cover from using these provided similar results. While we did not directly compare the cluster sampling approach described here to the use if the iTree application tool or hemispherical photographs, one might assume that the cluster sampling approach applied using high-resolution aerial imagery might also provide similar canopy cover estimates. If conducted well, a point-based sample should provide verifiable tree canopy cover estimates for use in carbon credit projects and carbon sequestration analyses. It also appears that the very latest versions of two freely available imagery products for the United States, Google Earth imagery and NAIP imagery, should both be adequate for providing estimates of tree canopy cover. Google Earth imagery may be more suitable for this type of analysis in urban areas due to its finer spatial resolution at varying scales. However, in using any composite aerial imagery, one must be aware of the potential for imagery mis-registration issues and feature displacement issues. In general, estimated tree canopy cover using NAIP imagery within ArcGIS and Google Earth imagery are similar when we compared the point-based sampling approach to the plot/grid sampling approach within the two cities of this study.

Protocols and procedures for estimating tree canopy cover from remotely sensed imagery continue to be tested for their usefulness in providing high quality information to support management decisions and policy analyses. The results of this study underline the importance of

selecting resource assessment methods (sampling design, intensity, and frequency) for the development of protocols for urban forest carbon projects. Sampling costs and their relationship to carbon credit prices are essential for the economic feasibility of carbon projects under consideration. While some of the tested procedures may seem to advance our ability to provide more precise and realistic tree canopy cover estimates, given advances in the resolution (spatial and spectral) of remotely sensed imagery, estimates from various sampling approaches seem no better than those provided by point-based sampling, and provide no advantages in terms of time, effort, or reduction in complexity.

Clearly, to have a viable carbon market reliable resource assessment methods are required in order to generate marketable carbon credits and provide assurances that these represent real, meeting specific registry criteria, carbon emission offsets. At the same time, carbon credits have relatively low values. While prices of forest or tree-based carbon credits vary greatly depending on the trading platform and credit attributes the average price of California carbon allowance futures has been in the $12 to 13 per tonne CO_2 equivalent range since mid-2013 (Climate Policy Initiative 2015). Climate Action Reserve carbon offset projects generate values of about $10 per tonne CO_2 equivalent on average (California Carbon 2015). As of May 2015, several *improved forest management* and *reforestation* projects have been registered with the Climate Action Reserve, yet no specific urban forestry projects have been registered, likely because of high project development and implementation costs which include carbon verification and monitoring efforts. Kerchner and Keeton (2015) also noted that high project development and long-term monitoring costs may prevent forest landowners from developing carbon projects.

While recognizing the differences between urban tree resources and forests in rural settings, forest inventories are typically taken at the time of timber sale or purchase and then not

more frequently than every five to ten years during the life of a forest stand (Borders et al. 2008). For example, planted pine stands in the U.S. South may be inventoried twice or three times during their lifetime, at the time of sale and then once or twice during mid-rotation. This sampling intensity is considered by and large as appropriate for the resources of such value. It can also be argued that timber stumpage prices in the U.S. South and carbon offset prices fall into similar ranges. Yet carbon inventories in forestry settings still require higher precision and frequency, and supplementary measurements (Holland 2013), which in turn rise project costs and may yield carbon project infeasible. Therefore, there is a tradeoff between the stringency of project development and implementation rules and the volume of carbon projects that are economically feasible. The challenge is, at least in our minds, to find a balance which would maximize environmental benefits expressed in additional carbon storage and offsets. It may be the case that the current rules may be too restrictive and therefore too expensive (given current carbon offset values), and this may prevent environmentally beneficial projects from being developed. Further research aimed at developing reliable yet cost-effective resource assessment methods may help to address these issues.

Organizations which are taking proactive leadership in the measurement of forest resources for carbon policy implementation should continue to allow their suggested protocols to undergo review. Deferring to the expertise of reviewers allows, in the case of the Urban Forest Management protocol (Nickerson, 2014b), landowners and agencies to select the process that best suits particular conditions. Research results, such as those presented here and elsewhere (e.g., Walton et al., 2008; Merry et al., 2014), provide guidance to others and help advance society's goals of making informed decisions with respect to climate change and carbon management.

Conclusion

The development of an accurate estimate of urban tree canopy cover can be a critical aspect of assessments of the carbon sequestration potential of an urban forest and the ecosystem services potentially provided by an urban forest (Nowak et al., 2008). Besides the more common sampling methods employed (point-based and polygon-based sampling approaches), a cluster sampling method was also proposed (Nickerson, 2014a), whose improvement in accuracy was heretofore unknown. While comparing point-based sampling approach to the plot/grid sampling approach, we found that the estimated tree canopy cover was similar within the two study areas (two medium-sized cities). Though with larger land coverage, the plot/grid sampling approach may represent actual tree cover better than the point-based sampling approach, yet the plot/grid sampling approach requires more time and effort. Like others have suggested, the point-based sampling approach may be the preferred method for assessments of tree canopy cover using remotely sensed imagery, particularly if fewer than 1,000 samples are collected. However, in cities where the average canopy cover is relatively high and the resulting standard error of sampled canopy cover in proportion with the mean canopy cover is relatively low, using Google Earth imagery and a plot/grid sampling approach may require equal or less time than the point-based sampling approach if the stopping point for sampling is determined as the number of samples required for the ±10% range in average canopy cover to equal the 90% confidence interval for canopy cover. However, given a fixed time window within which the assessment must be completed, distributing more points to the point-based approach may reduce the SEs more quickly, and therefore providing greater confidence in the results.

In our study, it also seemed that using different remotely sensed sources may influence the estimates of percentage tree canopy cover under the two different sampling approaches.

While some of the differences are statistically significant, the estimates of tree canopy cover were similar, and one should be comforted in knowing that some of the freely available remotely sensed data (e.g., airborne and satellite imagery) for the United States can provide reliable and repeatable results for purposes such as assessments of urban canopy cover. Remotely sensed imagery can help urban forest managers monitor current tree cover change levels and can facilitate processes that help to sustain desired tree canopy levels (e.g., McPherson et al., 2011), however when used for projects that influence financial outcomes or management policies, an explicit description of the sampling methods and data employed seems paramount.

Funding

This work was supported by the Warnell School of Forestry and Natural Resources at the University of Georgia, the Southern Research Station of the United States Forest Service, and The Republic of Turkey, Ministry of National Education. We are very grateful for the valuable comments provided by the Associate Editor and the anonymous reviewers.

References

Alig, R.J., Plantinga, A.J., Ahn, S.E., and Kline, J.D. (2003). Land use changes involving forestry in the United States: 1951 to 1997, with projections to 2050. General Technical Report PNW-GTR-587. U.S. Department of Agriculture, Forest Service, Pacific Northwest Research Station, Portland, OR.

Borders, B.E., Harrison, W.M., Clutter, M.L., Shiver, B.D., and Souter, R.A. (2008). The value of timber inventory information for management planning. Can. J. For. Res. 38, 2287–2294.

California Carbon. (2015). California Carbon info. http://californiacarbon.info/ (accessed 05/28/2015).

Climate Action Reserve. (2014a). Quantification guidance for use with forest carbon projects, January 21, 2014. Climate Action Reserve, Los Angeles, CA. 29 p.

Climate Action Reserve. (2014b). Summary of comments & responses, draft urban forest project protocol version 2.0. Climate Action Reserve, Los Angeles, CA. 18 p.

Climate Policy Initiative. (2015). California climate dashboard. http://calcarbondash.org/ (accessed 05/28/2015).

Congalton, R.G., and Green K. (2009). Assessing the accuracy of remotely sensed data, principles and practices, second ed. CRC Press, Boca Raton, FL.

ESRI. (2013). ArcGIS. http://www.esri.com/software/arcgis (accessed 09/21/2013).

Google, Inc. (2014). Google Earth (Version 7.1.2.2041). https://www.google.com/earth/ (accessed 12/27/2014).

Holland, K. (2013). A primer on forest carbon projects under California's new offset program. The Forestry Source 18(3): 7.

Irani F.M., and Galvin M.F. (2003). Strategic urban forests assessment: Baltimore, Maryland. Maryland Department of Natural Resources, Annapolis, MD.

Jensen, R., Gatrell, J., Boulton, J., and Harper, B. (2004). Using remote sensing and geographic information systems to study urban quality of life and urban forest amenities. Ecol. Soc. 9(5), 5.

Kerchner, D.C., and Keeton, W.S. (2015). California's regulatory forest carbon market: Viability for northeast landowners. For. Policy Econ. 50, 70–81.

King, K.L., and Locke, D.H. (2013). A comparison of three methods for measuring local urban tree canopy cover. Arboric. Urban For. 39, 62–67.

Levy, P.S., and Lemeshow, S. (1991). Sampling of populations: Methods and applications, second ed. John Wiley & Sons, Inc., New York.

Leuzinger, S., Vogt, R., and Körner, C. (2010). Tree surface temperature in an urban environment. Agric. For. Meteorol. 150, 56–62.

Lillesand, T.M., Kiefer, R.W., and Chipman, J.W. (2004). Remote Sensing and Image Interpretation. Seventh ed. John Wiley and Sons: New York, NY.

Macfie, B.P., and Nufrio, P.M. (2006). Applied statistics for public policy. M.E. Sharpe, Inc., Armonk, NY.

Mackun, P., Wilson, S., Fischetti, T., and Goworowska, J. (2011). Population distribution and change: 2000 to 2010. 2010 census briefs. C2010BR-01. U.S. Department of Commerce, Economics and Statistics Administration, U.S. Census Bureau, Suitland, MD.

McGee, J.A. III, Day, S.D., Wynne, R.H., and White, M.B. (2012). Using geospatial tools to assess the urban tree canopy: Decision support for local governments. J. For. 110, 275–286.

McPherson, E.G., Simpson, J.R., Xiao, Q., and Wu, C. (2011). Million trees Los Angeles canopy cover and benefit assessment. Landsc. Urban Plan. 99, 40–50.

Merry, K., Siry, J., Bettinger, P., and Bowker, J.M. (2014). Urban tree cover change in Detroit and Atlanta, USA, 1951–2010. Cities. 41, 123–131.

Nickerson, J. (2014a). Urban forest project protocol, version 2.0 for public comment, March 21, 2014. Climate Action Reserve, Los Angeles, CA. 58 p.

Nickerson, J. (2014b). Urban forest management project protocol, version 1.0, June 25, 2014. Climate Action Reserve, Los Angeles, CA.

Nowak, D.J. (1993). Historical vegetation change in Oakland and its implications for urban forest management. J. Arboric. 19, 313–319.

Nowak, D.J., Crane, D.E., Stevens, J.C., Hoehn, R.E., Walton, J.T., and Bond, J. (2008). A ground-based method of assessing urban forest structure and ecosystem services. Arboric. Urban For. 34, 347–358.

Nowak, D.J., and Greenfield, E.J. (2012). Tree and impervious cover change in U.S. cities. Urban For. Urban Greening. 11, 21–30.

Nowak, D.J., Rowntree, R.A., McPherson, E.G., Sisinni, S.M., Kerkmann, E.R., and Stevens, J.C. (1996). Measuring and analyzing urban tree cover. Landsc. Urban Plan. 36, 49–57.

Nowak, D.J., Stein, S.M., Randler, P.B., Greenfield, E.J., Comas, S.J., Carr, M.A., and Alig, R.J. (2010). Sustaining America's urban trees and forests. U.S. Department of Agriculture, Forest Service, Northern Research Station, State and Private Forestry, Newtown Square, PA. General Technical Report NRS-62.

Parlin, M., and Mead, M. (2009). Seattle, Washington urban tree canopy analysis: Project report: Looking back and moving forward. NCDC Imaging & Mapping, Colorado Springs, CO.

Richardson, J.J., and Moskal, L.M. (2014). Uncertainty in urban forest canopy assessment: Lessons from Seattle, WA, USA. Urban For. Urban Greening. 13, 152 –157.

Taylor, F. (2014). About Google Earth imagery. Google Earth Blog. http://www.gearthblog.com/blog/archives/2014/04/google-earth-imagery.html (accessed 12/26/2014).

U.S. Department of Agriculture. (2013). Imagery programs, NAIP imagery. U.S. Department of Agriculture, Farm Service Agency, Aerial Photography Field Office, Salt Lake City, UT. http://www.fsa.usda.gov/FSA/apfoapp?area=home&subject=prog&topic=nai (accessed

03/10/2014).

U.S. Census Bureau. (2014). State & County QuickFacts from U.S. Department of Commerce, Census Bureau, Suitland, MD. https://www.quickfacts.census.gov/qfd/states (accessed 12.15.2014).

Walton, J.T., Nowak, D.J., and Greenfield, E.J. (2008). Assessing urban forest canopy cover using airborne or satellite imagery. Arboric. Urban For. 34, 334–340.

CHAPTER 4

ESTIMATION OF URBAN VEGETATION COVER USING MULTISPECTRAL DATA AND LiDAR[3]

[3] Ucar, Z., Merry, K., Bettinger, P., Akbulut, R., Siry, J.

To be submitted to the *Urban Forestry & Urban Greening*, 2017.

Abstract

Urban vegetation are an important resource in built up environments, and estimation of urban canopy cover arising from trees and shrubs is an important metric in assessments of landscape quality. We used an image classification approach to estimate urban vegetation cover from trees and shrubs within two medium-sized cities in the United States. Four-band aerial imagery with 1 m spatial resolution, a vegetation index derived from this imagery, and two LiDAR-derived maps were used to examine the added value of LiDAR for this purpose. The classification results showed that using LiDAR derived data along with multispectral data or LiDAR derived data by itself improve the process of identifying vegetated areas. For Tallahassee, Florida, overall accuracy of six major classes (water, develop, vegetation, bare ground, grass and shadow) ranged from 51.3% to 69.3% among all scenarios. The user's accuracy of vegetation class was 69% when using NAIP imagery only. Adding LiDAR derived data into the classification increased the user's accuracy of vegetation class between 16% and 24%. Aggregating land cover classes into two major classes (vegetation, and non-vegetation) resulted in over 80% overall accuracy and user's accuracy across several scenarios. For Tacoma, Washington, the overall accuracy was between 60.3% and 72.8% for six major land cover classes. Similar to Tallahassee, using NAIP imagery alone produced the lowest user's accuracy of the vegetation class (67%) while LiDAR integrated scenarios resulted in over 80% of user's accuracy of vegetation class. Additionally, the overall accuracy for two major classes (vegetation and non-vegetation) was over 80%. The user's accuracy of the vegetation class using LiDAR integrated data or LiDAR data by itself exceeded 80% while using NAIP imagery alone was

70%. For both cities, estimates of vegetation using NAIP imagery alone were greater than the estimates of vegetation in other scenarios. Our results also suggest that LiDAR-derived information seemed to improve the overall accuracy of the six-class and two-class land cover classification results, when compared to using NAIP imagery alone for this purpose but improvement was not consistently very significant.

Keywords: Supervised classification, canopy cover, LiDAR, urban forestry

Introduction

Urban population growth has had an important impact on land cover change processes around the world (Berland, 2012). Since 1950, the world's urban human population has grown rapidly from 746 million to 3.9 billion (54% of the total world population), partly due to increases in population and partly due to the expansion of the urban land designation. Based on the continuing urbanization and overall growth of the world's population, it is projected that by 2050, 66% of all people will live in urban areas (United Nations, 2015). In the United States, the population increased from 281.4 million to 308.7 million between 2000 and 2010, and over 83% now live in urban areas (Berland, 2012; Mackun et al., 2011). While urbanization facilitates employment and other opportunities, it also increases the need for infrastructure such as educational facilities, health services, roads, and cultural amenities (Berland, 2012; United Nations, 2015), and exerts pressure upon the urban forests (McPherson et al., 2011; Nowak, 1993). For example, many urban areas in the United States were created from landscapes once previously forested; in the 1990s about 0.4 million hectares (ha) of forested land was converted to urban areas through urbanization (Alig et al., 2003).

Urban vegetation refers to all trees and shrubs within an urban area (Berland, 2012; Nowak et al., 2010; Ward and Johnson, 2007), and these structures can represent a significant component of the urban environment. Urban vegetation provides fundamental biophysical and socioeconomic benefits to humans, including recreational opportunities and aesthetic values that improve health, improve overall enjoyment, and increase the value of neighborhoods. Urban vegetation also can reduce energy use, facilitate cooling effects, improve water and air quality, and improve biodiversity (Leuzinger et al., 2010; Mariappan et al., 2015; McGee et al., 2012; Mincey et al., 2013; Myeong et al., 2006; Nowak et al., 2001; Nowak et al., 2008; Pasher et al., 2014; Richardson and Moskal, 2014; Singh et al. 2012; Ucar et al., 2016; Walton et al., 2008). Hence, accurately quantifying urban vegetation cover is crucial for proper management of vegetated areas within a city to help sustain or improve ecosystem services and quality of life (Nowak et al., 2008; Richardson and Moskal, 2014; Walton et al., 2008).

Remote sensing technologies such as aerial photography, satellite imagery, and airborne LiDAR (Light Detection and Ranging) are increasingly used to assess urban vegetation cover. When captured at an appropriate spatial resolution during an appropriate time of year, the use of these technologies can be more cost and time effective than field based inventories of urban vegetation cover (Mariappan et al., 2012; McPherson et al., 2011; Nowak et al., 1996; Singh et al., 2012). For instance, Nowak (1993) conducted a study using panchromatic aerial photographs spanning nearly 50 years to estimate long-term changes of urban forests in Oakland, California. Merry et al. (2014) also used digital aerial photography for a similar long-term change study of urban forests in Detroit and Atlanta, the United States. Nowak and Greenfield (2012) estimated tree cover change in 20 cities in the United States using stereo pairs of aerial photographs.

McGee et al. (2012) also recently estimated urban tree cover in Winchester, Virginia using digital aerial photography.

Aerial photography has a few limitations for these types of assessments that include the amount of ground coverage per image (unless bundled into a composite), the temporal revisiting periods, and the image acquisition cost. For these reason, some land cover change analyses in urban areas have been conducted with satellite imagery (Zhang et al., 2010). While larger areas are typically captured per image and while the temporal revisit period may be shorter, the use of the satellite imagery for urban canopy cover estimation is not without its limitations, as it may lack the spatial detail necessary to identify patchy vegetation cover (Nowak and Greenfield, 2012; Walton et al., 2008; Zhang et al., 2010). However, advances in satellite technology facilitate opportunities to describe urban vegetation cover (Zhang et al., 2010), such as with high spatial and spectral resolution satellite imagery provided through the IKONOS, QuickBird, GeoEye, and Worldview programs. These types of satellite imagery have been used to estimate urban vegetation cover in Seattle, Washington (Parlin and Mead, 2009), Baltimore and Annapolis, Maryland (Galvin et al., 2006; Irani and Galvin 2002), Nanjing City, China (Zhang et al., 2010), Atlanta, Georgia (Goetz et al., 2003), New York City (Bhaskaran et al., 2010), and Phoenix, Arizona (Myint et al., 2011).

More recently, airborne LiDAR (Light Detection and Ranging) technology has been employed for vertical feature description due to its ability to generate 3 dimensional point cloud data. Airborne LiDAR is a laser system that compares travel time differences of laser pulses emitted by an airborne sensor, interacting with earth objects, and returning to the sensor (Jia, 2015; Parmehr et al., 2016; Singh et al., 2012; Yan et al., 2015). In addition to describing the topographic profile of the Earth's surface, LiDAR data can be useful in estimating the urban

vegetation canopy because it can help eliminate the effects of relief displacement and shadows (Yan et al., 2015). Other natural resource applications (estimating forest inventory, deriving leaf area index, assessing tree canopy characteristics, etc.) also can benefit from the information provided by LiDAR data (Parmehr et al., 2016; Singh et al., 2012; Yan et al., 2015). In particular, the LiDAR data can contribute to studies in urban environments, such as estimations of impervious surfaces and assessments of infrastructure and environmental quality (Basgall, 2013; Chen et al., 2012; Hartfield et al., 2011; Jia, 2015; Parmehr et al., 2016), as well as individual tree detection, although it may be limited in cases where trees and shrubs of different crown classes reside due to decreased penetration of LiDAR through the vegetation profile (Hamraz et al., 2017).

One disadvantage of LiDAR data is that it lacks spectral information common to other types of imagery in the visible or near infrared spectrum, which may restrict its usefulness in land cover assessments in urban areas (Singh et al., 2012; Yan et al., 2015). Therefore, studies have been conducted on integrating LiDAR data with aerial or satellite imagery, providing descriptions of both radiometric and geometric data features. Hartfield et al. (2011) assessed the feasibility of combining multispectral aerial imagery and LiDAR-derived height information to improve a land use / land cover classification in Tucson, Arizona. The overall accuracy of a supervised classification process employed, which used only the 4-band multispectral data and Normalized Difference Vegetation Index (NDVI), was 84%. By adding LiDAR-derived height information to the supervised classification process, a 5% increase in classification accuracy was achieved. Singh et al. (2012) used Landsat and LIDAR data to assess large-area urban land cover in North Carolina and found that this increased the overall accuracy by 32% when compared to only using LiDAR, and by 8% when compared to only using Landsat data. Chen et al. (2012)

used NDVI and LiDAR for building detection in an urban area (Nanjing, China), and estimated that the total numbers of buildings in the area, 90% were correctly identified in LiDAR. Moreover, Jia (2015) conducted a study which combined LiDAR data and multispectral data for classification of an urban area in Sweden, and achieved a 95.2% overall accuracy in land cover class estimation, which was 6% higher than when only multispectral data was used, and 6.6% higher than when only LiDAR data were used.

Urban areas include impervious surface features such as buildings and roads, along with bare ground, open areas and vegetation that consist of trees, shrubs and grass. Our interest is in estimating canopy cover provided by urban vegetation (trees and shrubs). Since the use of multispectral data (aerial photography or satellite imagery) itself may not be sufficient for distinguishing heterogeneous land cover in urban areas, and since LiDAR data seem to add value to the classification process, we embarked on a study to utilize both. The objective was to assess whether the addition of the LiDAR data increased the accuracy of urban vegetation cover estimates when using a pixel-based supervised classification method.

Methods

Study Areas

Tallahassee and Tacoma are located in different regions of the United States (Figure 4.1), and contain different forms of vegetation cover. Tallahassee is in the humid, southern part of the United States, where prevalent natural tree species are pines (*Pinus* spp.) and oaks (*Quercus* spp.). Tacoma is in the Pacific Northwest of the United States, where prevalent natural tree species are mainly conifers (Douglas-fir (*Pseudotsuga menzeiesii*) and western hemlock (*Tsuga heterophylla*)). Each city has a variety of trees planted along streets that may not be typical of the area. In addition to their different locations, these two cities were selected based on the temporal

consistency of multispectral U.S. Department of Agriculture National Agricultural Imagery Program (NAIP) and LiDAR data available for this project. Further, each city is comparable in terms of population size; the estimated 2010 human population of Tallahassee (181,376) was similar to that of Tacoma (198,397), and the projected rates of population growth were similar (4.7% in Tallahassee, 4.8% in Tacoma) (U.S. Census Bureau 2010).

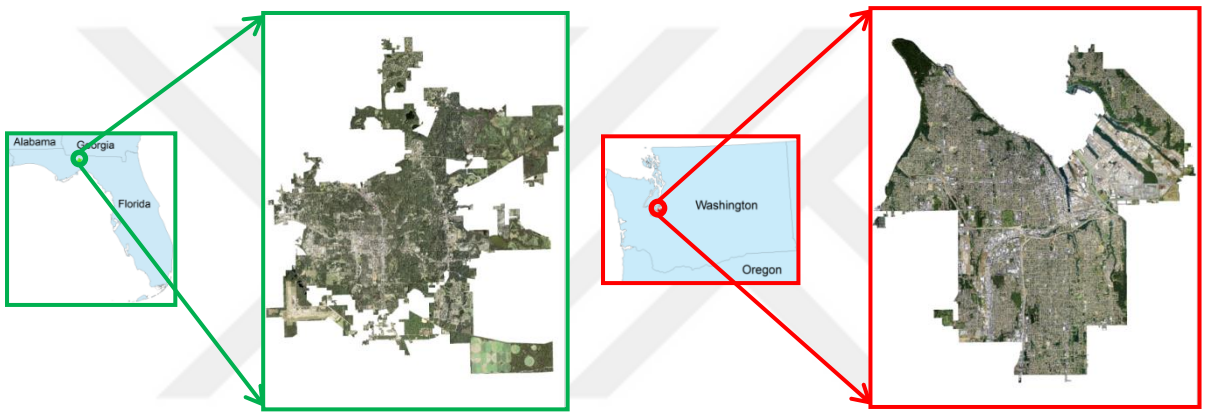

Figure 4.1. Administrative boundaries of (*left*) Tallahassee, and (*right*) Tacoma.

Aerial Imagery

The main goal of the NAIP program is to collect aerial imagery during the agricultural growing season and then provide the public digital, orthorectified photography with a 1 m spatial resolution, within one year of acquisition. NAIP imagery for Tallahassee and Tacoma were obtained from the U.S. Geological Survey (2017) National Map Viewer. Imagery for Tallahassee was captured between July 21, 2010 and October, 21 2010, while imagery for Tacoma was captured between August 26, 2011 and October 7, 2011. These multispectral databases contained reflectance values in four bands (red, green, blue, near infrared). More current NAIP imagery

may have been available at the time of the study, but we wanted the date of the NAIP imagery to coincide as closely as possible with the date of LiDAR data acquisition.

LiDAR Data

For Tallahassee, LiDAR data were commissioned by the Northwest Florida Water Management District for the Leon County in which the city resides. The LiDAR data were captured using a Lecia ALS50 Phase I device, which utilized a pulse rate of 55.4 kHz, a flying height of 1,676.4 m mean sea level (MSL), and a scan rate of 30 Hertz, and a scan angle (scan field of view) of 30°. The LiDAR data were captured between January 31, 2009 and February 6, 2009 and acquired from the National Oceanographic and Atmospheric Administration (2017). Horizontal and vertical control was used to establish positions and elevations for reference and correlation purposes and as input to an aerotriangulation process. Control consisted of Airborne GPS/IMU (Inertial Measurement Unit) and ground control points for ground reference. The LiDAR data set for this study area consisted of 204 tiles, each with dimensions of approximately 1,556 m x 1,556 m and an average point spacing of 1 m.

For Tacoma, LiDAR data were commissioned by Watershed Science, Inc. for Pierce County where Tacoma resides. The LiDAR for Tacoma was captured using a Lecia ALS50 Phase II device, which was utilized with a pulse rate of 83 to 105.9 kHz, a flying height of 900 to 1,300 m above ground level, and a scan angle of 1/3000th of the flying height above ground level. The resulting imagery had a maximum scan angle of approximately 14° from nadir and a side lap of 50%. The LiDAR data were captured between October 19, 2010 and September 6, 2011, and was acquired from the U.S. Geological Survey (2017). Airborne GPS / Inertial Measurement Unit and ground control points for ground reference were used as control points, similar to the horizontal and vertical control of the Tallahassee LiDAR data. The Tacoma study

area was covered by 217 tiles of airborne LiDAR data, each with dimensions of approximately 914.4 m x 914.4 m and an average point spacing of 0.8 m.

Urban Canopy Cover Estimation

For this study, we classified urban vegetation cover in two United States cities (Tallahassee, Florida and Tacoma, Washington) using a supervised maximum likelihood classification method. The data included multispectral aerial imagery with 1 m spatial resolution collected in with 4 spectral bands (red, green, blue, and near infrared) and LiDAR data. The workflow of the methodology to classify urban canopy cover included several steps (Figure 4.2) that involved (1) generating potential presence / absence data for trees and shrubs from LiDAR, (2) creating an impervious surface and water mask using NDVI, (3) performing an accuracy assessment of impervious surface and masked impervious surface data from vegetation presence / absence data, (4) stacking the imagery, (5) developing training areas and performing the supervised classification, and (6) performing an accuracy assessment of the land cover classification. Since the main objective of this research is to determine whether urban canopy cover estimates can be improved by incorporating LiDAR data into the supervised classification process, we used the LiDAR to both mask impervious surface features, such as buildings and roads, from the supervised classification process, and to further separate the classification of features during the supervised classification process.

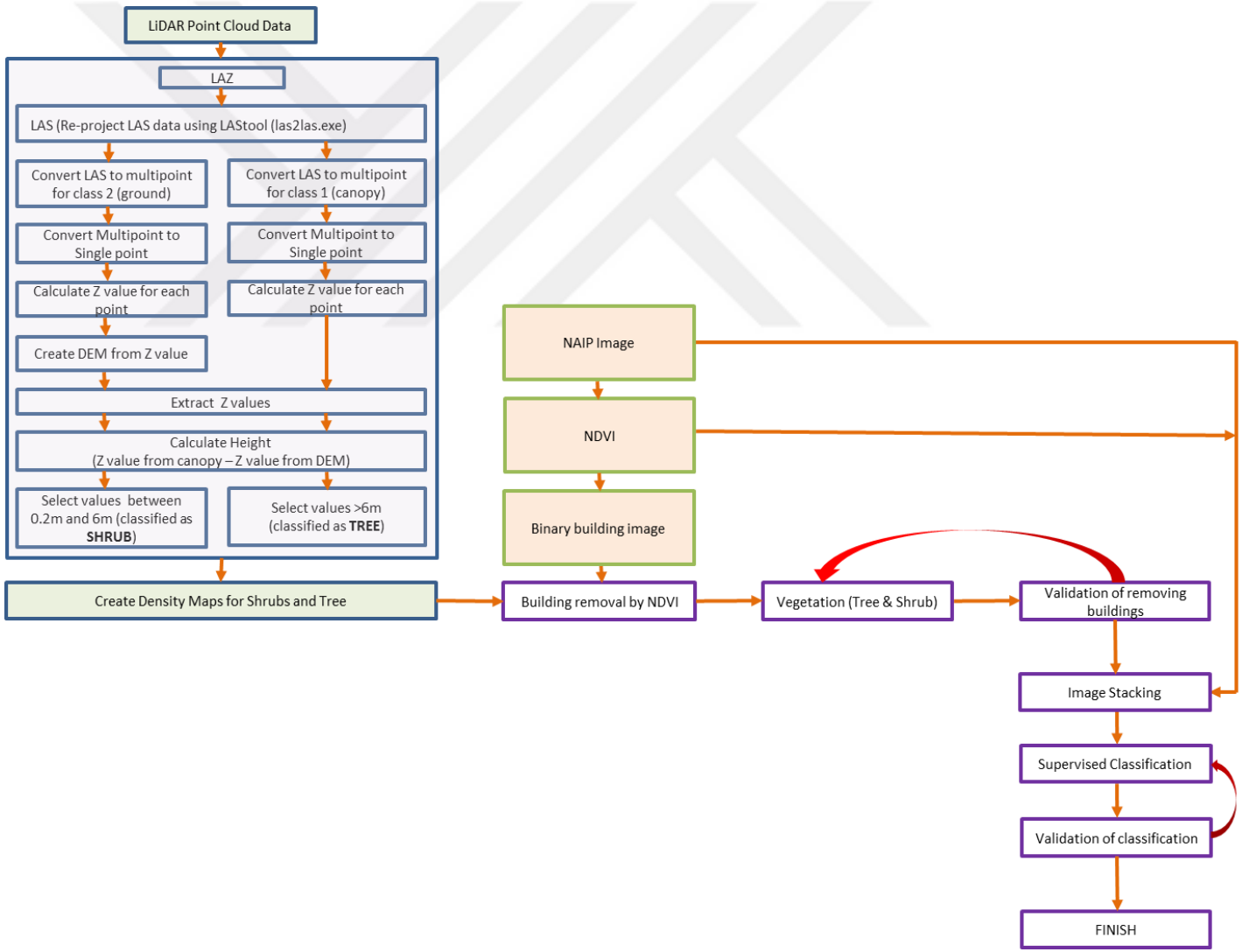

Figure 4.2. Flowchart describing workflow adapted in the study.

Generation of Potential Presence / Absence Data for Trees and Shrubs

In order to incorporate the LiDAR point cloud into the supervised classification process a presence / absence dataset for trees and shrubs was derived. We converted LAS files into two separate point cloud files using ArcGIS 10.4 (ESRI, 2016). The first point cloud file included only those points attributed as *ground* points. These were used to develop a digital elevation model (DEM). The second point cloud file included only those points attributed as *unclassified*. To obtain heights of the above-ground unclassified points, the z-values (elevations) of points from the *ground* point cloud were subtracted from the associated z-values of the *unclassified* point cloud. From here, two new point clouds were extracted from the above-ground set based on two height intervals: (1) points greater than 0.2 m and less than 6 m, and (2) points greater than 6 m. A shrub is defined as natural or semi-natural woody vegetation that are commonly less than 6 m tall (Cowardin et al., 1979). Therefore, the points from the LiDAR dataset that fell between 0.2 and 6 m were classified as shrubs (although it could be smaller trees that with time will exceed this threshold). Points with values below 0.2 m were not included in the shrub point cloud in an effort to eliminate any noise in the LiDAR returns that may exist between the ground-level and above-ground points. Those points from the above-ground LiDAR point cloud with heights greater than 6 m were classified as trees. Using these LiDAR point clouds, two raster datasets were created illustrating the potential presence / absence of trees and the presence / absence of shrubs. The spatial resolution of the LiDAR-derived data was set to 2 m. When we used 1 m as a cell size (similar to average point spacing of LiDAR data in both cities) to match the resolution of the NAIP imagery, the results were too fine and many gaps (NoData) were generated on the surface. The results were visually compared with the NAIP imagery, and the potential presence /

absence of trees and presence / absence of shrubs both seemed to be represented well at a 2 m spatial resolution.

Impervious Surface and Water Mask

NDVI is a commonly used vegetation index for delineating vegetation, water, bare soil, and developed areas (Bandyopadhyay et al., 2013; Chen et al., 2012; Wang et al., 2014). NDVI was calculated for each pixel in the NAIP imagery from the near infrared and red reflectance values, using following formula (Rouse et al., 1974):

$$NDVI = (near\ infrared - red) / (near\ infrared + red) \quad (1)$$

NDVI values ranged from -1 to +1 with higher NDVI values representing large amounts of green vegetation. In general, a threshold value of NDVI for vegetation is 0.2 or greater (Chen et al., 2012; McBride, 2011). However, this threshold value did not clearly distinguish vegetated areas from non-vegetated areas in our study areas when we visually compared the mask to the original NAIP imagery. Therefore, we used a threshold value of 0.1 for non-vegetated areas in this study. Smaller values represented barren rock, soil, roads, buildings, water, shadows, and a minimal amount of short grasses. This impervious surface and water database was then used as a mask to remove land and water areas from the LiDAR derived vegetation presence / absence datasets. This step was necessary following a visual assessment of the above-ground point cloud data because through this assessment, we found that some points fell on roof tops that were not representative of vegetation. Even with the Tacoma LiDAR data, where prior to acquisition the point cloud had been classified to include buildings, a number of points fell on rooftops.

In order to ensure that the impervious surface and water datasets was well-developed, we performed an accuracy assessment using 1,000 impervious surface and water points randomly located within the boundary of each city. This sample size is greater than the minimum samples size of 100 points per each class suggested by Congalton and Green (2009). We used Google Earth images obtained in January 2011 and August 2011 for Tallahassee and Tacoma, respectively, as a reference sources. Sample points were classified as shrub/tree vegetation or other land classes (impervious surface or water). The agreement between the impervious surface and water database and the Google Earth imagery was 92.5% for Tallahassee and 94.7% for Tacoma.

Image Stacking

We used an image stacking process (Figure 4.3) to combine the NAIP imagery (red, green, blue, near infrared), the NDVI derived from the NAIP imagery, and the potential presence / absence of trees and shrubs databases from LiDAR. We created several scenarios that would be subjected to supervised classification of the landscape:

- Scenario 1: NAIP + NDVI + potential presence / absence of trees and shrubs databases at 2 m resolution
- Scenario 2: NAIP + potential presence / absence of trees and shrubs databases at 2 m resolution
- Scenario 3: NDVI + potential presence / absence of trees and shrubs databases at 2 m resolution
- Scenario 4: NAIP imagery at 1 m resolution
- Scenario 5: Potential presence / absence of trees and shrubs databases vegetation at 2 m resolution

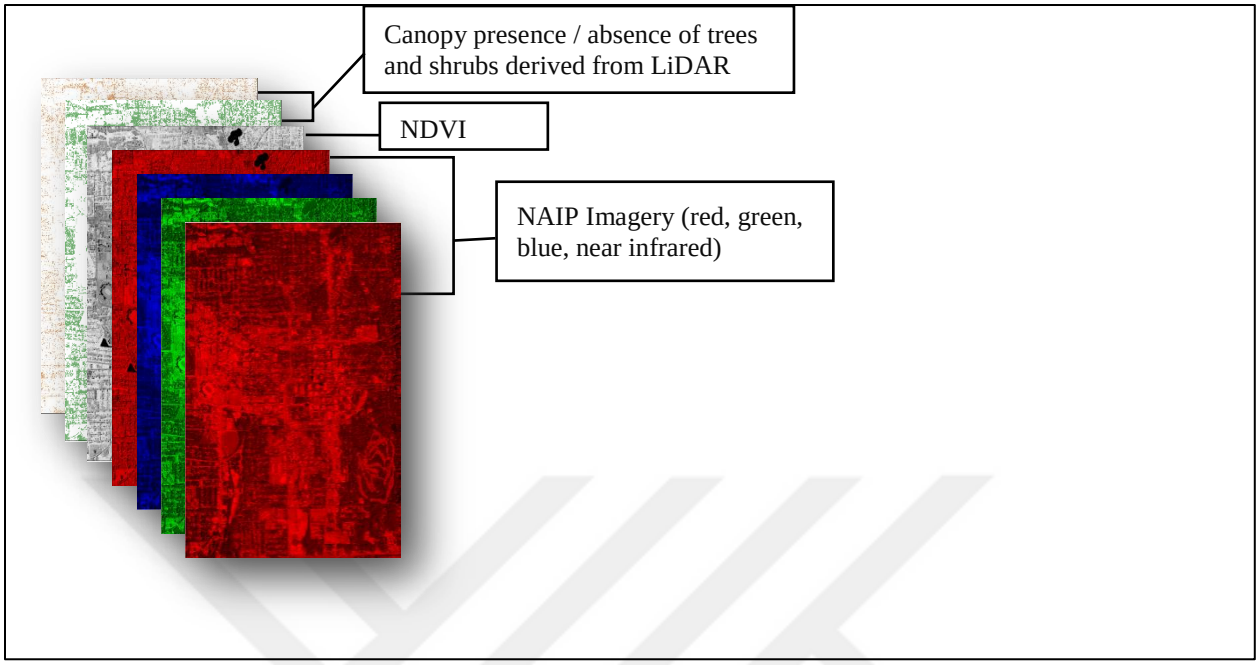

Figure 4.3. Conceptual model of the stacked images.

Supervised Classification Process

Based on landscape characteristics of our two study areas, we identified six major land cover classes: water, developed (buildings, roads, parking lots, etc.), vegetation (trees and shrubs), bare ground / soil, grasses, and shadows. We used a supervised maximum likelihood classifier process, which is a common pixel-based method for classifying a landscape (Bhaskaran et al., 2010; Campbell and Wynne, 2011). Given spectral heterogeneity in the major classes, several subclasses were developed (Table 4.1). A total of 940 training sets were developed for each city (24 subclasses × 40 training sets per subclass). Congalton (1991) suggested the appropriate number of training sets should be between 30 (as an absolute minimum) and 50. Our training sets for each subclass exceeds the minimum requirement, yet we could not develop 50 due to lack of sample areas for some subclasses. The minimum size of the training sets was 25 pixels; Campbell and Wynne (2011) recommended these should be between 10 and 40 pixels.

Table 4.1. Classification schemes for major classes and subclasses in the two study areas.

Major class	Tallahassee	Tacoma
Water (all water bodies)	4 subclasses: black; brown; light green; and green.	4 subclasses: light green; black/darkest blue; dark blue and green; and green.
Developed (buildings and roads)	5 building subclasses: purple; white; red/brown; dark gray; and light gray/metallic roof tops.	7 building subclasses: white; gray; light gray; black/darker smoke; brick red; brown; and yellowish brown roof tops.
	3 road subclasses: dark brown parking lots and weathered asphalt; light gray/ white concrete, overpasses, and medians, and limestone-surfaced roads; and lighter gray asphalt.	3 road subclasses: dark brown parking lots and weathered asphalt; light gray/ white concrete, overpasses, and medians, and limestone-surfaced roads; and lighter grey asphalt.
Vegetation (trees and shrubs)	4 tree subclasses: light green canopy representing young pine; dark green canopy representing older pine; two hardwood classes.	2 tree subclasses: light green canopy representing mostly hardwoods and young trees; and dark green canopy representing mostly evergreen and older trees.
	1 shrub subclass: small bushy vegetation mainly in yards and developed areas.	1 shrub subclass: small bushy vegetation mainly in yards and developed areas.
Bare ground	2 subclasses: areas of clayey soils, both natural and man-made (e.g., infields of baseball fields); sandy areas that were natural and man-made (e.g., sand traps on golf courses), and some recently plowed fields.	2 subclasses: representing areas of silt loam soils, both natural and man-made; glacial till and alluvium areas that were natural and man-made (e.g., sand traps on golf courses and infields of baseball fields).
Grass	4 subclasses: agricultural fields brown in color (dead vegetation); agricultural fields yellow or light brown in color; areas otherwise containing green and dark green vegetation; wet agricultural fields, wet grassy areas, non-grazed fields, medians, and recent clearcuts.	3 subclasses: dead vegetation areas yellow in color found along roads and in yards; dead vegetation areas brown in color found along roads and in yards; and areas otherwise containing green vegetation such as wet grassy areas, non-grazed fields, medians, and golf courses.
Shadows	1 class: edges along trees and buildings.	1 subclass: edges along trees and buildings.

They pointed out the importance of the training set size, noting that sets should include enough pixels for trustworthy assessments of the spectral characteristic of each class. With a minimum of 25 pixels in each training set, we provide a sufficient training set size for each subclass.

Training sets were selected so that pixel groupings were as homogeneous as possible in order to successfully represent each subclass (Bhaskaran et al., 2010; Campbell and Wynne, 2011). However, some classes might have variability in their spectral reflectance values (i.e., agricultural areas, developed areas). Hence, it is important to have a wide variety of training sets within each subclass in order to fully represent the landscape. While delineating the training sets, we used the Scenario 1 composite image as our base map.

To execute the supervised classification, we created a signature file for each composite image using the training sets. The results of the supervised classification using the 24 subclasses were then aggregated into six major land cover classes (water, developed, vegetation, bare ground, grass, and shadows). In addition, the results were aggregated further into non-vegetated (water, grass, developed, shadow, and bare ground) and vegetated (tree and shrub) classes since our original objective was to identify the urban vegetation cover.

Accuracy Assessment

As Congalton and Green (2009) suggested, one-hundred points were generated for each major class using an equalized stratified random sampling strategy in order to assess the accuracy of the supervised classification. We used different sets of randomly generated validation points for each scenario's land cover classification, to avoid any bias during decision making. As ground reference data, the NAIP imagery, temporally consistent with the study time frame, was used. On the rare occasion that the NAIP imagery was difficult to interpret, Google Earth imagery was referenced. An error matrix, which provides data on the comparison between

the land class assigned to each validation point and classification of that point through the supervised classification process (Congalton, 2001) was created, and indicates where confusion occurred between classes (Campbell and Wynne, 2011). The error matrix provided descriptive (user's and producer's accuracy, overall accuracy) and analytical (Kappa analysis) statistical summaries related to the ability of the process to assign land classes to the landscape. Overall accuracy is the simplest and most commonly used descriptive statistic for accuracy assessment (Campbell and Wynne, 2011; Congalton, 2001); it describes the proportion of correctly classified samples in the imagery by dividing the total number of correct sample (sum of the diagonal entries) by the total number of samples (Campbell and Wynne, 2011; Congalton, 1991; Congalton, 2001). The user's accuracy measures error of commission, and represents how well a pixel classified as a certain land cover type in land cover type matches the land cover type on the ground. It is calculated by dividing the total number of correctly classified sample points in a class by the total number of samples in that class. Producer's accuracy or omission error, measures how well a land cover class can be assigned to the landscape. It is computed by dividing number of correctly classified sample points in a class by the total number of sample points in that class (Congalton, 1991; Congalton, 2001; Jia, 2015; Peacock, 2014). The Kappa statistic represents the difference between actual agreement, and the agreement potentially obtained by chance. A Kappa value ranges between 0 and 1 with higher values indicating high levels of agreement (Campbell and Wynne, 2011; Congalton, 1991; Foody, 2002; Gómez and Montero, 2011; Jia 2015; Lo and Choi, 2004; Peacock, 2014; Yuan et al., 2005).

In this study, our objective was to obtain an overall accuracy of 70%, with no major class less than 70% user's and producer's accuracy. In particular, we focused on the accuracy of the vegetation class since this was the class of most interest to our work. Our threshold value for

accuracy assessment does not meet the minimum acceptable standard value (85%) for classification accuracy that was suggested by others (Anderson et al. 1976; Thomlinson et al. 1999), yet these standard minimum values may not be achievable in practice. The classification accuracy can be affected by factors such as characteristics of the remotely sensed data (e.g., spatial and spectral resolution), the classification method employed, the training sets constructed, and the validation scheme used (Kralova, 2013). For example, McBride (2011) using NAIP imagery for land cover classification in the Chicago area, found a wide range of overall accuracy, and noted that overall accuracy over 85% may be possible, yet could fall short of 80% depending on the situation. Myint et al. (2010) also compared two classification methods (per-pixel vs object based classification) using QuickBird imagery, and found that overall accuracy was about 68% for per-pixel classification (our method), and about 90% for object-based classification.

Results

Tallahassee, FL

In estimating the six major land classes in Tallahassee (Table 4.2), Scenario 1 had the highest overall accuracy (69.8%) and Kappa statistic (63.8%). This is below our 70% threshold value. However, the user's accuracy (90%) and producer's accuracy (87%) of the vegetation class were both well above our threshold. In Scenario 1 there was significant confusion between the water and shadow classes, and the bare ground and developed classes. This was expected due to the similar spectral reflectance values between dark water bodies in Tallahassee and the numerous shadows across the image. Likewise, the bare ground class (sandy soils) shared similar spectral reflectance values as some developed areas (concrete), which affected overall accuracy.

The overall classification accuracy of Scenario 2 was comparable but slightly less (67.7%) than Scenario 1, however the highest user's accuracy of the tree and shrub vegetation class (93%) was found here. On the other hand, the producer's accuracy of the vegetation class dropped to 74%. In this scenario, tree and shrub vegetation was more frequently confused with the grass class than it was in Scenario 1. And similar to Scenario 1, there was significant confusion between water and shadows, and bare ground and developed areas.

The lowest overall accuracy (51.3%) and Kappa (41.6%) were found in Scenario 3 which involved NDVI and LiDAR-derived vegetation data. Although the user's accuracy for the vegetation class was over 80%, there was a significant decline in the producer's accuracy of vegetation class (50%). This is likely due to confusion between vegetation and three other classes: water, developed, and shadows. The user's accuracy for the water and bare ground classes was 27% and 24%, respectively, which was also a marked decrease from other scenarios. Classification confusion for the water class most often occurred between the shadow, grass, and vegetation classes, while the bare ground class was often confused with developed areas.

In Scenario 4 (NAIP imagery only) the classification produced almost the same overall accuracy (69.3%) and Kappa statistic (63.2%) as Scenario 1. On the other hand, the lowest user's accuracy for vegetation class (69%) occurred in this scenario. Therefore, when using NAIP imagery by itself, other major classes were better identified to the detriment of the vegetation class.

Table 4.2. Classification matrices for four scenarios and six major land classes, Tallahassee.

	Reference								
Scenario 1	Water	Developed	Vegetation	Bare ground	Grass	Shadow	Total	UA (%)	PA (%)
Water	41	2	0	0	1	56	100	41.0	100.0
Developed	0	75	1	1	1	22	100	75.0	59.1
Vegetation	0	0	90	0	2	8	100	90.0	86.5
Bare ground	0	45	0	35	16	4	100	35.0	92.1
Grass	0	5	8	2	83	2	100	83.0	80.6
Shadow	0	0	5	0	0	95	100	95.0	50.8
Total	41	127	104	38	103	187	600		

Overall accuracy = 69.8%; Kappa statistic = 63.8%

Scenario 2	Water	Developed	Vegetation	Bare ground	Grass	Shadow	Total	UA (%)	PA (%)
Water	35	3	1	1	1	59	100	35.0	100.0
Developed	0	77	2	3	3	15	100	77.0	67.5
Vegetation	0	0	93	0	2	5	100	93.0	74.4
Bare ground	0	30	7	37	11	15	100	37.0	82.2
Grass	0	3	17	4	70	6	100	70.0	80.5
Shadow	0	1	5	0	0	94	100	94.0	48.5
Total	35	114	125	45	87	194	600		

Overall accuracy = 67.7%; Kappa statistic = 61.2%

Scenario 3	Water	Developed	Vegetation	Bare ground	Grass	Shadow	Total	UA (%)	PA (%)
Water	27	7	30	0	11	25	100	27.0	93.1
Developed	1	41	16	1	24	17	100	41.0	36.9
Vegetation	0	1	85	0	8	6	100	85.0	50.0
Bare ground	0	52	3	24	8	13	100	24.0	77.4
Grass	1	6	5	6	70	12	100	70.0	56.0
Shadow	0	4	31	0	4	61	100	61.0	45.5
Total	29	111	170	31	125	134	600		

Overall accuracy = 51.3%; Kappa statistic = 41.6%

Scenario 4	Water	Developed	Vegetation	Bare ground	Grass	Shadow	Total	UA (%)	PA (%)
Water	62	6	0	0	0	32	100	62.0	91.2
Developed	3	82	1	6	1	7	100	82.0	56.6
Vegetation	0	1	69	0	18	12	100	69.0	80.2
Bare ground	0	45	0	46	9	0	100	46.0	70.8
Grass	0	10	14	13	63	0	100	63.0	69.2
Shadow	3	1	2	0	0	94	100	94.0	64.8
Total	68	145	86	65	91	145	600		

Overall accuracy = 69.3%; Kappa statistic = 63.2%

UA = User's accuracy
PA = Producer's accuracy

We compared the area estimates for each major land cover class resulting from each scenario. The area of the vegetation class (Figure 4.4) was consistent and comparable between Scenarios 2 (42%) and 3 (42%), while the vegetation class in Scenario 1 was 4% greater. Scenario 4, using only NAIP imagery, estimated that 53% of Tallahassee was classified as vegetation. Scenario 3 estimated the greatest amount of developed areas (29%).

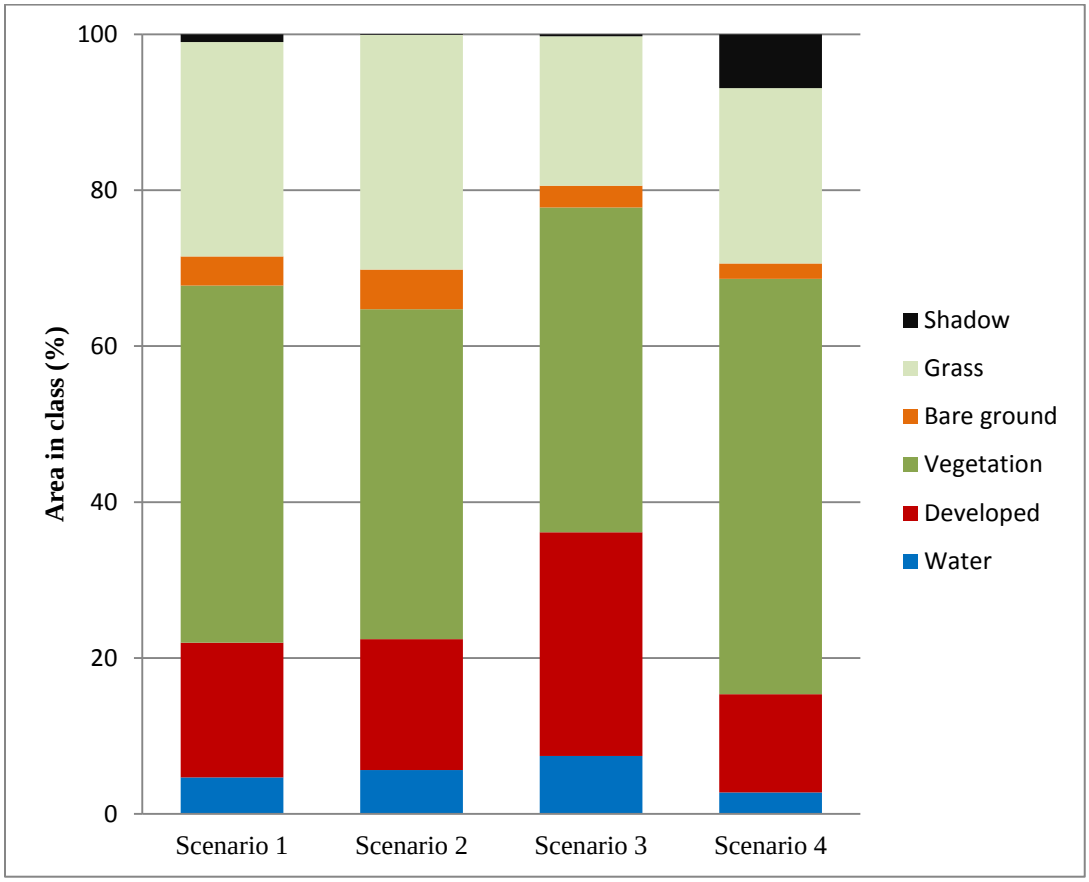

Figure 4.4. Percent area of the major land classes, Tallahassee.

Estimates of the developed class using NAIP imagery only (Scenario 4) produced 1,264.8 ha, 1,118.3 ha, and 4,309.7 ha less area than estimates of developed class in Scenario 1, 2 and 3, respectively (Table 4.3). The percentage area coverage of the water class within four scenarios

suggested similar relative results to the developed class, with the highest value (7%) from Scenario 3 and the lowest value (3%) from Scenario 4. The estimated area of bare ground ranged from 2 to 5% of the city. Area in the shadow class in Scenario 4 was greater than Scenarios 1-3, indicating that the LiDAR derived data and NDVI helped to minimize this.

Table 4.3. Difference in land cover between LiDAR-related scenarios (1-3) and using NAIP imagery only (Scenario 4), Tallahassee.

Land cover class	Scenario 1 - Scenario 4 (ha)	Scenario 2 - Scenario 4 (ha)	Scenario 3 - Scenario 4 (ha)
Water	513.5	773.1	1,252.2
Developed	1,264.8	1,118.3	4,309.7
Vegetation	-2,017.3	-2,944.7	-3,130.5
Bare ground	477.0	833.5	223.0
Grass	1,343.2	2,043.5	-892.9
Shadow	-1,588.3	-1,830.9	-1,783.2
Total	-7.1	-7.1	-21.7

When only two classes were estimated (vegetated and non-vegetated), overall classification accuracy was over 80.0% in all five scenarios (Table 4.4). This value is greater than our minimum acceptable classification accuracy of 70.0%. The highest overall classification accuracy (88.0%) and Kappa statistic (76.0%) was produced by Scenario 5, which included only LiDAR-derived data. Also, the user’s accuracy of the vegetation class in Scenario 5 was 95.0%, which was significantly higher than using only NAIP imagery (Scenario 4) or when combining LiDAR-derived data with multispectral data (Scenarios 1-3). Similar overall accuracy measurements were found in Scenario 2 and Scenario 4. Scenario 3 had a relatively high overall accuracy (87%), and the highest producer's accuracy for the trees and shrubs.

Table 4.4. Classification matrices for two major land classes, Tallahassee.

	Scenario 1		Scenario 2		Scenario 3		Scenario 4		Scenario 5	
Classes	UA (%)	PA (%)	UA (%)	PA (%)	UA (%)	PA (%)	UA (%)	PA (%)	UA (%)	PA (%)
Non-vegetation	85.0	83.3	81.0	81.0	87.0	87.0	92.0	76.0	81.0	94.2
Vegetation	83.0	84.7	81.0	81.0	87.0	87.0	71.0	89.9	95.0	83.3
Overall accuracy (%)	84.0		81.0		87.0		81.5		88.0	
Kappa statistic (%)	68.0		62.0		74.0		63.0		76.0	

UA = User's accuracy
PA = Producer's accuracy

In terms of estimating the percentage of urban canopy vegetation area (Figure 4.5), Scenario 5 (41.9% of the city), was not significantly different than the percentage of vegetated area in Scenario 1 (41.3%), 2 (42.3%), and 3 (41.7%). Though the estimated vegetation area in Scenario 4 was higher (53.3%), spectral similarities between grasses and trees / shrubs caused misclassification that resulted in an overestimation of the vegetation class.

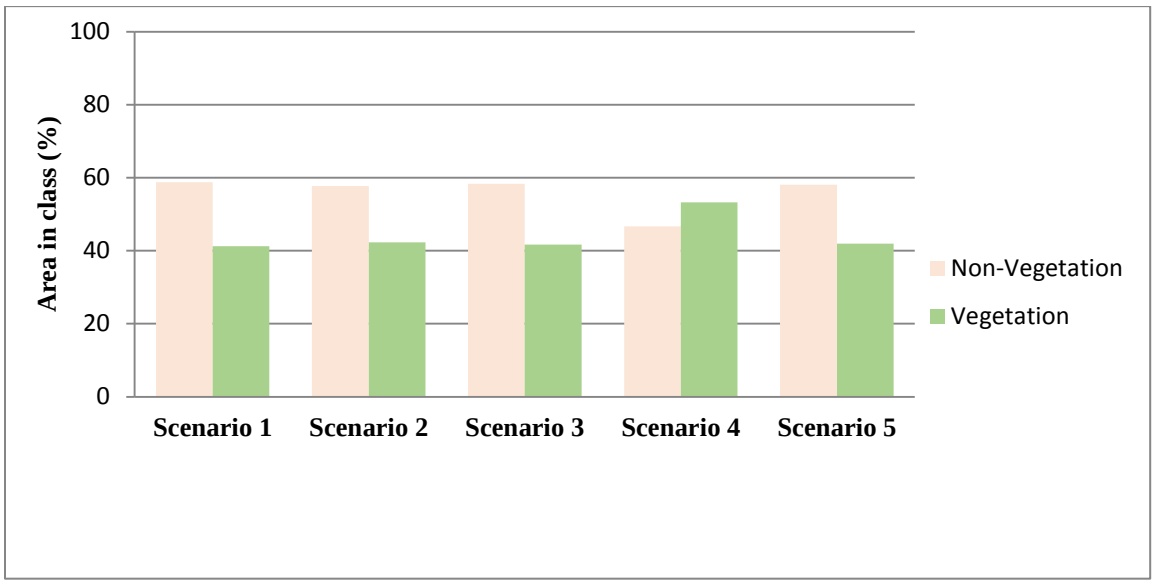

Figure 4.5. Comparison of land area estimated using the classification scenarios, Tallahassee.

Tacoma, WA

Scenario 1 had an overall accuracy of 70.5% and Kappa statistic of 64.6% (Table 4.5). The user's accuracy for tree and shrub vegetation was 86%, while the producer's accuracy was 75%. Confusion between the bare ground and developed classes led to a low user's accuracy of 8% for the bare ground class. Further, except for the developed and shadow classes, the producer's accuracy for other major classes was over 70 percent. Scenario 2's overall accuracy (72.0%) and Kappa statistic (66.4%) were higher, and Scenario 2 produced the highest user's accuracy (87%) for the vegetation and developed classes among all scenarios. However, the user's accuracy of the bare ground class was again 8% due to confusion with the developed class. In addition to developed and shadow classes, the producer's accuracy of the bare ground class was below 70%.

Scenario 3 had the lowest overall accuracy (60.3%) and Kappa statistic (52.4%) of the four scenarios. The user's accuracy of the vegetation class (85%) was similar to that of the vegetation class accuracy in Scenario 1 and 2. Again, there was confusion between the bare ground class and the developed class. The user's accuracy of the bare ground class did increase to 13%. However, the user's accuracy of water, developed, grass and shadow classes decreased when compared to Scenarios 1 and 2. The producer's accuracy was only over 70% for the water and tree / shrub vegetation classes.

Scenario 4 resulted in the best overall accuracy (72.8%) and Kappa statistic (67.4%). The user's accuracy of the vegetation class was lower (67%), with confusion occurring between the vegetation, grass and shadow classes. Scenario 4 had relatively high user's accuracy for the water, grass, shadow, and bare ground classes compared to the other Scenarios.

Table 4.5. Classification matrices for four scenarios and six major land classes, Tacoma.

	Reference								
Scenario 1	Water	Developed	Vegetation	Bare ground	Grass	Shadow	Total	UA (%)	PA (%)
Water	79	0	0	0	0	21	100	79.0	90.8
Developed	6	92	0	0	0	2	100	92.0	53.8
Vegetation	0	2	86	0	4	8	100	86.0	75.4
Bare ground	0	70	3	8	14	5	100	8.0	72.7
Grass	0	6	12	3	77	2	100	77.0	78.6
Shadow	2	1	13	0	3	81	100	81.0	68.1
Total	87	171	114	11	98	119	600		

Overall accuracy = 70.5%; Kappa statistic = 64.6%

Scenario 2	Water	Developed	Vegetation	Bare ground	Grass	Shadow	Total	UA (%)	PA (%)
Water	88	0	0	0	0	12	100	88.0	100.0
Developed	0	93	0	4	0	3	100	93.0	57.4
Vegetation	0	0	87	0	0	13	100	87.0	75.7
Bare ground	0	57	4	8	20	11	100	8.0	57.1
Grass	0	11	12	2	69	6	100	69.0	77.5
Shadow	0	1	12	0	0	87	100	87.0	65.9
Total	88	162	115	14	89	132	600		

Overall accuracy = 72.0%; Kappa statistic = 66.4%

Scenario 3	Water	Developed	Vegetation	Bare ground	Grass	Shadow	Total	UA (%)	PA (%)
Water	72	7	0	2	0	19	100	72.0	100.0
Developed	0	77	0	4	15	4	100	77.0	46.4
Vegetation	0	1	85	0	0	14	100	85.0	73.3
Bare ground	0	34	10	13	31	12	100	13.0	46.4
Grass	0	28	0	8	58	6	100	58.0	54.7
Shadow	0	19	21	1	2	57	100	57.0	50.9
Total	72	166	116	28	106	112	600		

Overall accuracy = 60.3%; Kappa statistic = 52.4%

Scenario 4	Water	Developed	Vegetation	Bare ground	Grass	Shadow	Total	UA (%)	PA (%)
Water	95	0	0	0	0	5	100	95.0	96.0
Developed	1	91	0	3	4	1	100	91.0	55.2
Vegetation	0	0	67	0	16	17	100	67.0	85.9
Bare ground	0	60	2	16	20	2	100	16.0	66.7
Grass	0	7	9	4	79	1	100	79.0	66.4
Shadow	3	7	0	1	0	89	100	89.0	77.4
Total	99	165	78	24	119	115	600		

Overall accuracy = 72.8%; Kappa statistic = 67.4%

UA = User's accuracy
PA = Producer's accuracy

Scenario 4, using only NAIP imagery, produced the highest estimates of tree and shrub vegetation (20%) (Figure 4.6). The greatest amount of developed areas was estimated in Scenario 3 (43%). The estimated area of the water class in Scenarios 1-3 was 3%, 1% greater than the estimated area of water class in Scenario 4. Scenario 4 produced the lowest estimated area of bare ground (20%) and the highest estimated area of the shadow class (5%). The difference in bare ground area between Scenario 2 and Scenario 4 (NAIP only) was relatively high (Table 6).

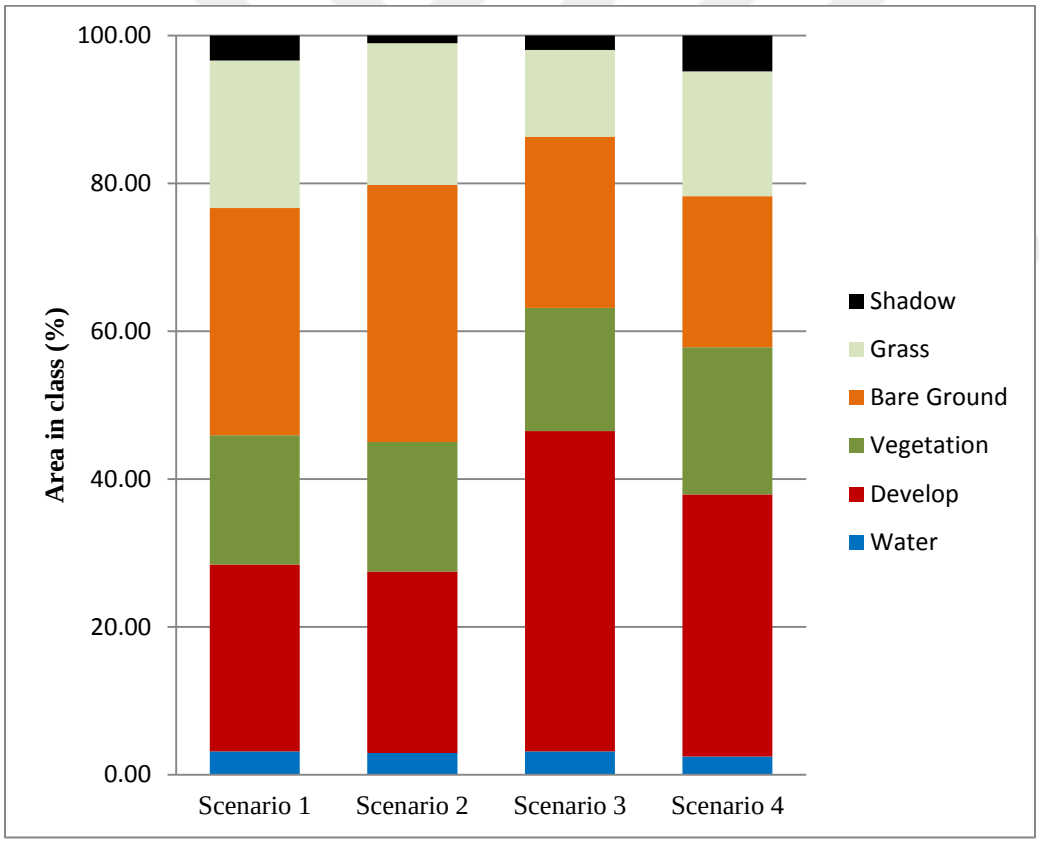

Figure 4.6. Percent area of the major land classes, Tacoma.

Table 4.6. Area difference of land cover between using LiDAR integrated data (Scenario 1, 2, and 3) and using NAIP imagery only (Scenario 4) into the classification, Tacoma.

Land cover class	Scenario 1 – Scenario 4 (ha)	Scenario 2 – Scenario 4 (ha)	Scenario 3 – Scenario 4 (ha)
Water	89.3	58.0	87.4
Developed	-1347.3	-1445.2	1051.0
Vegetation	-324.9	-315.1	-424.7
Bare ground	1365.8	1904.1	355.7
Grass	413.7	307.5	-683.0
Shadow	-195.4	-508.1	-385.1
Total	1.3	1.3	1.3

The results of overall accuracy by using a two-class classification for Tacoma (Table 4.7) were similar to the results of overall accuracy from Tallahassee. The overall accuracy was over 80% within all five scenarios as well. The best overall classification accuracy, produced by Scenarios 2 and 3, was 90.5% with Kappa statistic of 80.1%. The overall accuracy of Scenario 5 was only 1% less than the best overall accuracy. Also, Scenario 1 resulted in 88.5% overall accuracy with Kappa statistic of 77.0%. However, Scenario 4 resulted in lowest overall accuracy (83.0%) and Kappa statistic (66.0%). The accuracy of the vegetation classes among the scenarios was related to overall accuracy as well. While comparing area coverage of the vegetation classes (Figure 4.7), it can be seen that vegetated area in scenario 4 was about 20% greater than the vegetated area among scenarios that integrated LiDAR data into the classification.

Table 4.7. The summarized accuracy of two classes among five scenarios with Kappa statistic, Tacoma, WA

	Scenario 1		Scenario 2		Scenario 3		Scenario 4		Scenario 5	
Classes	UA (%)	PA (%)	UA (%)	PA (%)	UA (%)	PA (%)	UA (%)	PA (%)	UA (%)	PA (%)
Non-vegetation	96.0	83.5	96.0	86.5	97.0	85.8	96.0	76.2	95.0	85.6
Vegetation	81.0	95.3	85.0	95.5	84.0	96.6	70.0	94.6	84.0	94.4
Overall accuracy (%)	88.5		90.5		90.5		83.0		89.5	
Kappa statistic (%)	77.0		81.0		81.0		66.0		79.0	

UA = user's accuracy
PA = producer's accuracy

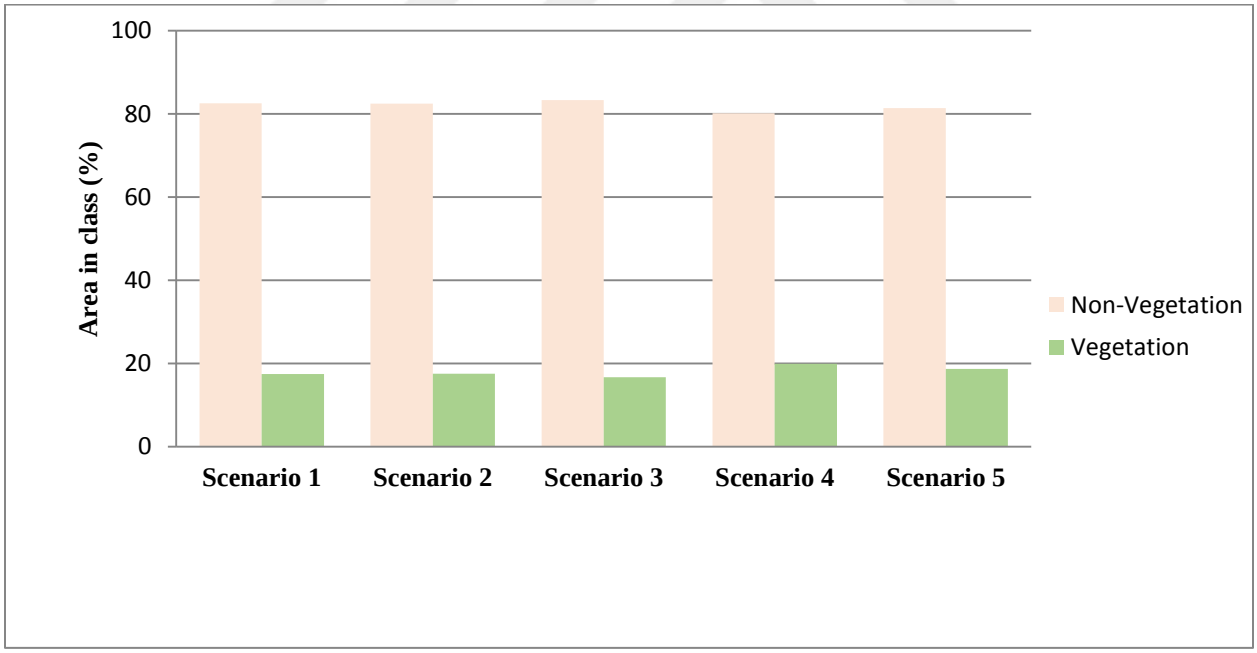

Figure 4.7. Comparison of land area estimated using the classification scenarios, Tacoma.

Discussion

The quality of outcomes from a supervised classification can be affected by a number of factors, including spatial resolution of the imagery, topographic displacement inherent in the imagery given characteristics of the landscape and flight mission (focal length, flying height), shadows, tone and texture issues along edges of individual image frames within a composite, classification method (i.e., pixel based or object-based classification), training dataset quality and extent, and classification scheme (number of classes and subclasses) (Alpin et al., 1999; Kralova, 2013). Several of these may have affected our results. For example, we noticed some tone and texture issues along edges of individual frames within the NAIP mosaic for each of the counties within which the cities reside. These issues were not adjusted or smoothed prior to the supervised classification process. Further, our classification method (6 major classes, 24 subclasses) was necessary given that a single major class (e.g., water) could have contained landscape features that had several different spectral reflectance ranges. Water areas (ponds, lakes, pools, etc.) in Tallahassee, for example, ranged from black to blue. At the onset of the project, we created four subclasses with sufficient number of training areas for this major class, and found that the results of supervised classification were very poor due to the wide range of spectral values that represented water. Shadows were somewhat of a problem, as was found in other work that classified NAIP 1 m spatial resolution imagery (Merry et al., 2014). The addition of LiDAR-derived information seemed to improve the overall accuracy in Tallahassee, but with respect to this metric and the estimation of six major classes, using NAIP alone seemed sufficient (albeit with the area estimation problem noted above). However, by adding LiDAR-derived vegetation presence / absence data to supervised classification, the user's accuracy (how well validation pixels classified as vegetation matched the vegetation land cover type on the ground) of the

vegetation class (trees and shrubs) increased even though the producer's accuracy (how well the vegetation cover types were assigned to the landscape) decreased.

Based on visual assessment and error matrices, it can be clearly seen that confusion between water and shadow class was the main issue in Tallahassee when compared to Tacoma (Figure 4.8). The vegetation class was more commonly confused with the shadow class in Tacoma than Tallahassee. There were likely differences between the two cities in terms of the time of day of imagery acquisition, atmospheric conditions, and shapes and sizes of trees and buildings, and natural colors of dominant vegetation. These situations can affect the reflectance values of vegetation canopy and areas around the vegetation canopy, thus vegetation can often be misclassified as shadow and vice versa (Goetz et al., 2003; Merry et al., 2013). In addition, due to similarities between reflectance values of dark building roof tops and shadows, the developed class sometimes was confused with the shadow class. Contrary to our expectations, LiDAR integrated scenarios could not eliminate shadow effects; using only NAIP imagery (Scenario 4) seemed to determine shadow classes better and promoted less confusion of these with other classes.

Moreover, using high spatial resolution imagery for the urban land cover classification helps to recognize the detail in complex urban environment where discrete and continuous features are found together (Alpin, 2003; Lo and Choi, 2004). However, the high spatial resolution imagery reduces mixed pixels that increase spectral variability within-and-between classes. Thus, many different land cover in urban environments might be represented with same or similar spectral value (e.g., white roof tops, bright sandy soil, cement roads, dirty brown soil, and red brick roof top, water, shadow).

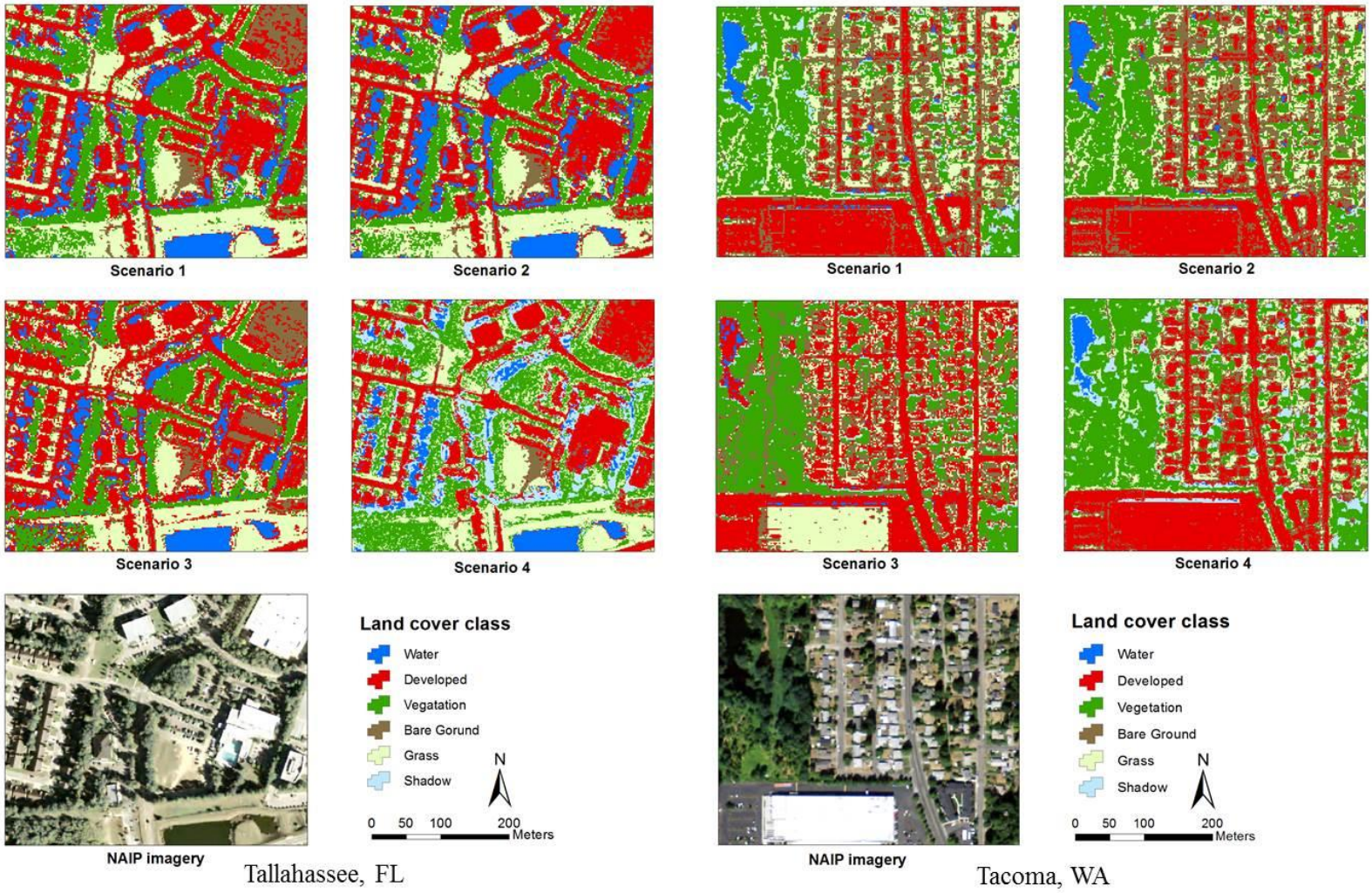

Figure 4.8. An example of classification results for six major classes (*left*) Tallahassee, and (*right*) Tacoma.

This can lead to misclassification problems in pixel-based classification methods, which use only spectral information (pixel value), and do not consider spatial information between groups of pixels (Bhaskaran et al., 2010; Alpin et al., 2003; Lo and Choi, 2004; Myint et al., 2011), even if sufficient number of training datasets were created to represent each major class. Additional research using different classification methods (e.g., per-field classification, object-based classification) might be useful to reduce the confusion between the classes, and increase the overall accuracy of the classification.

Within these urban environments, there was a significant collection of heterogeneous, man-made features. In a more natural environment, the results of supervised classification may be of higher quality. When we reduced the classification to two simple classes, vegetated (trees and shrubs) and non-vegetated (all other classes), our results suggest that using LiDAR-derived information alone (Scenario 5) could provide results of comparable quality to the other scenarios. Overall accuracy, user's accuracy, and producer's accuracy were all very high (85% or greater) in these cases. If our goal was to simply delineate the urban canopy cover in this manner (two classes), either using LiDAR-derived data alone or combining it with NDVI or basic four-band NAIP imagery would seem to be sufficient. At the two-class level, however, using NAIP imagery alone produced results lower in quality than the other scenarios. Therefore, the structural information provided by the LiDAR data was of value in reducing many sources of confusion (water, shadows, etc.) and assigning land classes more correctly to pixels in the imagery.

Our main focus was to determine vegetation class accurately to assess urban vegetation canopy cover for our study areas. The results from our two-class process complements findings from previous studies (Hartfield et al., 2011; Jia, 2015; Singh et al., 2012) that suggest

integrating LiDAR-derived data into land cover classification may again increase the accuracy of the vegetation class. With respect to simply estimating urban canopy cover, our results for these two cities using image classification are similar to a previous study where point sampling methods were employed (Ucar et al., 2016). In the previous study, urban canopy cover in Tacoma was estimated to be roughly 15-20% (95% confidence) depending on the sampling approach. In the current study, all five scenarios estimated urban vegetation cover in this range, and were similar to other recent estimates (Nowak and Greenfield, 2012) as well. In the previous study, urban canopy cover in Tallahassee was estimated to be roughly 41-51% (again 95% confidence). In the current study, Scenario 4 (NAIP imagery only) seemed to overestimate canopy cover while the other scenarios estimated urban vegetation cover in this range. Therefore, in some environments the structural information provided by LiDAR data, and perhaps the use of a vegetation index such as NDVI, will be of value in reducing many sources of confusion and assigning the land classes more correctly (Figure 4.9).

Conclusion

In this study we assessed urban land cover classification using remotely sensed multispectral data and LiDAR-derived vegetation presence / absence data. Six major land cover classes were estimated under four data scenarios, and in order to assess urban vegetation cover across the cities, land cover classes were further aggregated into two land cover classes under five scenarios. Twenty-four subclasses informed the development of this classification, given the heterogeneity in tone and color of the class features within each major class. For both cities, the results suggest that incorporating LiDAR-derived information into supervised classification seemed to improve the overall accuracy of the six-class results and the two-class, when compared to using NAIP imagery alone, but not significantly.

Figure 4.9. An example of classification results for two major classes (*left*) Tallahassee, and (*right*) Tacoma.

However, using LiDAR derived data along with multispectral data or LiDAR data by itself helps delineate the boundary of vegetation areas so that the accuracy of vegetation class improves compared to using NAIP imagery alone. In addition, estimates of land areas in each class were quite different when NAIP alone was used as the source of imagery (Scenario 4). In these cases, the extent of land area classified as vegetation (trees or shrubs) was generally greater than the other scenarios, even when LiDAR-derived information was used alone (Scenario 5).

Overall, the methodology of this study was effective in distinguishing vegetated areas from non-vegetated areas in an urban environment. However, further examination of this issue should be conducted to determine why the accuracy was similar but the land area estimated for the major class of interest (vegetation) was different. Also, different land cover class (e.g., buildings, roads, bare ground, parking areas) can share same or similar spectral reflectance in complex urban environment that can cause low overall accuracy in pixel-based classification. To eliminate the limitation of pixel based classification, and increase the overall accuracy of the classification, different classification methods (e.g., per-field classification, object based classification) that consider relationship between spectral and spatial features of the imagery could be addressed in further research.

Funding

This study was supported by the U.S. Forest Service, Southern Research Station in Athens, Georgia, and the Republic of Turkey, Ministry of National Education.

Reference

Alig, R.J., Plantinga, A.J., Ahn, S.E., and Kline, J.D. (2003). Land use changes involving forestry in the United States: 1951 to 1997, with projections to 2050. General Technical Report PNW-GTR-587. U.S. Department of Agriculture, Forest Service, Pacific Northwest Research Station, Portland, OR.

Alpin, P. (2003). Comparison of simulated IKONOS and SPOT HRV imagery for classifying urban areas, in: Mesev, V. (eds.), Remotely sensed cities. Taylor & Francis, London and New York, pp. 23-45.

Alpin, P., Atkinson, P.M., and Curran, P.J. (1999). Fine spatial resolution simulated satellite sensor imagery for land cover mapping in the United Kingdom. Remote Sens. Environ. 68, 206–216.

Anderson, J.R., Hardy, E.E., Roach, J.T., and Witmer, R.E. (1976). A land use and land cover classification system for use with remote sensor data. U.S. Geological Survey, Professional Paper 964.: US Government Printing Office, Washington, DC.

Bandyopadhyay, M., van Aardt, J.A., and Cawse-Nicholson, K. (2013). Classification and extraction of trees and buildings from urban scenes using discrete return LiDAR and aerial color imagery. *In* Proceedings of SPIE, Laser Radar Technology and Applications XVIII, Turner, M.D., and G.W. Kamerman (eds.). International Society for Optics and Photonics. 8731, 873105.

Basgall, P.L. (2013). Lidar point cloud and stereo image point cloud fusion. Master of Science thesis. Naval Postgraduate School, Monterey, CA. 81 p.

Berland, A.M. (2012). Twin Cities urbanization and implications for urban forest ecosystem services. PhD dissertation. University of Minnesota, Minneapolis, MN. 142 p.

Bhaskaran, S., Paramananda, S., and Ramnarayan, M. (2010). Per-pixel and object-oriented classification methods for mapping urban features using Ikonos satellite data. Appl. Geogr. 30, 650–665.

Campbell, J.B., and Wynne, R.H. (2011). Introduction to remote sensing, fifth ed. The Guilford Press, New York.

Chen, L., Zhao, S., Han, W., and Li, Y. (2012). Building detection in an urban area using Lidar data and QuickBird imagery. Int. J. Remote Sens. 33, 5135–5148.

Congalton, R.G. (1991). A review of assessing the accuracy of classifications of remotely sensed data. Remote Sens. Environ. 37, 35–46.

Congalton, R.G. (2001). Accuracy assessment and validation of remotely sensed and other spatial information. Int. J. Wildland Fire. 10, 321–328.

Congalton, R.G., and Green K. (2009). Assessing the accuracy of remotely sensed data, principles and practices, second ed. CRC Press, Boca Raton, FL.

Cowardin, L.M., Carter, V., Golet, F.C., and LaRoe, E.T. (1979). Classification of wetlands and deepwater habitats of the United States. U.S. Fish and Wildlife Service, Washington, DC. FWS/OBS-79/31.

ESRI. (2016). ArcGIS 10.4.1. Released May 2016 http://www.esri.com/ (accessed 27.04.17).

Foody, G.M. (2002). Status of land cover classification accuracy assessment. Remote Sens. Environ. 80, 185–201.

Galvin, M.F., Grove, J.M. and O'Neil-Dunne, J. (2006). A report on Annapolis' present and potential urban tree canopy. Maryland Department of Natural Resources, Annapolis, MD.

Goetz, S.J., Wright, R.K., Smith, A.J., Zinecker, E., and Schaub, E. (2003). IKONOS imagery for resource management: Tree cover, impervious surfaces, and riparian buffer analyses in the mid-Atlantic region. Remote Sens. Environ. 88, 195–208.

Gómez, D., and Montero, J. (2011). Determining the accuracy in image supervised classification problems. *In* Proceedings of the EUSFLAT – LFA European Society for Fuzzy Logic and Technology. Advances in Intelligent Systems Research. Atlantis Press, Paris. 1, 342–349.

Hamraz, H., Contreras, M.A., and Zhang, J. (2017). A scalable approach for tree segmentation within small-footprint airborne LiDAR data. Computers & Geosciences. 102, 139–147.

Hartfield, K.A., Landau, K.I., and van Leeuwen, W.J.D. (2011). Fusion of high resolution aerial multispectral and LiDAR data: land cover in the context of urban mosquito habitat. Remote Sens. 3, 2364–2383.

Irani F.M., and Galvin M.F. (2003). Strategic urban forests assessment: Baltimore, Maryland. Maryland Department of Natural Resources, Annapolis, MD.

Jia, Y. (2015). Object-based land cover classification with orthophoto and Lidar data. Masters Thesis. Royal Institute of Technology, Stockholm, Sweden.

Králová, M. (2013). Accuracy assessment and classification efficiency of object-based image analysis of aerial imagery. AUC Geographica. 1, 15–23.

Leuzinger, S., Vogt, R., and Körner, C. (2010). Tree surface temperature in an urban environment. Agric. For. Meteorol. 150, 56–62.

Lo, C.P., and Choi, J. (2004). A hybrid approach to urban land use/cover mapping using Landsat 7 Enhanced Thematic Mapper Plus (ETM+) images. Int. J. Remote Sens. 25, 2687–2700.

Mackun, P., Wilson, S., Fischetti, T., and Goworowska, J. (2011). Population distribution and change: 2000 to 2010. 2010 census briefs. C2010BR-01. U.S. Department of Commerce, Economics and Statistics Administration, U.S. Census Bureau, Suitland, MD.

Mariappan, M., Krishnan, V., Murugaiya, R., and Kolanuvada, S.R. (2015). Urban forest canopy extraction using LiDAR data. Environ. Eng. Manag. J. 14, 2333–2340.

McBride, J. (2011). Mapping Chicago area urban tree canopy cover using color infrared imagery. Master of Science thesis. Lund University, Lund, Sweden. 52 p.

McGee, J.A. III, Day, S.D., Wynne, R.H., and White, M.B. (2012). Using geospatial tools to assess the urban tree canopy: Decision support for local governments. J. For. 110, 275–286.

McPherson, E.G., Simpson, J.R., Xiao, Q., and Wu, C. (2011). Million trees Los Angeles canopy cover and benefit assessment. Landsc. Urban Plan. 99, 40–50.

Merry, K., Siry, J., Bettinger, P., and Bowker, J.M. (2013). Assessing potential urban tree planting sites in the Piedmont of the United States: a comparison methods. Southeastern Geographer. 53, 79–101.

Merry, K., Siry, J., Bettinger, P., and Bowker, J.M. (2014). Urban tree cover change in Detroit and Atlanta, USA, 1951–2010. Cities. 41, 123–131.

Mincey, S.K., Schmitt-Harsh, M., and Thurau, R. (2013). Zoning, land use, and urban tree canopy cover: the importance of scale. Urban For. Urban Greening. 12, 191–199.

Myeong, S., Nowak, D.J., and Duggin, M.J. (2006). A temporal analysis of urban forest carbon storage using remote sensing. Remote Sens. Environ. 101, 277–282.

Myint, S.W., Gober, P., Brazel, A., Grossman-Clarke, S., and Weng, Q. (2011). Per-pixel vs. object-based classification of urban land cover extraction using high spatial resolution imagery. Remote Sens. Environ. 115, 1145–1161.

National Oceanographic and Atmospheric Administration. (2017). Office for Coastal Management, Charleston, SC. https://coast.noaa.gov/ (accessed 27.04.17).

Nowak, D.J. (1993). Historical vegetation change in Oakland and its implications for urban forest management. J. Arboric. 19, 313–319.

Nowak, D.J., Crane, D.E., Stevens, J.C., Hoehn, R.E., Walton, J.T., and Bond, J. (2008). A ground-based method of assessing urban forest structure and ecosystem services. Arboric. Urban For. 34, 347–358.

Nowak, D.J., and Greenfield, E.J. (2012). Tree and impervious cover change in U.S. cities. Urban For. Urban Greening. 11, 21–30.

Nowak, D.J., Noble, M.H., Sisinni, S.M., and Dwyer, J.F. (2001). People and trees: assessing the US urban forest resource. J. For. 99(3), 37–42.

Nowak, D.J., Rowntree, R.A., McPherson, E.G., Sisinni, S.M., Kerkmann, E.R., and Stevens, J.C. (1996). Measuring and analyzing urban tree cover. Landsc. Urban Plan. 36, 49–57.

Nowak, D.J., Stein, S.M., Randler, P.B., Greenfield, E.J., Comas, S.J., Carr, M.A., and Alig, R.J. (2010). Sustaining America's urban trees and forests. U.S. Department of Agriculture, Forest Service, Northern Research Station, State and Private Forestry, Newtown Square, PA. General Technical Report NRS-62.

Parlin, M., and Mead, M. (2009). Seattle, Washington urban tree canopy analysis: Project report: Looking back and moving forward. NCDC Imaging & Mapping, Colorado Springs, CO.

Parmehr, E.G., Amati, M., Taylor, E.J., and Livesley, S.J. (2016). Estimation of urban tree canopy cover using random point sampling and remote sensing methods. Urban For. Urban Greening. 20, 160–171.

Pasher, J., McGovern, M., Khoury, M., and Duffe, J. (2014). Assessing carbon storage and

sequestration by Canada's urban forests using high resolution earth observation data. Urban For. Urban Greening. 13, 484–494.

Peacock, R. (2014). Accuracy assessment supervised and unsupervised classification using Landsat imagery of Little Rock, Arkansas. Master of Science thesis. Northwest Missouri State University, Maryville, MO. 48 p.

Richardson, J.J., and Moskal, L.M. (2014). Uncertainty in urban forest canopy assessment: Lessons from Seattle, WA, USA. Urban For. Urban Greening. 13, 152–157.

Rouse, J.W. Jr., Haas, R.H., Schell, J.A., and Deering, D.W. (1974). Monitoring vegetation systems in the Great Plains with ERTS. *In* Goddard Space Flight Center Third ERTS-1 Symposium. Volume 1, Section A. pp. 309–317.

Singh, K.K., Vogler, J.B., Shoemaker, D.A., and Meentemeyer, R.K. (2012). LiDAR-Landsat data fusion for large-area assessment of urban land cover: Balancing spatial resolution, data volume and mapping accuracy. ISPRS J. Photogramm. Remote Sens. 74, 110–121.

Thomlinson, J.R., Bolstad, P.V., and Cohen, W.B. (1999). Coordinating Methodologies for scaling landcover classification from site-specific to global map products. Remote Sens. Environ. 70, 16–28.

Ucar, Z., Bettinger, P., Merry, K., Siry, J., Bowker, J.M., and Akbulut, R. (2016). A comparison of two sampling approaches for assessing the urban forest canopy cover from aerial photography. Urban For. Urban Greening. 16, 221–230.

United Nations. (2015). World urbanization prospects. United Nations Department of Economic and Social Affairs, Population Division, New York. ST/ESA/SER.A/366. 493 p.

U.S. Census Bureau. (2010). U.S. QuickFacts from the US Census Bureau. https://www.census.gov/quickfacts/table/PST045216/00 (accessed 05.05.2017).

U.S. Geological Survey. (2017). The National Map. https://viewer.nationalmap.gov/launch/ (accessed 27.04.17).

Walton, J.T., Nowak, D.J., and Greenfield, E.J. (2008). Assessing urban forest canopy cover using airborne or satellite imagery. Arboric. Urban For. 34, 334–340.

Wang, J.L., Ma, Y.T., and Sun, L.S. (2014). Analysis of EVI and NDVI Characteristics in Different Land Cover Types in Liaoning Province. *In PIERS 2014 Guangzhou*. The Electromagnetics Academy, Cambridge, MA. pp. 2386–2390.

Ward, K.T., Johnson, G.R. (2007). Geospatial methods provide timely and comprehensive urban forest information. Urban For. Urban Greening. 6, 15–22.

Yan, W.Y., Shaker, A., and El-Ashmawy, N. (2015). Urban land cover classification using airborne LiDAR data: A review. Remote Sens. Environ. 158, 295–310.

Yuan, F., Sawaya, K.E., Loeffelholz, B.C., and Bauer, M.E. (2005). Land cover classification and change analysis of the Twin Cities (Minnesota) Metropolitan Area by multitemporal Landsat remote sensing. Remote Sens. Environ. 98, 317–328.

Zhang, X., Feng, X., and Jiang, H. (2010). Object-oriented method for urban vegetation mapping using IKONOS imagery. Int. J. Remote Sens. 31, 177–196.

CHAPTER 5

CONCLUSION

Application of advanced technology in precision forestry and natural resources management increases progressively, and endeavors in this field require continuous evaluation in order to determine efficiency and accuracy of the technology. In this dissertation, three studies have been performed to examine the use of remote sensing technologies, GIS and GPS, and their accuracy in precision forestry practices.

The study described in Chapter 2, "Dynamic accuracy of recreation-grade GPS receivers in oak-hickory forests," presents results of a highly controlled dynamic (kinematic) accuracy of a single model of recreation-grade receiver, within deciduous forest, across two seasons of the year (winter and summer). The goals of the study were to gauge the area of agreement with a relatively small but well-defined closed area, to assess the variation of waypoints recorded around true boundaries of the area, and to determine whether there were significant differences in area determination among the two seasons of the year. The following hypotheses were tested to evaluate the accuracy of this model of recreational-grade GPS receiver:

1. Difference in areas estimated by recreational grade GPS units from the true area is the same whether the GPS data are collected in winter or in summer.
2. Differences in the percentage of vertices within 1 m bands (1 m, 2 m, 3 m, etc.) of the true area boundary are not different during the two seasons.
3. The area of agreement between the true sample area and the areas estimated using the

GPS receiver (using an intersect process in a geographic information systems) is the same in winter as in summer.

In addition to these hypotheses, we simulated larger areas of different sizes (1 to 49 ha) to examine how the effects of the observed error from our small study area might impact area measurements when applied to larger land areas. This work was published in the journal *Forestry* in 2014.

A number of studies have been employed in the past for statistical horizontal position accuracy while the assessment of the dynamic (kinematic) accuracy of a recreation-grade receiver has been lacking. The result of the study showed that there were general differences between the samples collected in the summer and the samples that were collected in the winter. The average of closed areas collected using the recreation-grade GPS receiver was closer to the true area during the winter season (leaf-off), and the range of the sample areas during the winter season varied less than summer season (leaf-on). The average area of agreement was greater in the winter season than in the summer season as well. It seemed that the percentage of the vertices within 1 m bands around the true boundary line illustrated only minor differences among the seasons. However, based on the statistical test results, no significant differences were observed, and all three hypotheses could not be rejected. Hence, it cannot be stated that vegetative conditions associated with a deciduous forest in winter and in summer had any effect on the area determined, the area of agreement (with the true area), or the distribution of vertices around the true area boundary. Additionally, after simulating larger areas of different sizes (1 to 49 ha), our results suggested that areas greater than 25 ha produced 2 percent or less error in both winter and summer seasons. This research could be expand by employing similar study protocols to the

assessment of current mapping-grade GPS receiver, and exploring impacts of variations in receiver settings on the results obtained.

In Chapter 3, "A Comparison of two sampling approaches for assessing the urban forest canopy cover from aerial photography," we assessed the percentage of the tree canopy cover in two United States cities (Tacoma, Washington and Tallahassee, Florida). The main goal of this study was to compare two sampling approaches (random point-based and plot/grid) for estimating urban tree canopy cover using two different remotely sensed imagery sources (NAIP imagery and Google Earth imagery) . The following hypotheses were developed:

1. When employing the random point-based sampling approach, there is no significant difference in the estimated tree canopy cover derived from using the NAIP imagery in ArcGIS and the estimated tree canopy cover derived from using the Google Earth imagery.
2. When employing the plot/grid sampling approach, there is no significant difference in the estimated tree canopy cover derived from using the NAIP imagery in ArcGIS and the estimated tree canopy cover derived from using the Google Earth imagery.

Assessments of tree canopy cover from remotely sensed imagery using new protocols or procedures require continuous testing for their usefulness to support management decisions and policy analyses. When comparing a point-based sampling approach (a common sampling method) to a plot/grid sampling approach, the estimated tree canopy cover was similar within two study areas. The results of the estimates of tree canopy cover in Tallahassee, Florida, were 48.6 to 49.1 % using Google Earth imagery and 44.5 to 45.1% using NAIP imagery within ArcGIS. Statistical tests results showed that there seemed to be significant difference between the two sampling approaches using the two different imagery sources. For Tacoma, Washington,

the estimated tree canopy cover was about 19.2 to 20.0% using Google Earth imagery and 17.3 to 18.1% when using NAIP imagery in ArcGIS. The statistical test results suggested that there was no significant difference between the random point-based sampling approach using the two different image sources but the result of the plot/grid sampling approach showed a significant difference. It can be stated that our findings showed some similarities between the two sampling approaches; therefore, the random point-based sampling approach might be preferred due to the time and effort required, and causing less classification problems. This work was published in the journal *Urban Forestry and Urban Greening* in 2016.

The study in Chapter 4, "Estimation of urban vegetation cover using multispectral imagery and LiDAR," reports the results of assessing urban vegetation cover using a supervised maximum likelihood classification method in two United States cities (Tacoma and Tallahassee). The primary goal of this study was to determine whether the incorporation of the LiDAR data into a pixel-based supervised maximum likelihood classification method increased the accuracy of urban vegetation cover estimations. The following general hypotheses were developed:

1. When employing LiDAR in a supervised classification of urban vegetation, the overall accuracy of the resulting vegetation level improves when used in conjunction with high spatial resolution remotely sensed imagery.
2. When employing LiDAR data by itself to identify urban vegetation, the overall accuracy of the resulting vegetation level is no different than if it is used in conjunction with high spatial resolution remotely sensed imagery.

Chapter 4 represents continuous test results of the protocols and procedures associated with using remotely sensed data for estimating urban canopy cover within two study areas. In order to address hypothesis 1, six major land cover classes were developed under four scenarios.

For both cities, the results suggested that incorporating LiDAR-derived information into supervised classification seemed to improve the overall accuracy of the six-class results when compared to using NAIP imagery alone, but not significantly. In particular, by adding LiDAR derived information into the classification, the accuracy of vegetation class increased between 16% and 24% while comparing to using NAIP imagery only. For hypothesis 2, land cover classes were aggregated into two land cover classes under five scenarios. The results of the two land cover class were similar to the six-class results. Also, estimated urban vegetation areas in Chapter 4 where the supervised classification method was used suggested similarities with the results of Chapter 3 where sampling methods were employed. Overall, the results suggested that using LiDAR derived information along with high resolution remotely sensed imagery or LiDAR data by itself improved the process of identifying vegetated areas so that the accuracy of vegetation class increases and the estimates of vegetated land areas were more appropriate, when compared to using NAIP imagery alone.

In general, our methodology was useful for differentiating vegetated areas from non-vegetated areas in an urban environment. However, further analysis could be conducted to determine why the accuracy was similar but the land area estimated for the major class of interest (vegetation) was different. Also, land cover class (e.g., buildings, roads, bare ground, and parking areas) in heterogeneous urban environment can share same or similar spectral reflectance that results in low overall accuracy in pixel-based classification. To eliminate the limitation of pixel based classification, and increase the overall accuracy of the classification, different classification methods (e.g., per-field classification, object based classification) that consider relationship between spectral and spatial features of the imagery could be addressed in further research. Additionally, in our study, size of the data was huge, and it took long time to process

the data. We sometimes used around 10 computers to process the data. With recent advanced technology and tools such as Google Earth Engine (a cloud platform that can be used as both data archive and analysis tool), we may not only be able to access imagery from different sources in different time periods but also analyze large data sets in a relatively short amount of time (Google Inc., 2015). Thus, new tools like this might require further investigation into their usefulness in urban cover assessment at regional, national and global scales.

In this dissertation, the three precision forestry studies provided scientific accuracy assessments of the application of modern tools and technologies to forestry and natural resource management concerns. The studies suggested many reasons inherent to the tools and technologies that can affect the accuracy significantly. We hope that developing new protocols and procedures with modern technologies and tools will help to reduce undesirable effects and produce the most accurate data that can assist foresters, natural resource managers, and policy makers in addressing a variety of management issues.

REFERENCES

Alig, R.J., Plantinga, A.J., Ahn, S.E., and Kline, J.D. (2003). Land use changes involving forestry in the United States: 1951 to 1997, with projections to 2050. General Technical Report PNW-GTR-587. U.S. Department of Agriculture, Forest Service, Pacific Northwest Research Station, Portland, OR.

Alpin, P. (2003). Comparison of simulated IKONOS and SPOT HRV imagery for classifying urban areas, in: Mesev, V. (eds.), Remotely sensed cities. Taylor & Francis, London and New York, pp. 23-45.

Alpin, P., Atkinson, P.M., and Curran, P.J. (1999). Fine spatial resolution simulated satellite sensor imagery for land cover mapping in the United Kingdom. Remote Sens. Environ. 68, 206–216.

Anderson, H.E., Clarkin, T., Winterberger, K., and Strunk, J. (2009). An accuracy assessment of positions obtained using survey- and recreational-grade global positioning system receivers across a range of forest conditions within the Tanana Valley of Interior Alaska. West. J. Appl. For. 24, 128–136.

Anderson, J.R., Hardy, E.E., Roach, J.T., and Witmer, R.E. (1976). A land use and land cover classification system for use with remote sensor data. U.S. Geological Survey, Professional Paper 964.: US Government Printing Office, Washington, DC.

Bare, B.B. (2001). Opening remarks and welcome to the First International Precision Forestry Symposium. *In* Proceedings of the First International Precision Forestry Cooperative Symposium. University of Washington, College of Forest Resources, Seattle, WA. pp. 1.

Bandyopadhyay, M., van Aardt, J.A., and Cawse-Nicholson, K. (2013). Classification and extraction of trees and buildings from urban scenes using discrete return LiDAR and aerial color imagery. *In* Proceedings of SPIE, Laser Radar Technology and Applications XVIII, Turner, M.D., and G.W. Kamerman (eds.). International Society for Optics and Photonics. 8731, 873105.

Basgall, P.L. (2013). Lidar point cloud and stereo image point cloud fusion. Master of Science thesis. Naval Postgraduate School, Monterey, CA. 81 p.

Beran, T., Langley, R.B., Bisnath, S.B., and Serrano, L. (2007). High-accuracy point positioning with low-cost GPS receivers. Navig. 54, 53–63.

Berland, A.M. (2012). Twin Cities urbanization and implications for urban forest ecosystem services. PhD dissertation. University of Minnesota, Minneapolis, MN. 142 p.

Bettinger, P., and Fei, S. (2010). One year's experience with a recreation-grade GPS receiver. Math. Comp. For. Nat. Res. Sci. 2, 153–160.

Bettinger, P., and Merry, K.L. (2011). Global navigation satellite system research in forest management. LAP Lambert Academic Publishing, Saarbrücken, Germany. 64 p.

Bettinger, P., and Merry, K. (2012a). Static horizontal positions determined with a consumer-grade GNSS receiver: One assessment of the number of fixes necessary. Croat. J. For. Eng. 33, 149–157.

Bettinger, P., and Merry, K.L. (2012b). Influence of the juxtaposition of trees on consumer-grade GPS position quality. Math. Comp. For. Nat. Res. Sci. 4, 81–91.

Bhaskaran, S., Paramananda, S., and Ramnarayan, M. (2010). Per-pixel and object-oriented classification methods for mapping urban features using Ikonos satellite data. Appl. Geogr. 30, 650–665.

Borders, B.E., Harrison, W.M., Clutter, M.L., Shiver, B.D., and Souter, R.A. (2008). The value of timber inventory information for management planning. Can. J. For. Res. 38, 2287–2294.

Buerkert, A., and Schlecht, E. (2009). Performance of three GPS collars to monitor goats' grazing itineraries on mountain pastures. Comput. Electron. Agr. 65, 85–92.

California Carbon. (2015). California Carbon info. http://californiacarbon.info/ (accessed 05/28/2015).

Campbell, J.B., and Wynne, R.H. (2011). Introduction to remote sensing, fifth ed. The Guilford Press, New York.

Chen, L., Zhao, S., Han, W., and Li, Y. (2012). Building detection in an urban area using Lidar data and QuickBird imagery. Int. J. Remote Sens. 33, 5135–5148.

Climate Action Reserve. (2014a). Quantification guidance for use with forest carbon projects, January 21, 2014. Climate Action Reserve, Los Angeles, CA. 29 p.

Climate Action Reserve. (2014b). Summary of comments & responses, draft urban forest project protocol version 2.0. Climate Action Reserve, Los Angeles, CA. 18 p.

Climate Policy Initiative. (2015). California climate dashboard. http://calcarbondash.org/ (accessed 05/28/2015).

Congalton, R.G. (1991). A review of assessing the accuracy of classifications of remotely sensed data. Remote Sens. Environ. 37, 35–46.

Congalton, R.G. (2001). Accuracy assessment and validation of remotely sensed and other spatial information. Int. J. Wildland Fire. 10, 321–328.

Congalton, R.G., and Green K. (2009). Assessing the accuracy of remotely sensed data, principles and practices, second ed. CRC Press, Boca Raton, FL.

Cowardin, L.M., Carter, V., Golet, F.C., and LaRoe, E.T. (1979). Classification of wetlands and deepwater habitats of the United States. U.S. Fish and Wildlife Service, Washington, DC. FWS/OBS-79/31.

Danskin, S.D., Bettinger, P., Jordan, T.R., and Cieszewski, C. (2009). A comparison of GPS performance in a southern hardwood forest: Exploring low-cost solutions for forestry applications. South. J. Appl. For. 33, 9–16.

Deckert, C. and Bolstad, P.V. (1996). Forest canopy, terrain, and distance effects on global positioning system point accuracy. Photogramm. Eng. Rem. Sens. 62, 317–321.

Dussault, C., Courtios, R., Ouellet, J., and Huot, J. (2001). Influence of satellite geometry and differential correction on GPS location accuracy. Wildl. Soc. Bull. 29, 171–179.

Ehlers, M., Edwards, G., and Bedard, Y. (1989). Integration of remote sensing and GIS: data and data access. Photogramm. Eng. Rem. Sens. 55, 1619–1627.

ESRI. (2013). ArcGIS. http://www.esri.com/software/arcgis (accessed 09/21/2013).

ESRI. (2016). ArcGIS 10.4.1. Released May 2016 http://www.esri.com/ (accessed 04/27/2017).

Foody, G.M. (2002). Status of land cover classification accuracy assessment. Remote Sens. Environ. 80, 185–201.

Franklin, S.E. (2001). Remote sensing for sustainable forest management. CRC Press, Boca Raton, FL.

Galvin, M.F., Grove, J.M. and O'Neil-Dunne, J. (2006). A report on Annapolis' present and potential urban tree canopy. Maryland Department of Natural Resources, Annapolis, MD.

Garmin International Inc. (2013). Oregon® 450t. Garmin International Inc., Olathe, KS.

https://buy.garmin.com/en-US/US/on-the-trail/handhelds/oregon-450t/prod63350.html (accessed 09/21/2013).

Gervasi, V., Brunberg, S., and Swenson, J.E. (2006). An individual-based method to measure animal activity levels: A test on brown bears. Wildl. Soc. Bull. 34, 1314–1319.

Goetz, S.J., Wright, R.K., Smith, A.J., Zinecker, E., and Schaub, E. (2003). IKONOS imagery for resource management: Tree cover, impervious surfaces, and riparian buffer analyses in the mid-Atlantic region. Remote Sens. Environ. 88, 195–208.

Google, Inc. (2014). Google Earth (Version 7.1.2.2041). https://www.google.com/earth/ (accessed 12/27/2014)

Google, Inc. (2015). Google Earth Engine. https://earthengine.google.com/ (accessed 07/12/2017).

Gómez, D., and Montero, J. (2011). Determining the accuracy in image supervised classification problems. *In* Proceedings of the EUSFLAT – LFA European Society for Fuzzy Logic and Technology. Advances in Intelligent Systems Research. Atlantis Press, Paris. 1, 342–349.

Hamraz, H., Contreras, M.A., and Zhang, J. (2017). A scalable approach for tree segmentation within small-footprint airborne LiDAR data. Computers & Geosciences. 102, 139–147.

Hartfield, K.A., Landau, K.I., and van Leeuwen, W.J.D. (2011). Fusion of high resolution aerial multispectral and LiDAR data: land cover in the context of urban mosquito habitat. Remote Sens. 3, 2364–2383.

Holden, N.M., Martin, A.A., Owende, P.M.O., and Ward, S.M. (2001). A method for relating GPS performance to forest canopy. Int. J. For. Eng. 12, 51–56.

Holland, K. (2013). A primer on forest carbon projects under California's new offset program. The Forestry Source 18(3): 7.

Holopainen, M., Vastaranta, M., and Hyypä, J. (2014). Outlook for the next generation's precision forestry in Finland. Forests. 5, 1682–1694.

Irani F.M., and Galvin M.F. (2003). Strategic urban forests assessment: Baltimore, Maryland. Maryland Department of Natural Resources, Annapolis, MD.

Jensen, R., Gatrell, J., Boulton, J., and Harper, B. (2004). Using remote sensing and geographic information systems to study urban quality of life and urban forest amenities. Ecol. Soc. 9(5), 5–15.

Jia, Y. (2015). Object-based land cover classification with orthophoto and Lidar data. Masters Thesis. Royal Institute of Technology, Stockholm, Sweden.

Kerchner, D.C., and Keeton, W.S. (2015). California's regulatory forest carbon market: Viability for northeast landowners. For. Policy Econ. 50, 70–81.

King, K.L., and Locke, D.H. (2013). A comparison of three methods for measuring local urban tree canopy cover. Arboric. Urban For. 39, 62–67.

Kiser, J., Solmie, D., Kellogg, L., and Wing, M.G. (2005). Efficiencies of traditional and digital technologies for forest operations. West. J. Appl. For. 20, 138–143.

Kovácsová, P. and Antalová, M. (2010). Precision forestry–definition and technologies. Šumarski List. 134(11-12), 603–610.

Králová, M. (2013). Accuracy assessment and classification efficiency of object-based image analysis of aerial imagery. AUC Geographica. 1, 15–23.

Levy, P.S., and Lemeshow, S. (1991). Sampling of populations: Methods and applications, second ed. John Wiley & Sons, Inc., New York.

Leuzinger, S., Vogt, R., and Körner, C. (2010). Tree surface temperature in an urban environment. Agric. For. Meteorol. 150, 56–62.

Lillesand, T.M., Kiefer, R.W., and Chipman, J.W. (2004). Remote Sensing and Image Interpretation. Seventh ed. John Wiley and Sons: New York, NY.

Liu, C.J., and Brantigan, R. (1995). Using Differential GPS for forest traverse surveys. Can. J. For. Res. 25, 1795–1805.

Lo, C.P., and Choi, J. (2004). A hybrid approach to urban land use/cover mapping using Landsat 7 Enhanced Thematic Mapper Plus (ETM+) images. Int. J. Remote Sens. 25, 2687–2700.

Loveland, T.R. and Johnson, G.E. (1983). The role of remotely sensed and other spatial data for predictive modelling: The Umatilla, Oregon example. Photogramm. Eng. Rem. Sens. 49, 1183–1192.

Lyon, J.G. (1983). Landsat derived landcover classifications for locating potential kestrel nesting habitat. Photogramm. Eng. Rem. Sens. 49, 245–250.

Macfie, B.P., and Nufrio, P.M. (2006). Applied statistics for public policy. M.E. Sharpe, Inc., Armonk, NY.

Mackun, P. J., Wilson, S., Fischetti, T. R., and Goworowska, J. (2011). Population distribution and change: 2000 to 2010. 2010 census briefs. C2010BR-01.U.S. Department of Commerce, Economics and Statistics Administration, U.S. Census Bureau, Suitland, MD.

Mariappan, M., Krishnan, V., Murugaiya, R., and Kolanuvada, S.R. (2015). Urban forest canopy extraction using LiDAR data. Environ. Eng. Manag. J. 14, 2333–2340.

McGee, J.A. III, Day, S.D., Wynne, R.H., and White, M.B. (2012). Using geospatial tools to assess the urban tree canopy: Decision support for local governments. J. For. 110, 275–286.

McPherson, E.G., Simpson, J.R., Xiao, Q., and Wu, C. (2011). Million trees Los Angeles canopy cover and benefit assessment. Landsc. Urban Plan. 99, 40–50.

McRoberts, R.E. (2010). The effects of rectification and Global Positioning system errors on

satellite image-based estimates of forest area. Remote Sens. Environ. 114, 1710–1717.

Merry, K., Siry, J., Bettinger, P., and Bowker, J.M. (2013). Assessing potential urban tree planting sites in the Piedmont of the United States: a comparison methods. Southeastern Geographer. 53, 79–101.

Merry, K., Siry, J., Bettinger, P., and Bowker, J.M. (2014). Urban tree cover change in Detroit and Atlanta, USA, 1951–2010. Cities. 41, 123–131.

Mincey, S.K., Schmitt-Harsh, M., and Thurau, R. (2013). Zoning, land use, and urban tree canopy cover: the importance of scale. Urban For. Urban Greening. 12, 191–199.

Minitab Inc. (2013). Minitab 16. Minitab Inc., State College, PA. www.minitab.com (accessed 09/21/2013).

Minnesota Department of Natural Resources. (2012). DNRGPS application, 6.0.0.15. St. Paul, MN. http://www.dnr.state.mn.us/mis/gis/DNRGPS/DNRGPS.html (accessed 09/21/2013).

Myeong, S., Nowak, D.J., and Duggin, M.J. (2006). A temporal analysis of urban forest carbon storage using remote sensing. Remote Sens. Environ. 101, 277–282.

Myint, S.W., Gober, P., Brazel, A., Grossman-Clarke, S., and Weng, Q. (2011). Per-pixel vs. object-based classification of urban land cover extraction using high spatial resolution imagery. Remote Sens. Environ. 115, 1145–1161.

Naesset, E., and Jonmeister, T. (2002). Assessing point accuracy of DGPS under forest canopy before data acquisition, in the field and after postprocessing. Scand. J. For. Res. 17, 351–358.

National Oceanographic and Atmospheric Administration. (2017). Office for Coastal Management, Charleston, SC. https://coast.noaa.gov/ (accessed 04/27/2017).

Nickerson, J. (2014a). Urban forest project protocol, version 2.0 for public comment, March 21, 2014. Climate Action Reserve, Los Angeles, CA. 58 p.

Nowak, D.J. (1993). Historical vegetation change in Oakland and its implications for urban forest management. J. Arboric. 19, 313–319.

Nowak, D.J., and Crane, D.E. Carbon storage and sequestration by urban trees in the USA. Environ. Pollution. 116, 381–389.

Nowak, D.J., Crane, D.E., Stevens, J.C., Hoehn, R.E., Walton, J.T., and Bond, J. (2008). A ground-based method of assessing urban forest structure and ecosystem services. Arboric. Urban For. 34, 347–358.

Nowak, D.J., and Greenfield, E.J. (2012). Tree and impervious cover change in U.S. cities. Urban For. Urban Greening. 11, 21–30.

Nowak, D.J., Noble, M.H., Sisinni, S.M., and Dwyer, J.F. (2001). People and trees: assessing the US urban forest resource. J. For. 99(3), 37–42.

Nowak, D.J., Rowntree, R.A., McPherson, E.G., Sisinni, S.M., Kerkmann, E.R., and Stevens, J.C. (1996). Measuring and analyzing urban tree cover. Landsc. Urban Plan. 36, 49–57.

Nowak, D.J., Stein, S.M., Randler, P.B., Greenfield, E.J., Comas, S.J., Carr, M.A., and Alig, R.J. (2010). Sustaining America's urban trees and forests. U.S. Department of Agriculture, Forest Service, Northern Research Station, State and Private Forestry, Newtown Square, PA. General Technical Report NRS-62.

Olivera, A., and Visser, R. (2014). Integration of GNSS in harvesters as a tool for site-specific management in plantation forests; a literature review. Future Forest Research Ltd. Rotorua, New Zealand.

Parlin, M., and Mead, M. (2009). Seattle, Washington urban tree canopy analysis: Project report: Looking back and moving forward. NCDC Imaging & Mapping, Colorado Springs, CO.

Parmehr, E.G., Amati, M., Taylor, E.J., and Livesley, S.J. (2016). Estimation of urban tree canopy cover using random point sampling and remote sensing methods. Urban For. Urban Greening. 20, 160–171.

Pasher, J., McGovern, M., Khoury, M., and Duffe, J. (2014). Assessing carbon storage and sequestration by Canada's urban forests using high resolution earth observation data. Urban For. Urban Greening. 13, 484–494.

Peacock, R. (2014). Accuracy assessment supervised and unsupervised classification using Landsat imagery of Little Rock, Arkansas. Master of Science thesis. Northwest Missouri State University, Maryville, MO. 48 p.

Pirti, A. (2005). Using GPS near the forest and quality control. Surv. Rev. 38, 286–299.

Ransom, M.D., Rhynold, J., and Bettinger, P. (2010). Performance of mapping-grade GPS receivers in southeastern forest conditions. RURALS: Rev. Undergrad. Res. Agric. Life Sci. 5(1), Article 2.

Richardson, J.J., and Moskal, L.M. (2014). Uncertainty in urban forest canopy assessment: Lessons from Seattle, WA, USA. Urban For. Urban Greening. 13, 152–157.

Rodriguez-Perez, J.R., Alvarez, M.F., Sanz, E., and Gavela, A. (2006). Comparision of GPS receiver accuracy and precision in forest environments. Practical recommendations regarding methods and reciever selection. Shaping the Change XXIII FIG Congress. Munich, Germany.

Rodriguez-Perez, J.R., Alvarez, M.F., and Sanz-Ablanedo, E. (2007). Assessment of low-cost GPS receiver accuracy and precision in forest enviroments. J. Surv. Eng. 133, 159–167.

Rouse, J.W. Jr., Haas, R.H., Schell, J.A., and Deering, D.W. (1974). Monitoring vegetation systems in the Great Plains with ERTS. *In* Goddard Space Flight Center Third ERTS-1 Symposium. Volume 1, Section A. pp. 309–317.

Singh, K.K., Vogler, J.B., Shoemaker, D.A., and Meentemeyer, R.K. (2012). LiDAR-Landsat data fusion for large-area assessment of urban land cover: Balancing spatial resolution, data volume and mapping accuracy. ISPRS J. Photogramm. Remote Sens. 74, 110–121.

Tachiki, Y., Yoshimura, T., Hasegawa, H., Mita, T., Sakai, T., and Nakamura, F. (2005). Effects of polyline simplification of dynamic GPS data under forest canopy on area and perimeter estimations. J. For. Res. 10, 419–427.

Taylor, F. (2014). About Google Earth imagery. Google Earth Blog. http://www.gearthblog.com/blog/archives/2014/04/google-earth-imagery.html (accessed 12/26/2014).

Taylor, R.K., Schrock, M.D., Bora, G., Bloomfield, J., Brockmeier, G., Burton, W., Carlson, B., Gattis, J., Groening, R., Kopriva, J., Oleen, N., Ney, J., Simmelink, C., and Vondracek. J. (2004). Dynamic testing of GPS receivers. Trans. ASAE 47, 1017–1025.

Taylor, S.E., McDonald, T.P., Fulton, J.P., Shaw, J.N., Corley, F.W., and Brodbeck, C.J. (2006). Precision forestry in the Southeast US. *In* Proceedings of the Precision Forestry in Plantations, Semi-Natural and Natural Forests, Ackerman, P.A., Längin, D.W., and Antonides, M.C. (eds.). pp. 397–414.

Thomlinson, J.R., Bolstad, P.V., and Cohen, W.B. (1999). Coordinating Methodologies for scaling landcover classification from site-specific to global map products. Remote Sens. Environ. 70, 16–28.

Ucar, Z., Bettinger, P., Merry, K., Siry, J., Bowker, J.M., and Akbulut, R. (2016). A comparison

of two sampling approaches for assessing the urban forest canopy cover from aerial photography. Urban For. Urban Greening. 16, 221–230.

United Nations. (2015). World urbanization prospects. United Nations Department of Economic and Social Affairs, Population Division, New York. ST/ESA/SER.A/366. 493 p.

U.S. Census Bureau. (2010). U.S. QuickFacts from the US Census Bureau. https://www.census.gov/quickfacts/table/PST045216/00 (accessed 05/05/2017)

U.S. Census Bureau. (2014). State & County QuickFacts from U.S. Department of Commerce, Census Bureau, Suitland, MD. https://www.quickfacts.census.gov/qfd/states (accessed 12/15/2014).

U.S. Department of Agriculture. (2013). Imagery programs, NAIP imagery. U.S. Department of Agriculture, Farm Service Agency, Aerial Photography Field Office, Salt Lake City, UT. http://www.fsa.usda.gov/FSA/apfoapp?area=home&subject=prog&topic=nai (accessed 03/10/2014).

U.S. Geological Survey. (2017). The National Map. https://viewer.nationalmap.gov/launch/ (accessed 04/27/2017).

Veal, M.W., Taylor, S.E., McDonald, T.P., McLemore, D.K., and Dunn, M.R. (2001). Accuracy of tracking forest machines with GPS. Trans. ASAE. 44, 1903–1911.

Walton, J.T., Nowak, D.J., and Greenfield, E.J. (2008). Assessing urban forest canopy cover using airborne or satellite imagery. Arboric. Urban For. 34, 334–340.

Wang, J.L., Ma, Y.T., and Sun, L.S. (2014). Analysis of EVI and NDVI Characteristics in Different Land Cover Types in Liaoning Province. *In PIERS 2014 Guangzhou*. The Electromagnetics Academy, Cambridge, MA. pp. 2386–2390.

Ward, K. T., and Johnson, G.R. (2007). Geospatial methods provide timely and comprehensive

urban forest information. Urban For. Urban Greening. 6, 15–22.

Weaver, S.A. (2015). Precision forestry studies: Laser calipers and GPS receivers. Master of Science thesis. University of Georgia, Athens, GA. 71 p.

Weaver, S.A., Z. Ucar, P. Bettinger, K. Merry, K. Faw, and C.J. Cieszewski. (2015). Assessing the accuracy of tree diameter measurements collected at a distance. Croatian J. For. Engineering. 36(1), 73–83.

Welch, R., Remillard, M., and Slack, R. (1988). Remote Sensing and geographic information techniques for aquatic resource evaluation. Photogramm. Eng. Rem. Sens. 54, 177–185.

Wing, M.G. (2008). Consumer-grade Global Positioning Systems (GPS) receiver performance. J. For. 106, 185–190.

Wing, M.G. (2009). Consumer-grade Global Positioning Systems performance in an urban forest setting. J. For. 107, 307–312.

Wing, M.G. (2011). Consumer-grade GPS receiver measurement accuracy in varying forest conditions. Res. J. For. 5, 78–88.

Wing, M.G., Eklund, A., and Kellogg, L.D. (2005). Consumer-grade Global Positioning System (GPS) accuracy and reliability. J. For. 103, 169–173.

Wulder, M.A., Hall, R.J., and Franklin, S.E. (2005) Remote sensing and GIS in forestry. *In* Remote sensing for GIS managers, Aronoff, S. (ed.). ESRI Press, Redlands, CA. pp. 351–362.

Yan, W.Y., Shaker, A., and El-Ashmawy, N. (2015). Urban land cover classification using airborne LiDAR data: A review. Remote Sens. Environ. 158, 295–310.

Yuan, F., Sawaya, K.E., Loeffelholz, B.C., and Bauer, M.E. (2005). Land cover classification and change analysis of the Twin Cities (Minnesota) Metropolitan Area by multitemporal Landsat remote sensing. Remote Sens. Environ. 98, 317–328.

Zenner, E.K., Fauskee, J.T., Berger, A.L., and Puettmann, K.J. (2007). Impacts of skidding traffic intensity on soil disturbance, soil recovery, and aspen regeneration in north central Minnesota. North. J. Appl. For. 24, 177–183.

Zhang, X., Feng, X., and Jiang, H. (2010). Object-oriented method for urban vegetation mapping using IKONOS imagery. Int. J. Remote Sens. 31, 177–196.